Hyperspectral remote sensing (imaging Spectroscopy) of agriculture and vegetation:
knowledge gains and knowledge gaps after 40 years of research

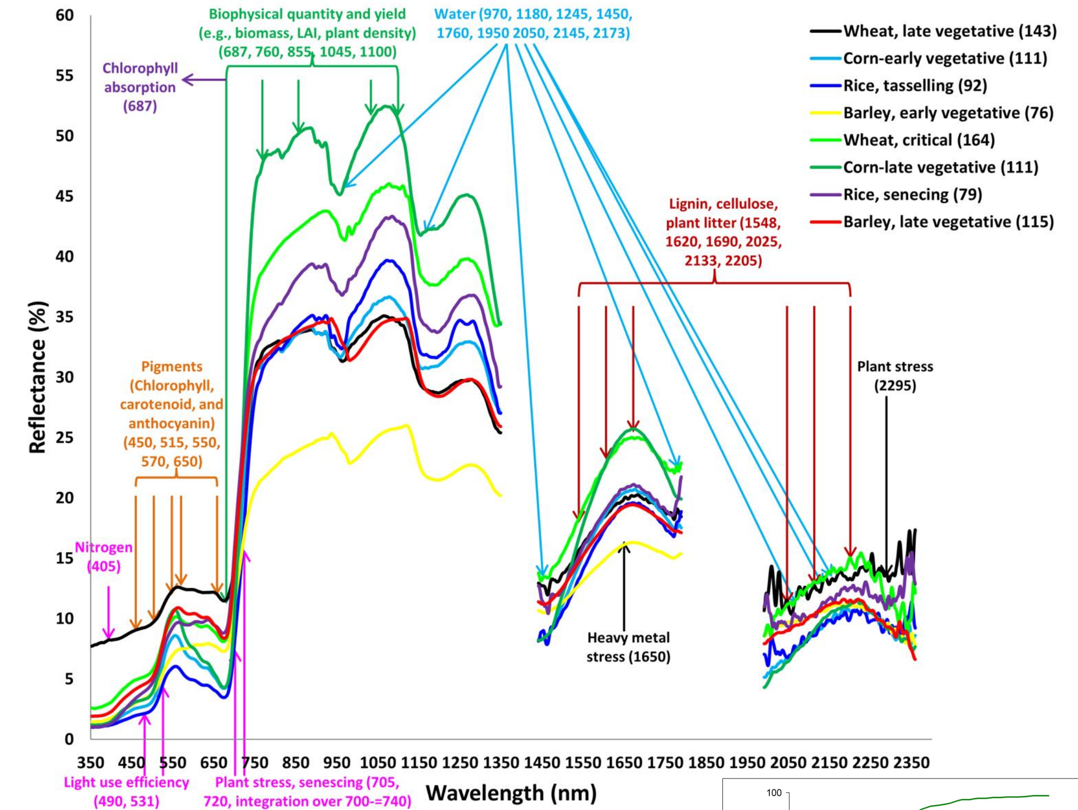

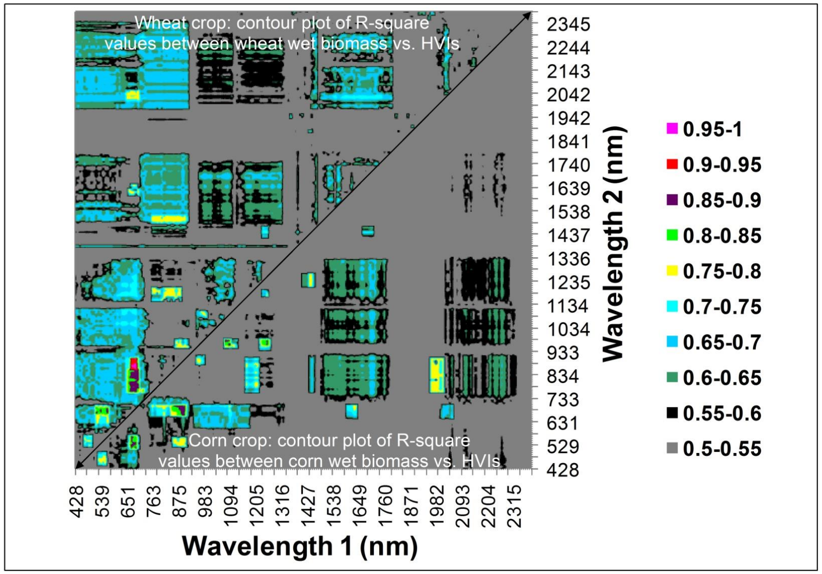

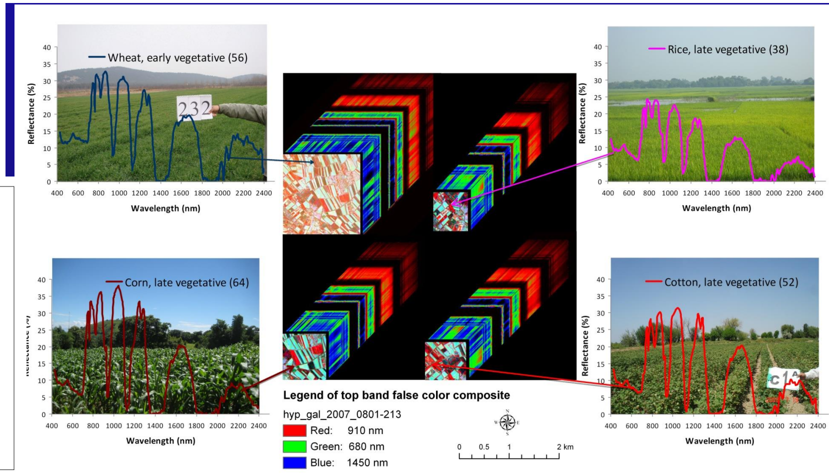

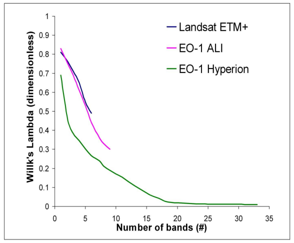

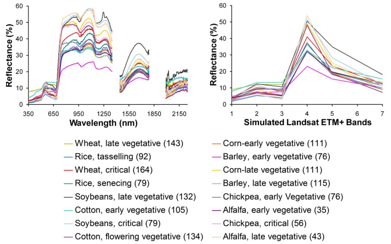

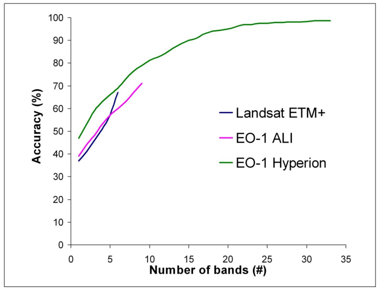

USGS
science for a changing world
U.S. Geological Survey
U.S. Department of Interior

Workshop on

Prasad S. Thenkabail
Research Geographer, U.S. Geological Survey (USGS)

April 21-22, 2015

@ Space Studies Department, University of North Dakota, Grand Forks, ND, USA

Hyperspectral Data Importance

in Study of Agriculture and Vegetation

Hyperspectral Remote Sensing (Imaging Spectroscopy) of Vegetation

Importance of Hyperspectral Sensors in Study of Vegetation

More specifically…………..hyperspectral Remote Sensing, originally used for detecting and mapping minerals, is increasingly needed for to characterize, model, classify, and map agricultural crops and natural vegetation, specifically in study of:

(a)Species composition (e.g., *chromolenea odorata vs. imperata cylindrica*);
(b)Vegetation or crop type (e.g., soybeans vs. corn);
(c)Biophysical properties (e.g., LAI, biomass, yield, density);
(d)Biochemical properties (e.g, Anthrocyanins, Carotenoids, Chlorophyll);
(e)Disease and stress (e.g., insect infestation, drought),
(f)Nutrients (e.g., Nitrogen),
(g)Moisture (e.g., leaf moisture),
(h)Light use efficiency,
(i)Net primary productivity and so on.

……….in order to increase accuracies and reduce uncertainties in these parameters……..

Hyperspectral Remote Sensing (Imaging Spectroscopy) of Vegetation

Spectral Wavelengths and their Importance in the Study of Vegetation Biophysical and Biochemical properties

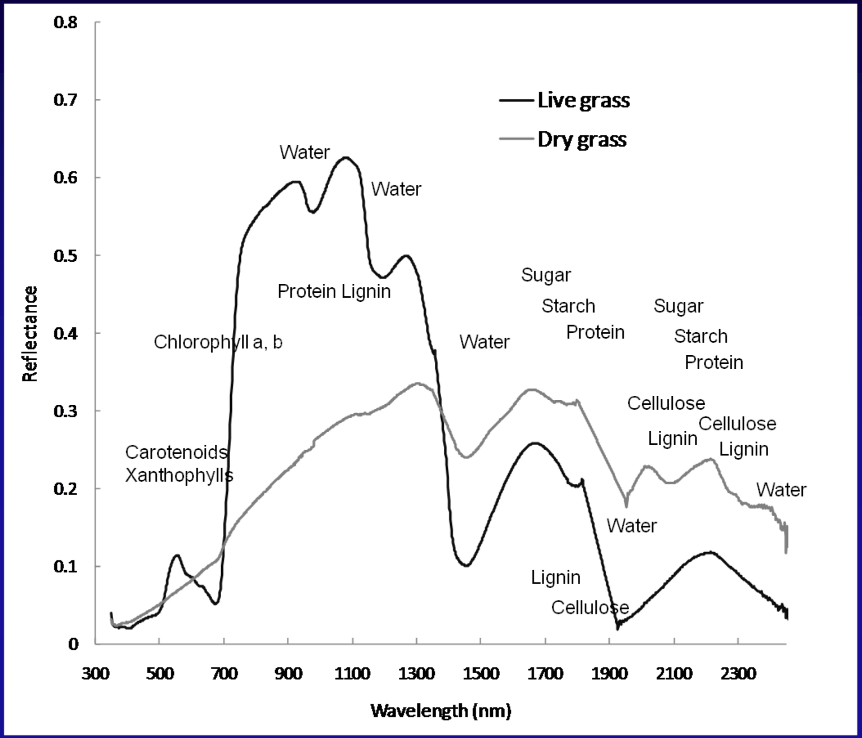

The reflectance spectra with characteristic absorption features associated with plant biochemical constitutents for live and dry grass (Adapted from Hill [13]).

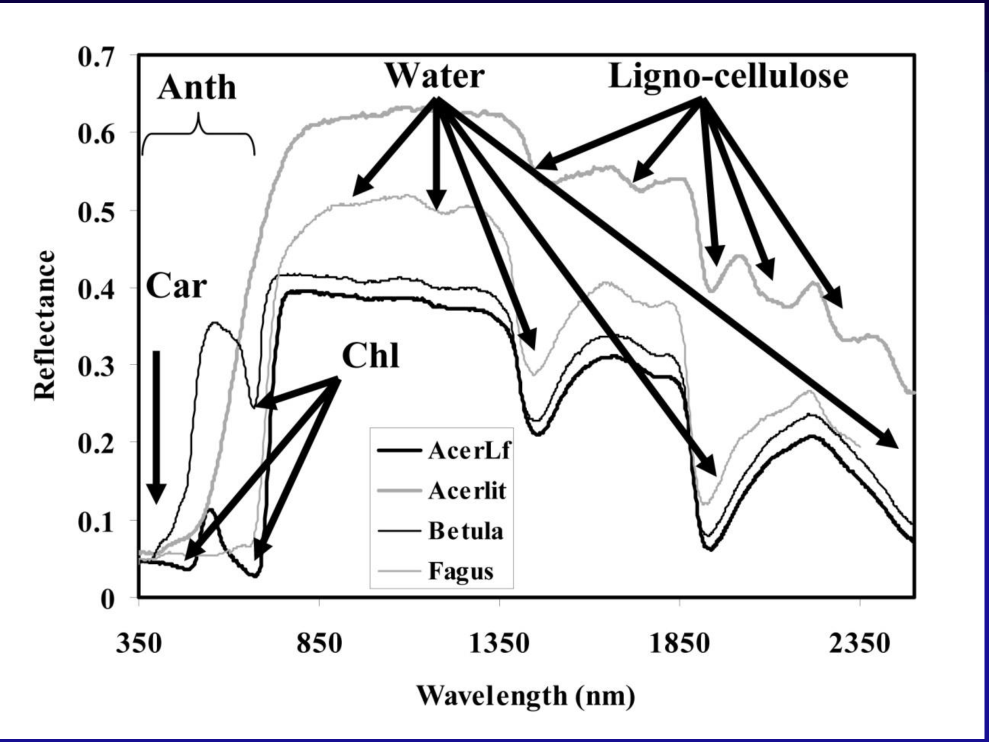

Reflectance spectra of leaves from a senesced birch (Betula), ornamental beech (Fagus) and healthy and fully senesced maple (AcerLf, Acerlit) illustrating Carotenoid (Car), Anthocyanin (Anth), Chlorophyll (Chl), Water and Ligno-cellulose absorptions.

USGS
science for a changing world

U.S. Geological Survey
U.S. Department of Interior

Hyperspectral Remote Sensing of Vegetation

Typical Hyperspectral Signatures of Certain Land Components

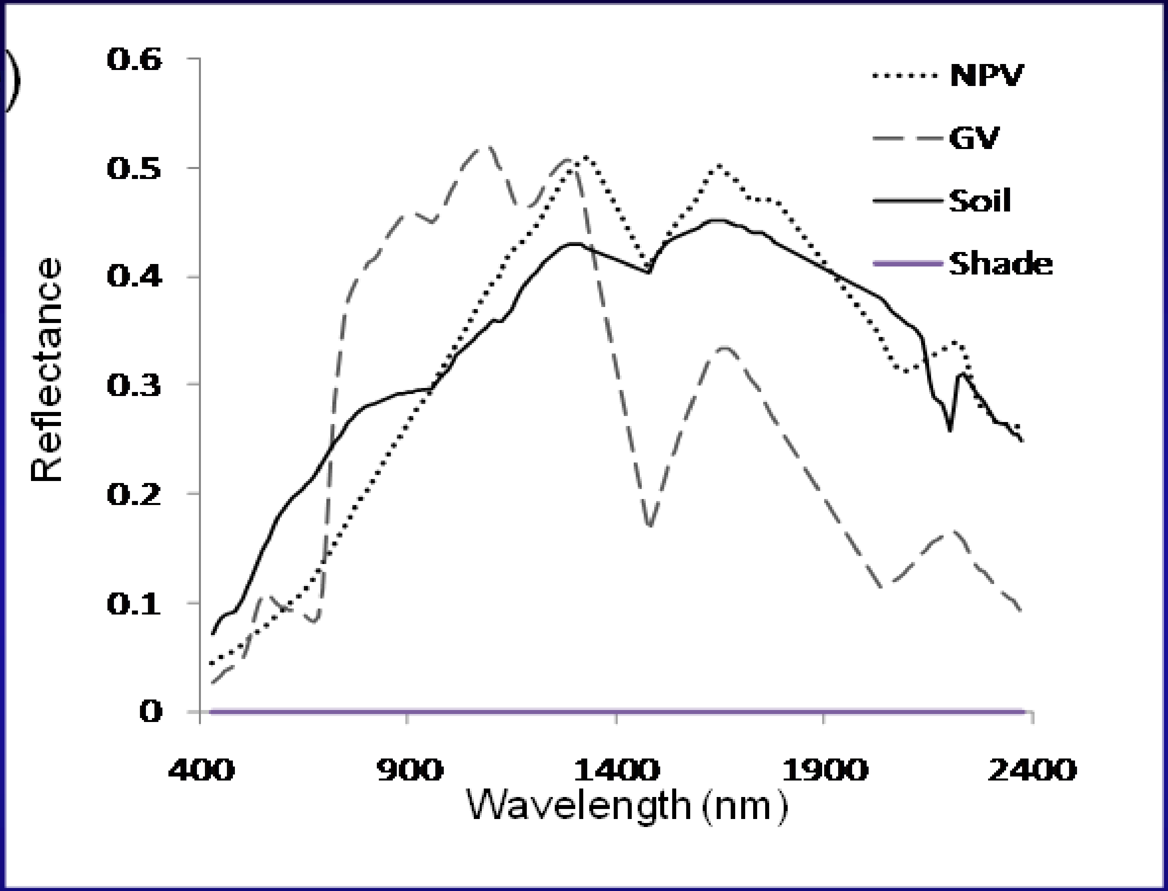

Fraction images of a pasture property in the Amazon derived from EO-1 Hyperion imagery. Four endmembers: (a) nonphotosynthetic vegetation (NPV); (b) green vegetation (GV); (c) Soil; and (d) Shade.

See chapter 9, Numata et al.

Hyperspectral
Definition

Hyperspectral Remote Sensing (Imaging Spectroscopy) of Vegetation

Definition of Hyperspectral Data

A. consists of hundreds or thousands of narrow-wavebands (as narrow as 1; but generally less than 5 nm) along the electromagnetic spectrum;
B. it is important to have narrowbands that are contiguous for strict definition of hyperspectral data; and not so much the number of bands alone (Qi et al. in Chapter 3, Goetz and Shippert).

…………Hyperspectral Data is fast emerging to provide practical solutions in characterizing, quantifying, modeling, and mapping natural vegetation and agricultural crops.

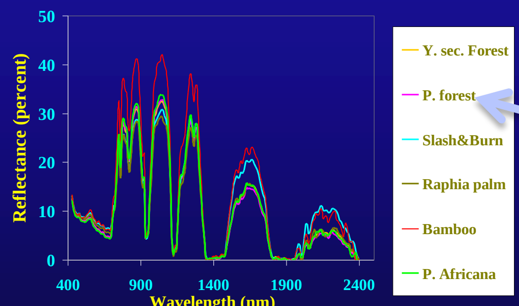

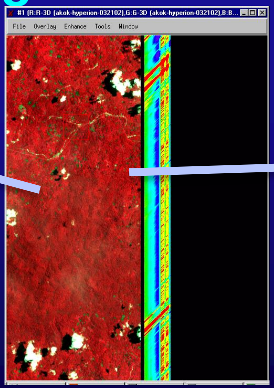

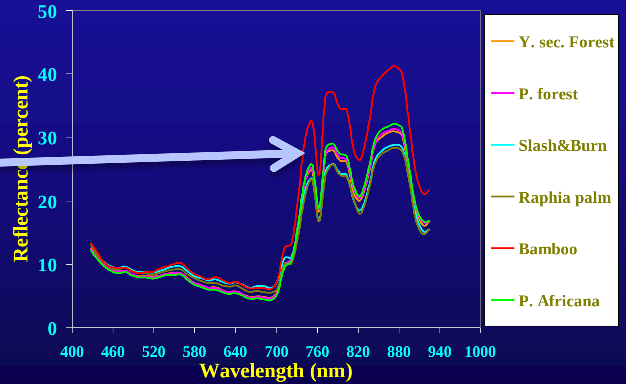

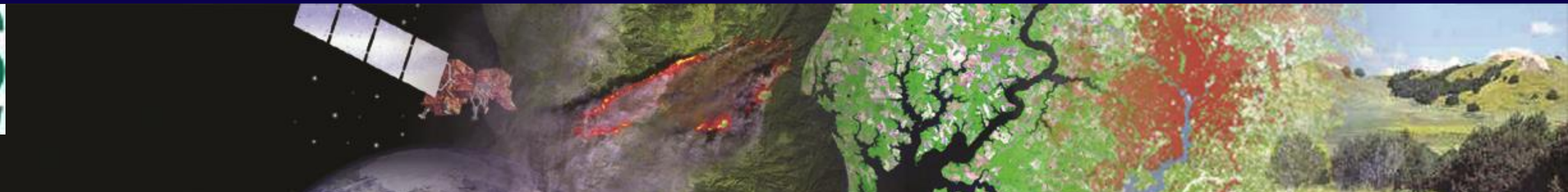

Hyperspectral Remote Sensing (Imaging Spectroscopy) of Vegetation

Truck-mounted Hyperspectral sensors

The advantage of airborne, ground-based, and truck-mounted sensors are that they enable relatively cloud free acquisitions that can be acquired on demand anywhere; over the years they have also allowed careful study of spectra in controlled environments to advance the genre.

(a) (b) (c)

Truck-mounted Hyperspectral Data Acquisition example

Hyperspectral Sensors and their Characteristics

Hyperspectral Remote Sensing (Imaging Spectroscopy) of Vegetation

Spaceborne Hyperspectral Imaging Sensors: Some Characteristics

Instrument (Satellite)	Altitude, km	Pixel Size, m	Number Bands	Spectral Range, nm	Spectral Resolution, nm	IFOV, μrad	Swath, km
HSI (SIMSA)	523	25	220	430-2400	20	47.8	7.7
FTHSI (MightySatII)	565	30	256	450-1050	10-50	50	13
Hyperion (EO-1)	705	30	220	400-2500	10	42.5	7.5
CHRIS (PROBA)	580	25	19	400-1050	1.25-11.0	43.1	17.5
COIS (NEMO)	605	30	210	400-2500	10	49.5	30
ARIES-1 (ARIES-1)	500	30	32 32 32	400–1100 2000-2500 1000-2000	22 16 31	60	15
UKON-B	400	20	256	400-800	4-8	50	15
Warfighter-1 (OrbView-4)	470	8	200 80	450-2500 3000-5000	11	20	5
EnMAP	675	30	92 108	420-1030 950-2450	5-10 10-20	30	30
HypSEO (MITA)	620	20	~210	400-2500	10	40	20
MSMI (SUNSAT)	660	15	~200	400-2350	10	22	15
PRISMA	695	30	250	400-2500	<10	40	30
ARTEMIS (TacSat-3)	425	4	400	400-2500	5	70	~10
HyspIRI	~700	60	>200	380-2500	10	80	145
SUPERSPEC (MYRIADE)	720	20	8	430-910	20	30	120
VENμS	720	5.3	12	415-910	16-40	8	27.5
Global Imager (ADEOS-2)	802	250-1000	36	380-1195	10-1000	310-1250	1600
WFIS (like MODIS)	705	1400	630	400-1000	1-5	2000	2400

Existing hyperspectral spaceborne missions:
1. Hyperion (USA's NASA),
2. PROBA (Europe's ESA;'s), and

There are some twenty spaceborne hyperspectral sensors

The advantages of spaceborne systems are their capability to acquire data: (a) continuously, (b) consistently, and (c) over the entire globe. A number of system design challenges of hyperspectral data are discussed in Chapter 3 by Qi et al. Challenges include cloud cover and large data volumes.

The 4 near future hyperspectral spaceborne missions:
1. PRISMA (Italy's ASI's),
2. EnMAP (Germany's DLR's), and
3. HISUI (Japanese JAXA);
4. HyspIRI (USA's NASA).

will all provide 30 m spatial resolution hyperspectral images with a 30 km swath width, which may enable a provision of high temporal resolution, multi-angular hyperspectral observations over the same targets for the hyperspectral BRDF characterization of surface.

The multi-angular hyperspectral observation capability may be one of next important steps in the field of hyperspectral remote sensing.

Comparison of Hyperspectral Data with Data from Other Advanced Sensors

Hyperspectral Sensors for Land and Atmospheric Studies

Table 1. Characteristics of spaceborne hyperspectral sensors (either in orbit or planned for launch) for Ocean, atmosphere, land, and water applications compared with ASD spectroradiometer[a] [modified and adopted from Thenkabail et al., 2011, 2014, and Qi et al., 2011].

Sensor, Satellite[c]	Spatial (meters)	Spectral (#)	Swath (km)	band range (μm)	band widths (μm)	Irradiance ($W\ m^{-2} sr^{-1}\ \mu m^{-1}$)	Data Points (# per hectares)	Launch (Date)
I. Coastal Hyperspectral Spaceborne Imagers								
3. HICO, ISS USA	90	128	42	353-1080	5.7	See data in Neckel and Labs (1984). Plot it	0.81	2009-present
II. Atmosphere\Ozone Hyperspectral Spaceborne Imagers								
3. OMI, Aura USA	13000x12000	740	145	270-500	0.45-1	See data in Neckel and Labs (1984). Plot it	1/16900	2004-present
3. SCIAMACHY, ENVISAT ESA	30000 x60000	~2000	960	212-2384	0.2-1.5	See data in Neckel and Labs (1984). Plot it	1/180000	2002-present
III. Land and Water Hyperspectral Spaceborne Imagers								
1. Hyperion, EO-1 USA	30	220 (196[b])	7.5	196 effective Calibrated bands VNIR (band 8 to 57 427.55 to 925.85 nm SWIR (band 79 to 224) 932.72 to 2395.53 nm	10 nm wide (approx.) for all 196 bands	See data in Neckel and Labs (1984). Plot it and obtain values for Hyperion bands	11.1	2000-present
2. CHRIS, PROBA ESA	25	19	17.5	200-1050	1.25-11	same as above	16	2001-present
3. HyspIRI VSWIR USA	60	210	145	210 bands in 380-2500 nm	10 nm wide (approx.) for all 210 bands	See data in Neckel and Labs (1984). Plot it	2.77	2020+
4. HyspIRI TIR USA	60	8	145	7 bands in 7500-12000 nm and 1 band in	7 bands in 7500-12000 nm	See data in Neckel and Labs (1984). Plot it	2.77	2020+

Comparison of Hyperspectral Data with Data from Other Advanced Sensors
Hyperspectral Sensors for Land and Atmospheric Studies

				3000-5000 nm (3980 nm center)				
5. EnMAP Germany	30	92 108	30	420-1030 950-2450	5-10 10-20	same as above	11.1	2015+
6. PRISMA Italy	30	250	30	400-2500	<10	same as above	11.1	2014+
I. Land and Water Hand-held spectroradiometer								
7. ASD spectroradiometer	1134 cm^2 @ 1.2 m Nadir view 18 degree Field of view	2100 bands 1 nm width between 400-2500 nm	N\A	2100 effective bands	1 nm wide (approx.) in 400-2500nm	See data in Neckel and Labs (1984). Plot it and obtain values for Hyperion bands	88183	last 30+ years

Note:

a = information for the table modified and adopted from Thenkabail et al., 2011, Thenkabail et al., 2014, and Qi et al., 2014.

b = Of the 242 bands, 196 are unique and calibrated. These are: (A) Band 8 (427.55 nm) to band 57 (925.85 nm) that are acquired by visible and near-infrared (VNIR) sensor; and (B) Band 79 (932.72 nm) to band 224 (2395.53 nm) that are acquired by short wave infrared (SWIR) sensor

c = HICO = **Hyperspectral** Imager for the Coastal Ocean onboard International Space Station. OMI = Ozone Monitoring Instrument onboard AURA of NASA; SCIAMACHY (Scanning Imaging Absorption Spectrometer for Atmospheric CHartographY) of ESA; Hyperion EO-1= hyperspectral sensor onboard EO-1= Earth observing 1; CHRIS PROBA = Compact High Resolution Imaging Spectrometer Project for On Board Autonomy satellite of ESA; HyspIRI VSWIR = Hyperspectral Infrared Imager Visible to Short Wavelength InfraRed of NASA; HyspIRI TIR = Hyperspectral Infrared Imager thermal infrared of NASA; Environmental Mapping and Analysis Program of Germany; PRISMA =PRecursore IperSpettrale della Missione Applicativa of Italy.

Hyperspectral Remote Sensing (Imaging Spectroscopy) of Vegetation

Earth and Planetary Hyperspectral Remote Sensing Instruments

		Hyperspectral Instrument	Spectral Range (nm)	# of Channels	Spectral Bandpass	Spatial Resolution	Operational Dates
Earth							
	Airborne	AVIRIS[1]	380 - 2500	224	10 nm	4 - 20 m	1989 - present
		ProSpecTIR-VS[2]	400 - 2450	256	2.3 - 20 nm	1 - 10 m	~2000 - present
		HyMap[3]	400 - 2500	128	15 nm	2 - 10 m	~1997 - present
		CASI[4]	400 - 1000	288	2 - 12 nm	0.5 - 10 m	~1990 - present
		SFSI[5]	1230 - 2380	230	10 nm	0.5 - 10 m	1990 - present
	Spaceborne	EO-1 Hyperion[6]	400 - 2500	220	10 nm	30 m	2001 - present
Mercury		MESSENGER MASCS[7]	220 - 1450	768	0.2 - 0.5 nm	1 - 650 km	2004 - present
Moon		Chandrayaan-1 Moon Mineralogy Mapper[8]	400 - 2900	260	10 nm	70 - 140 m	2008 - 2009
Mars		Mars Express OMEGA[9]	350 - 5100	352	7 - 20 nm	300 m - 4.8 km	2003 - present
		Mars Reconnaissance Orbiter CRISM[10]	362 - 3920	545	6.55 nm	15.7 m - 200 m	2005 - present
Jupiter		Galileo NIMS[11]	700 - 5200	1 - 408	12.5 & 25 nm	50 - 500 km	1989 - 2003
Saturn		Cassini VIMS[12]	300 - 5100	352	7 & 14 nm	10 - 20 km	1997 - present

1 - Airborne Visible Infrared Imaging Spectrometer (http://aviris.jpl.nasa.gov)
2 - Spectral Technology and Innovative Research Corporation Hyperspectral Imaging Spectrometer (http://www.spectir.com/assets/Images/Capabilities/ProspecTIR%20specs.pdf)
3 - HyVista Corporation Hyperspectral Mapper, developed by Integrated Spectronics (http://www.hyvista.com/main.html and http://www.intspec.com)
4 - Compact Airborne Spectrographic Imager (http://www.geomatics-group.co.uk/GeoCMS/Products/CASI.aspx)
5 - SWIR Full Spectrum Imager (http://www.borstad.com/sfsi.html)
6 - Hyperion (http://eo1.gsfc.nasa.gov/Technology/Hyperion.html)
7 - Mercury Atmospheric and Surface Composition Spectrometer (http://www.messenger-education.org/instruments/mascs.htm)
8 - M[3] (http://moonmineralogymapper.jpl.nasa.gov/INSTRUMENT/)
9 - Observatoire pour la Minéralogie, l'Eau, les Glaces et l'Activité (http://sci.esa.int/science-e/www/object/index.cfm?fobjectid=34826&fbodylongid=1598)
10 - Compact Reconnaissance Imaging Spectrometer for Mars (http://crism.jhuapl.edu/)
11 - Near-Infrared Mapping Spectrometer (http://www2.jpl.nasa.gov/galileo/instruments/nims.html)
12 - Visual and Infrared Mapping Spectrometer (http://wwwvims.lpl.arizona.edu/)

See chapter 27, Vaughan et al.

Hyperspectral Sensors
Relative
to Multispectral Sensors

Comparison of Hyperspectral Data with Data from Other Advanced Sensors

Hyperspectral, Hyperspatial, and Advanced Multi-spectral Data

Satellite/Sensor or pixels	spatial resolution (meters)	spectral bands (#)	data points per hectare
Earth Observing-1			
Hyperion	30	196 (400-2500 nm)	11.1
ALI	10 m (P), 30 m (M)	1, 9	100, 11.1
IKONOS 2 SpaceImaging	1 m (P), 4 m (M)	4	10000, 625
QUICKBIRD Digital Globe	0.61 m (P), 2.44 m (M)	4	16393, 4098
Terra: Earth Observing System (EOS)			
ASTER	15 m, 30 m, 90 m (VNIR,SWIR,TIR)	4,6,5	44.4,11.1,1.26
MODIS	250-1000 m	36	0.16, 0.01
Landsat-7 ETM+	15 m (P), 30 m (M)	7	44.4,11.1
Landsat-4, 5 TM	30 m (M)	7	11.1
SPOT-1,2,3, 4,5 HRV	2.5 m. 5m, 10 m (P/M), 20 m (M)	4	1600,400,100,25
IRS-1C LISS	5 m (P), 23.5 m (M)	3	400, 18.1
IRS-1D LISS	5 m (P), 23.5 m (M)	3	400, 18.1

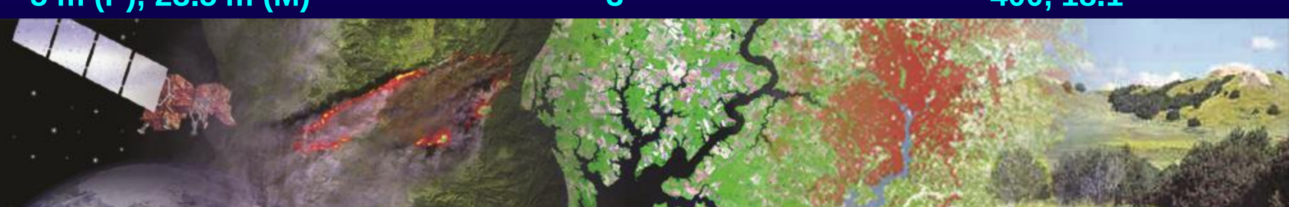

Comparison of Hyperspectral Data with Data from Other Advanced Sensors

Hyperspectral, Hyperspatial, and Advanced Multi-spectral Data

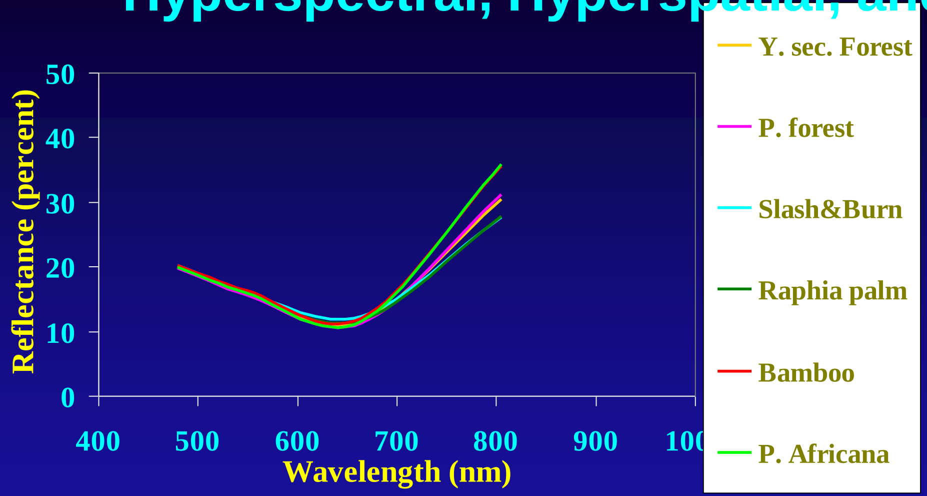

IKONOS: Feb. 5, 2002 (hyper-spatial)

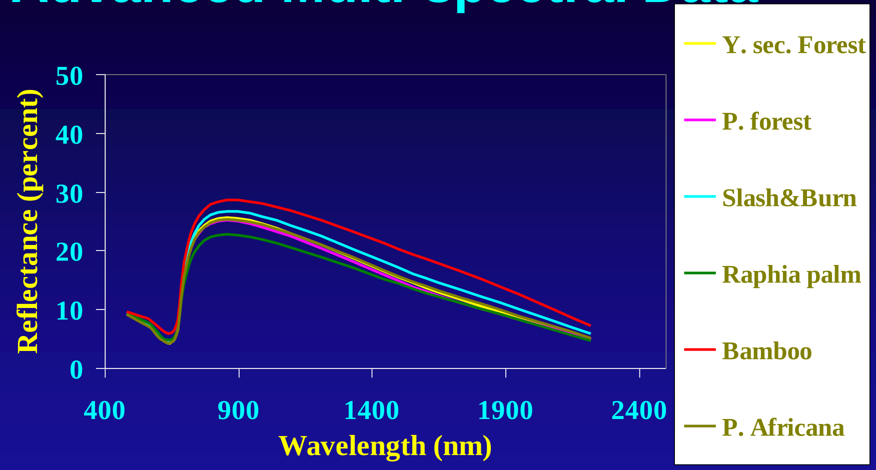

ETM+: March 18, 2001 (multi-spectral)

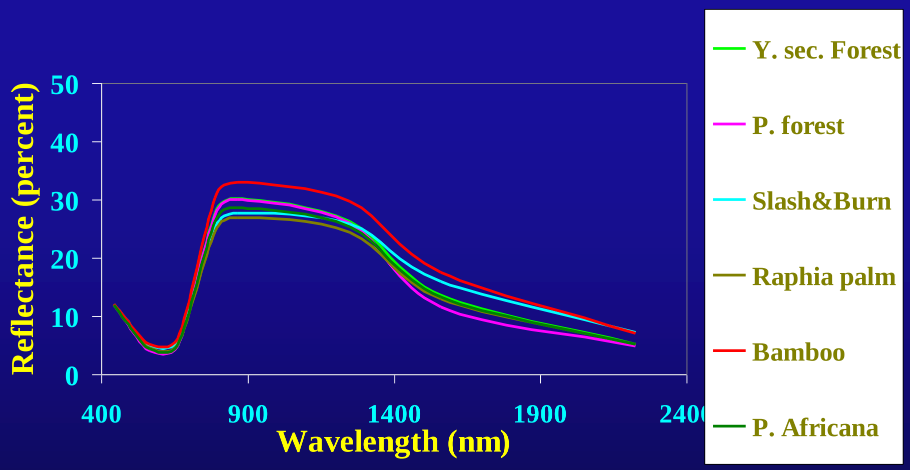

ALI: Feb. 5, 2002 (multi-spectral)

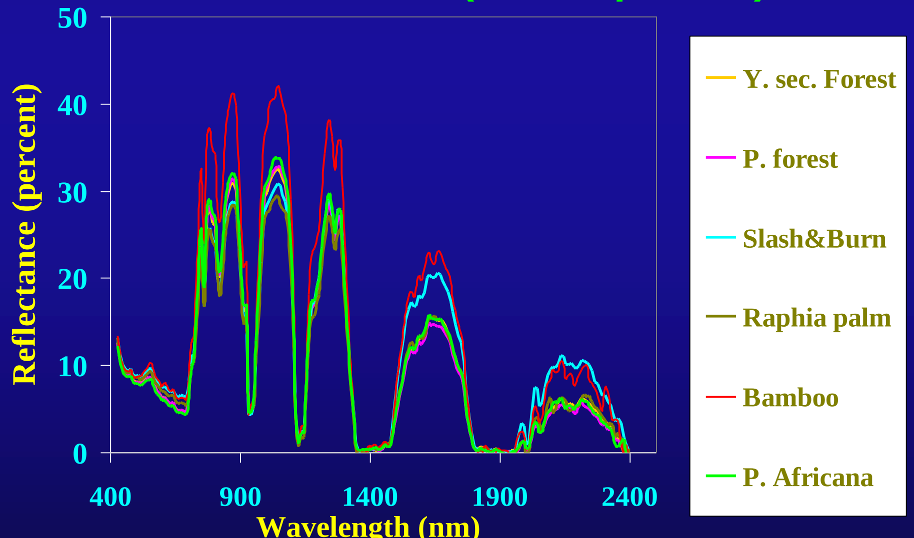

Hyperion: March 21, 2002 (hyper-spectral)

Hyperion

the First Spaceborne Hyperspectral Sensor

Hyperspectral Remote Sensing (Imaging Spectroscopy) of Vegetation
~64,000 Hyperspectral Hyperion Images of the World (2001-2013)

185 km by 7.5 km; 242 bands, 10 nm wide in 400-2500 nm; 30 m spatial resolution

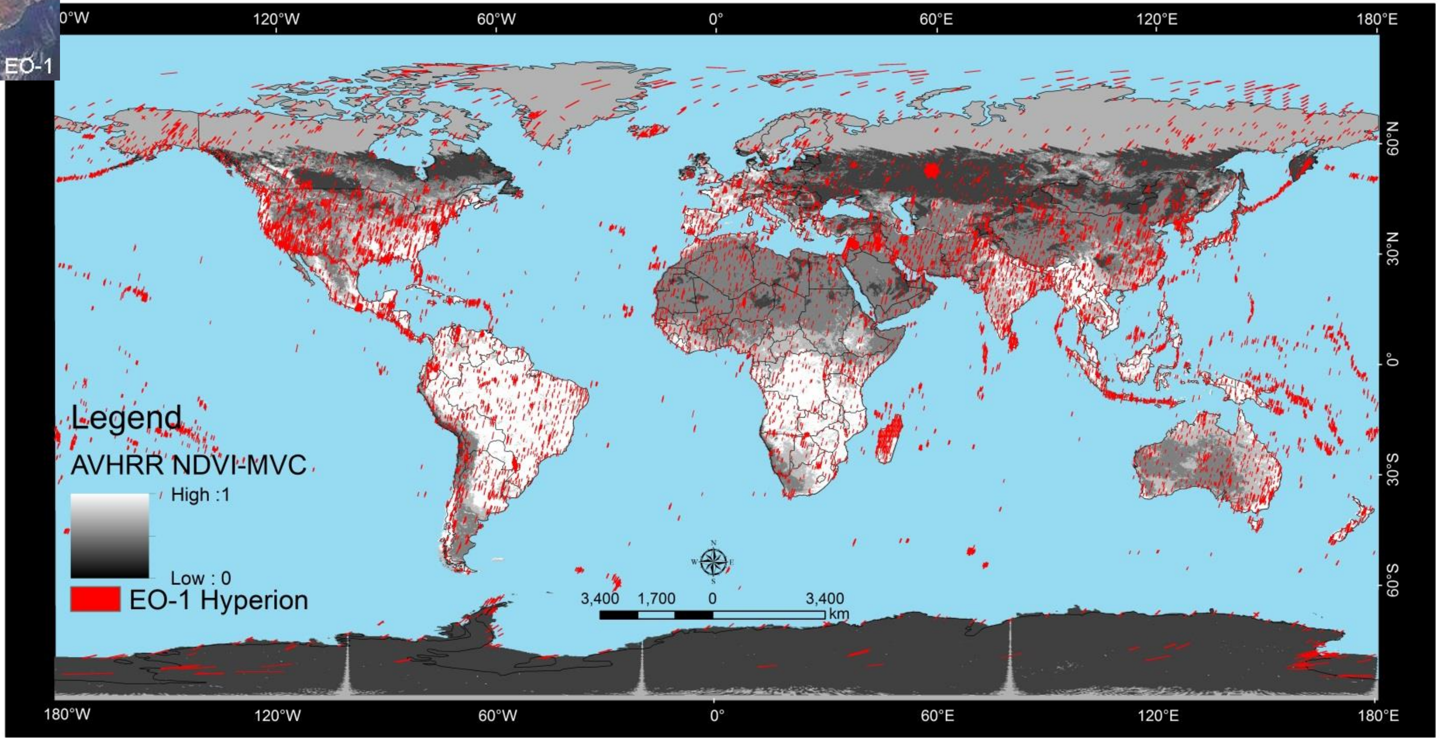

http://earthexplorer.usgs.gov/; http://eo1.usgs.gov/

USGS
science for a changing world

U.S. Geological Survey
U.S. Department of Interior

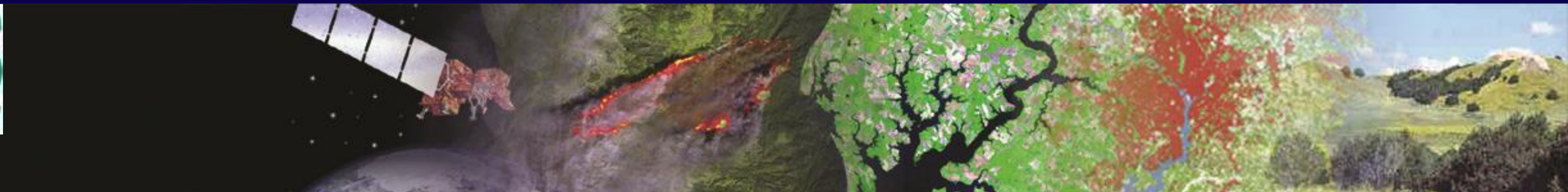

Hyperspectral Remote Sensing of Vegetation
Mega file Data Cube (MFDC) of Hyperion Sensor onboard EO-1

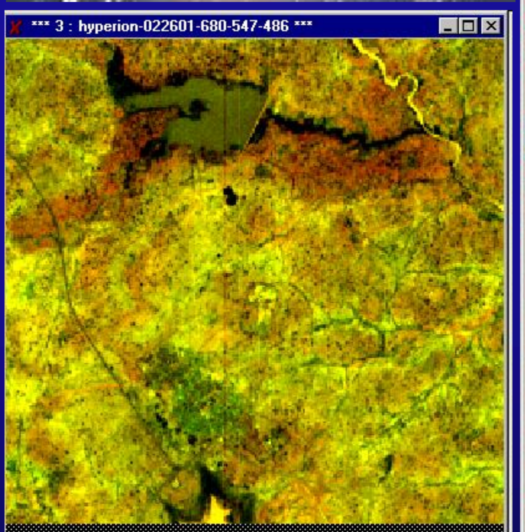

FCC (RGB): 680, 547, 486

e.g., MFDC of African Rainforests in Cameroon

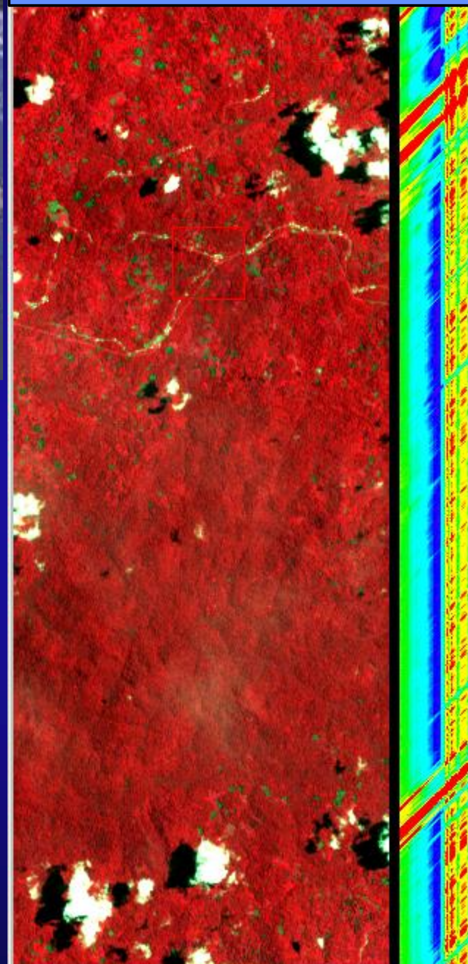

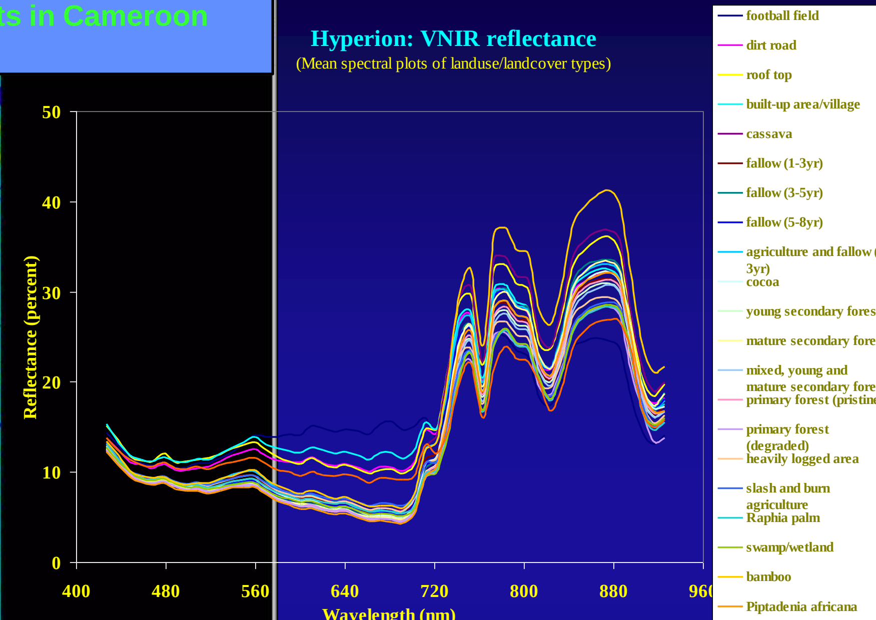

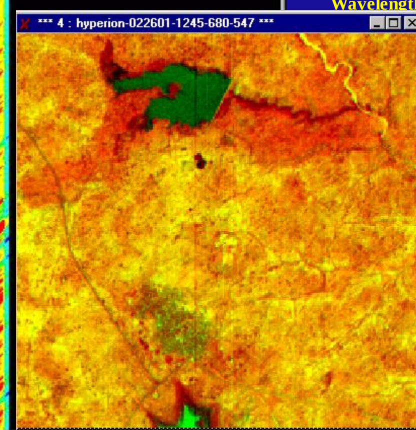

Hyperion has 220 bands in 400-2500 nm

Note: Currently NASA is planning a next Spaceborne Hyperspectral mission called: HyspIRI

FCC (RGB): 1245, 680, 547

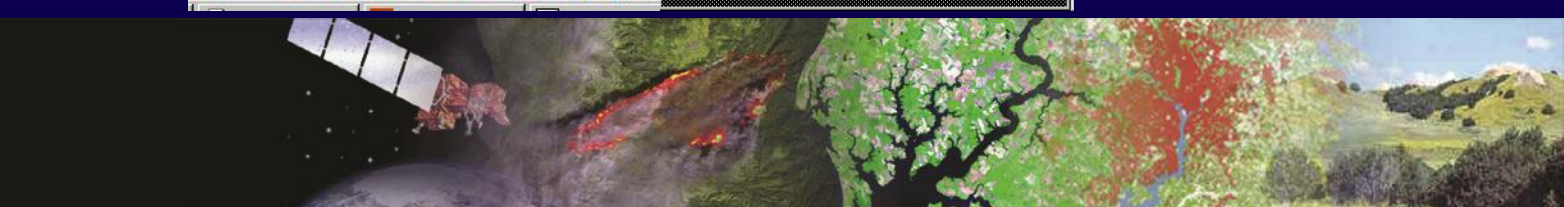

Hyperion Narrow-Band Data from EO-1 Vs. ETM+ Broad-band Data

Hyperspectral Data Provides Numerous Ways of Looking at Data

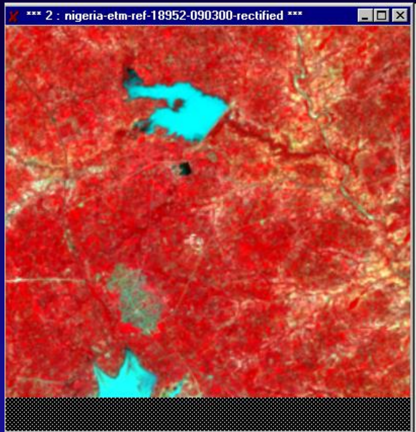

ETM+:4,3,2

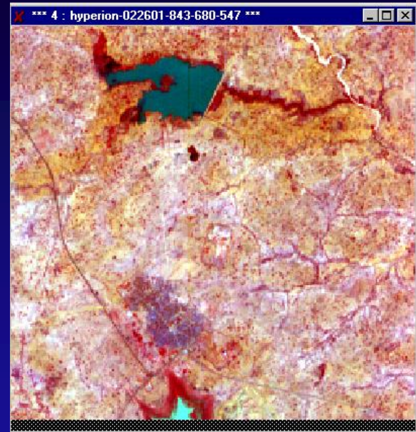

Hyperion:843, 680, 547

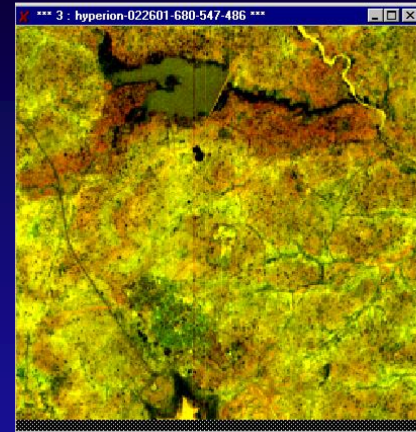

Hyperion: 680, 547, 486

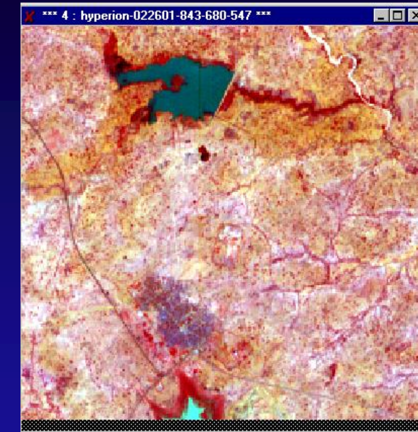

Hyperion:905, 680, 547

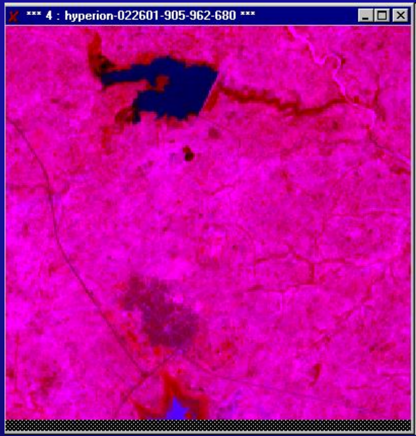

Hyperion:905, 962, 680

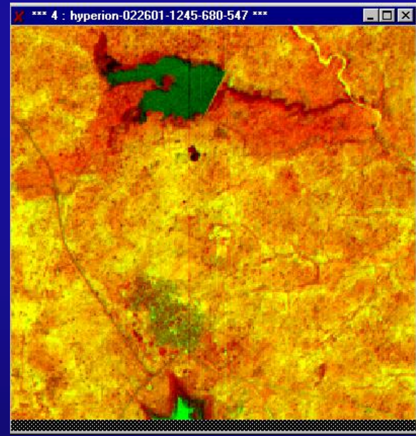

Hyperion:1245, 680, 547

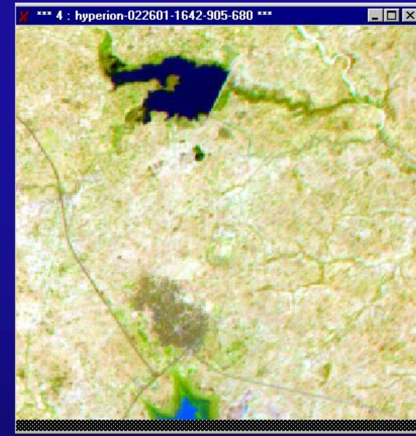

Hyperion:1642, 905, 680

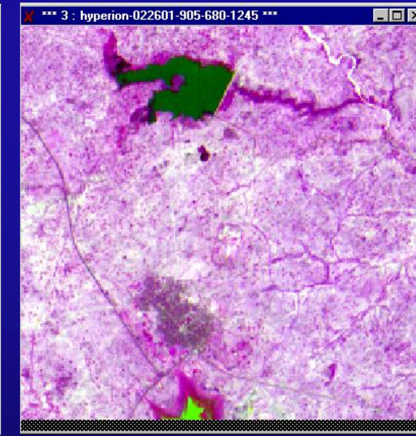

Hyperion:904,680,1245

Hyperspectral Data in Study of Complex Vegetation

e.g., Hyperion EO-1 Data for Biophysical Characteristics of African rainforests

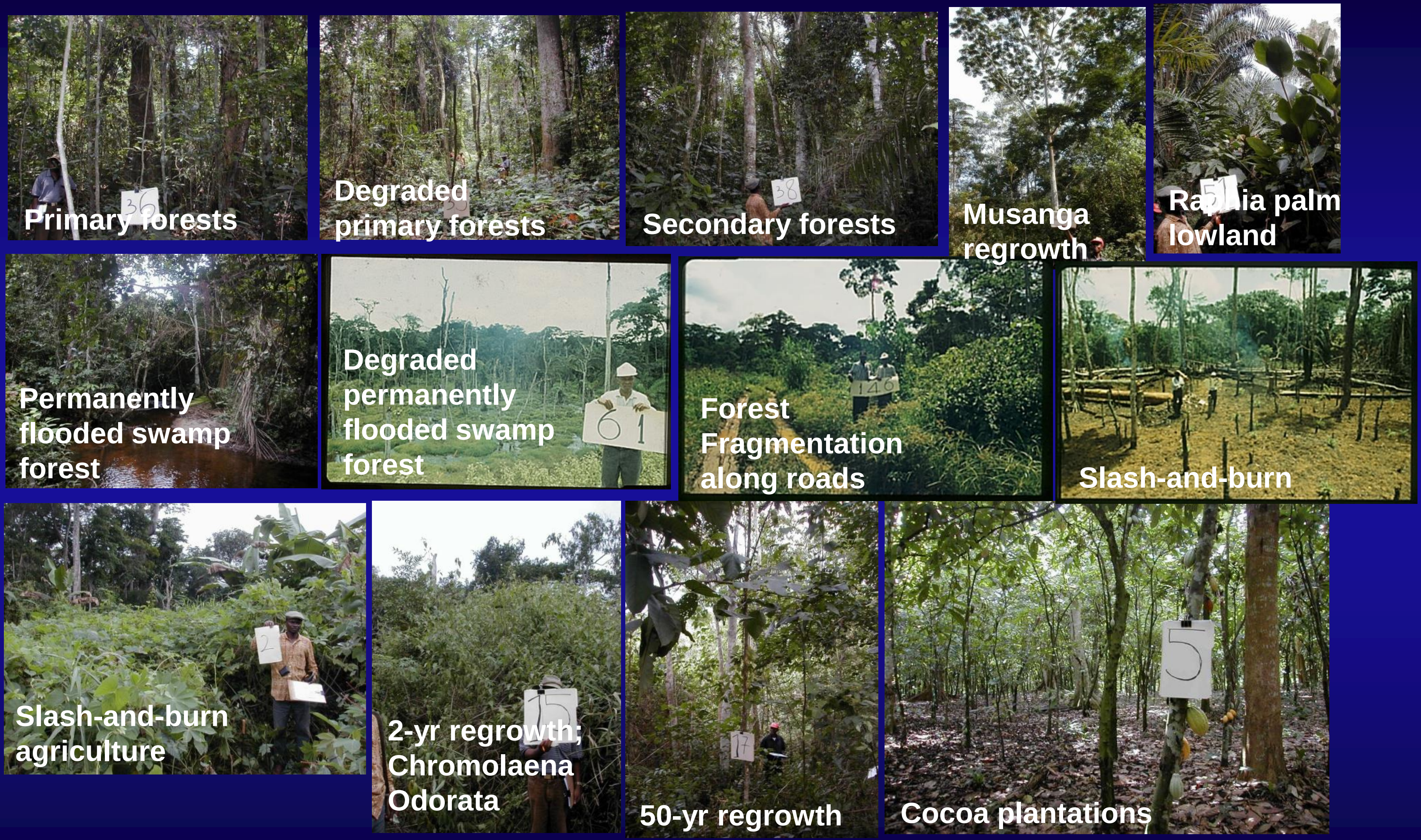

USGS
science for a changing world
U.S. Geological Survey
U.S. Department of Interior

Hyperion Data from EO-1 (e.g., in Rainforests of Cameroon)

Hyperspectral Data Cube Providing Near-continuous data of 100's of Wavebands

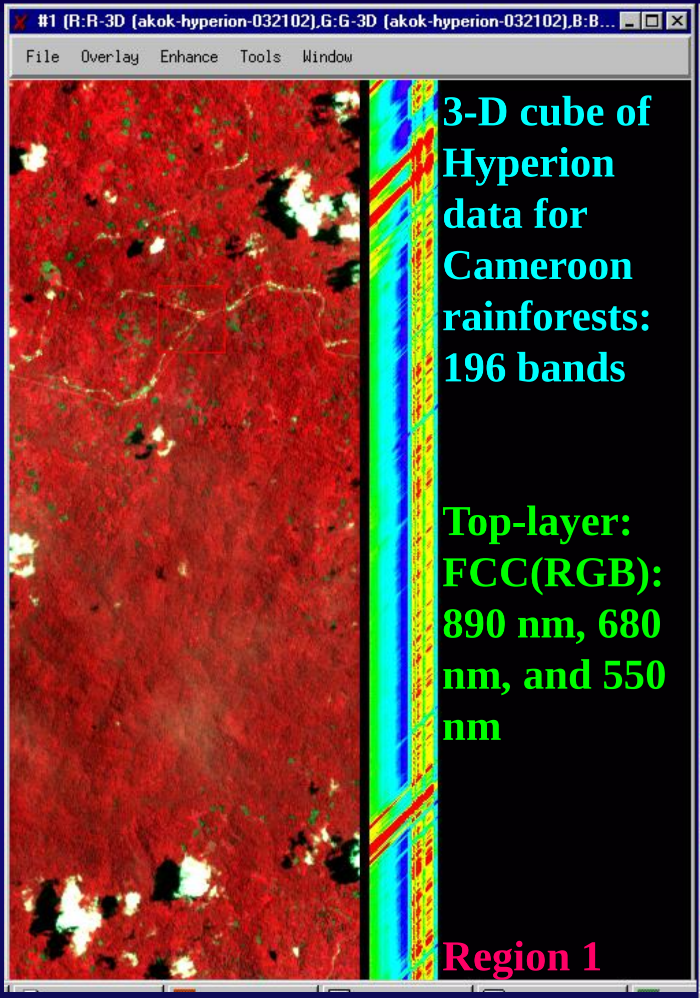

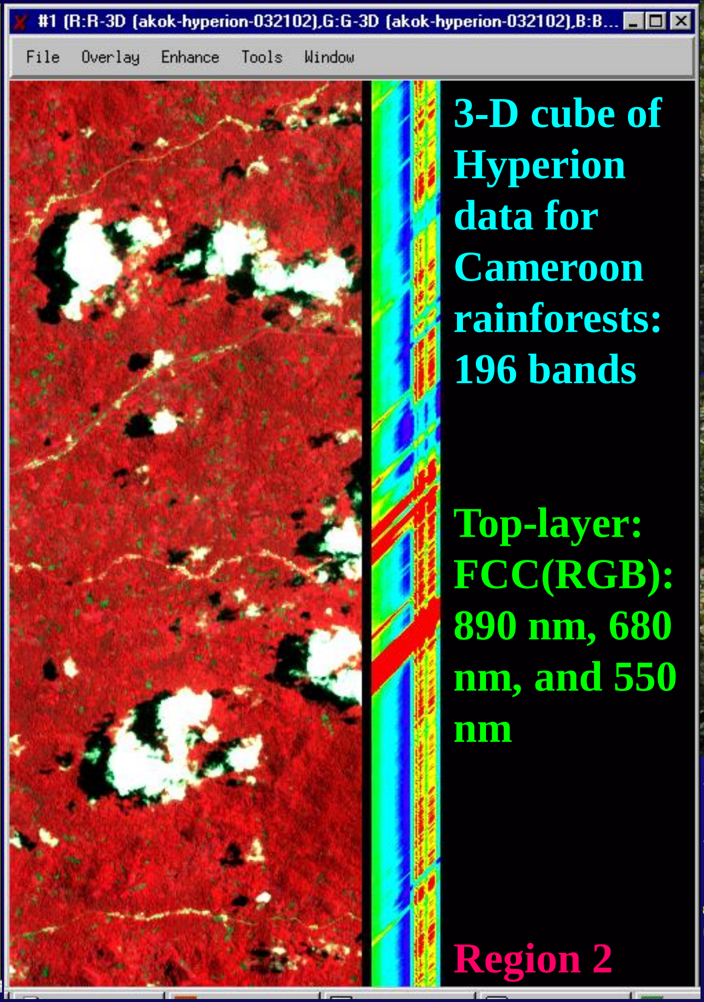

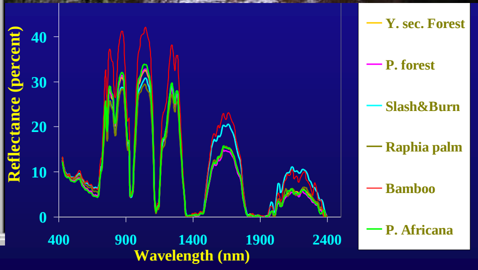

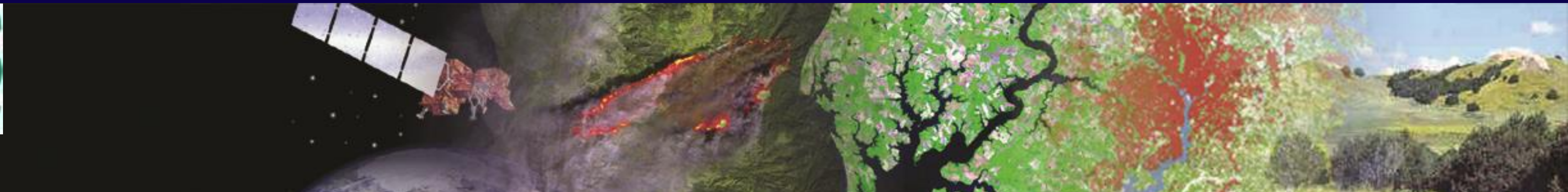

USGS
science for a changing world
U.S. Geological Survey
U.S. Department of Interior

Hyperion Data from EO-1 (e.g., in Rainforests of Cameroon)

Hyperspectral Data Cube Providing Near-continuous data of 100's of Wavebands

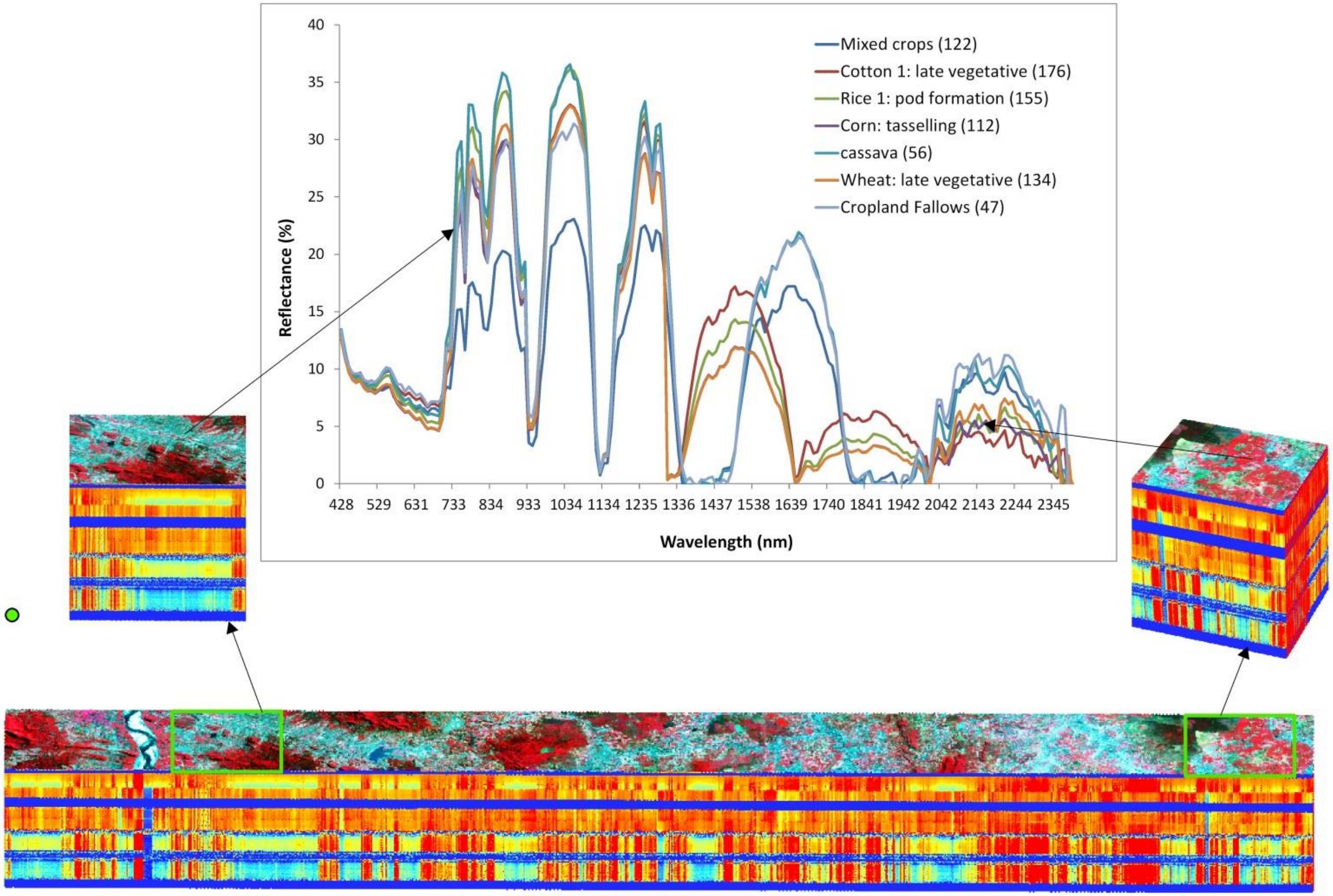

Hyperspectral Data Gathered for the Following Rainforest Vegetation

using Hyperion EO-1 Data

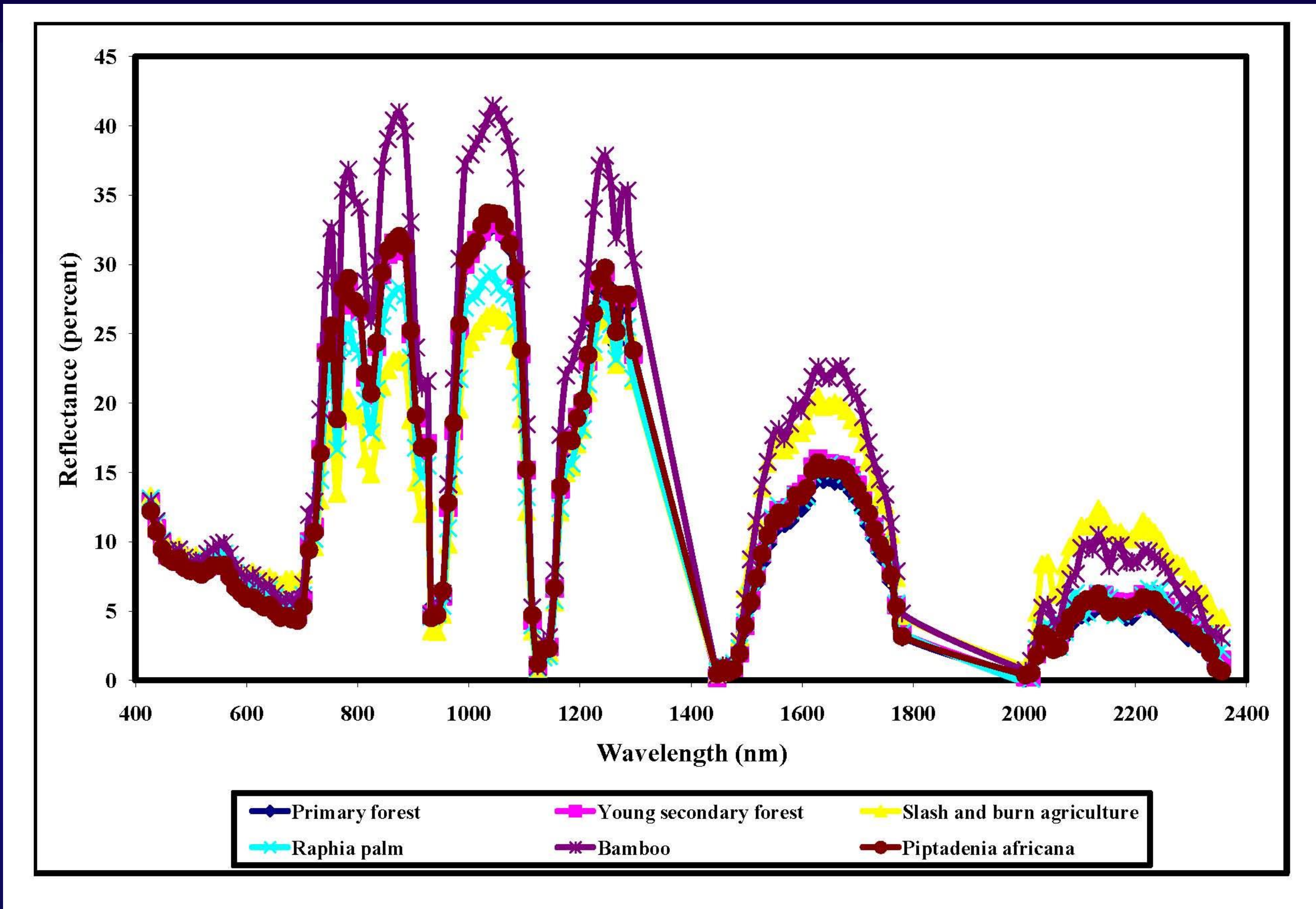

Hyperspectral Data Gathered for the Following Rainforest Vegetation

using Hyperion EO-1 Data

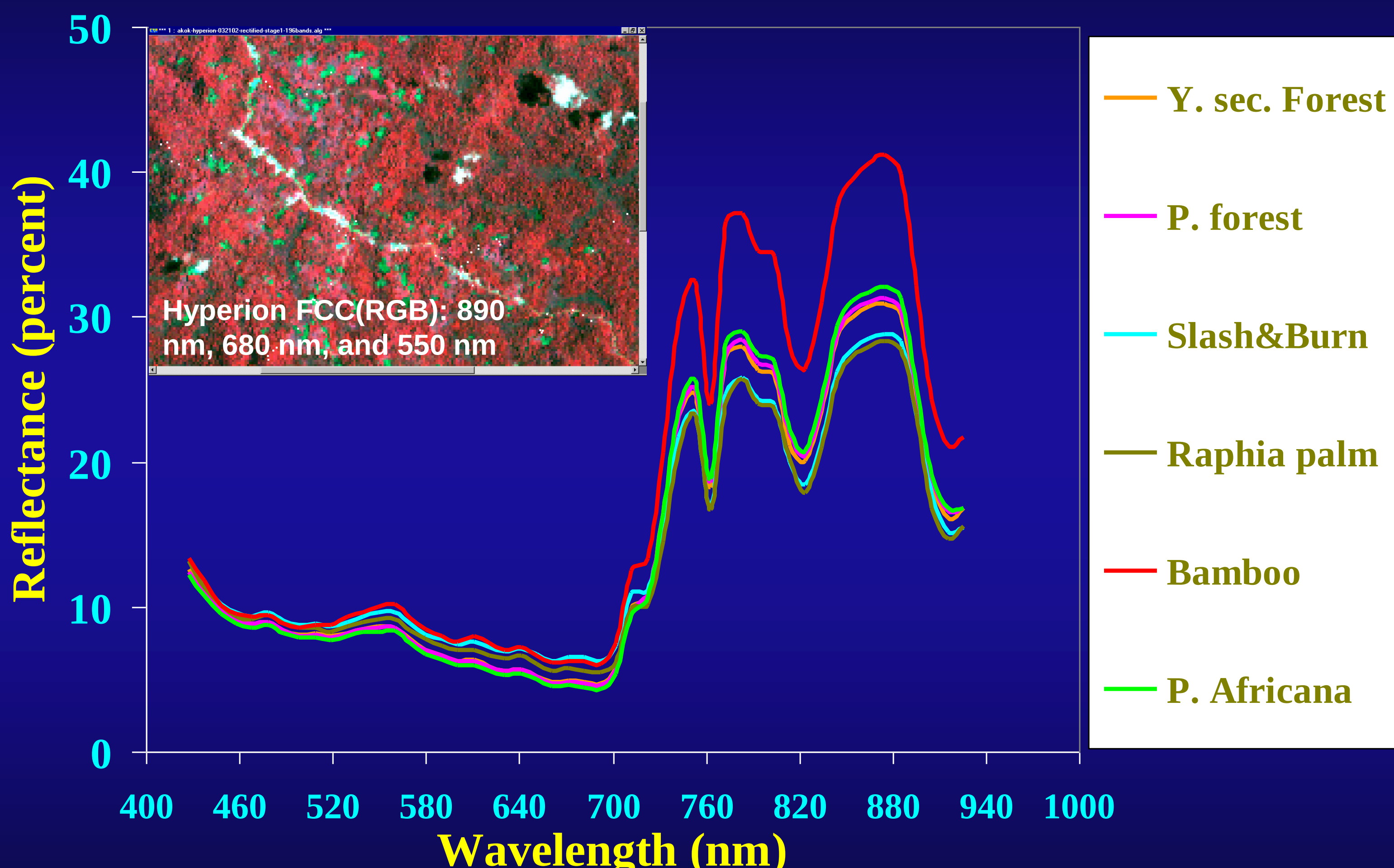

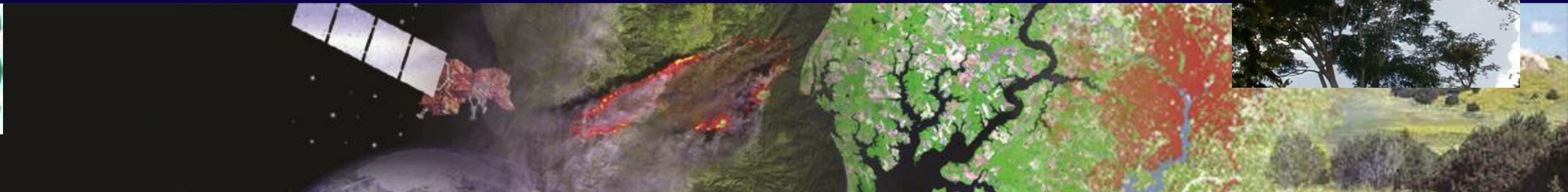

Hyperspectral Data of Two Dominant Weeds

Chromolaena Odorata in African Rainforests vs. *Imperata Cylindrica* in African Savannas

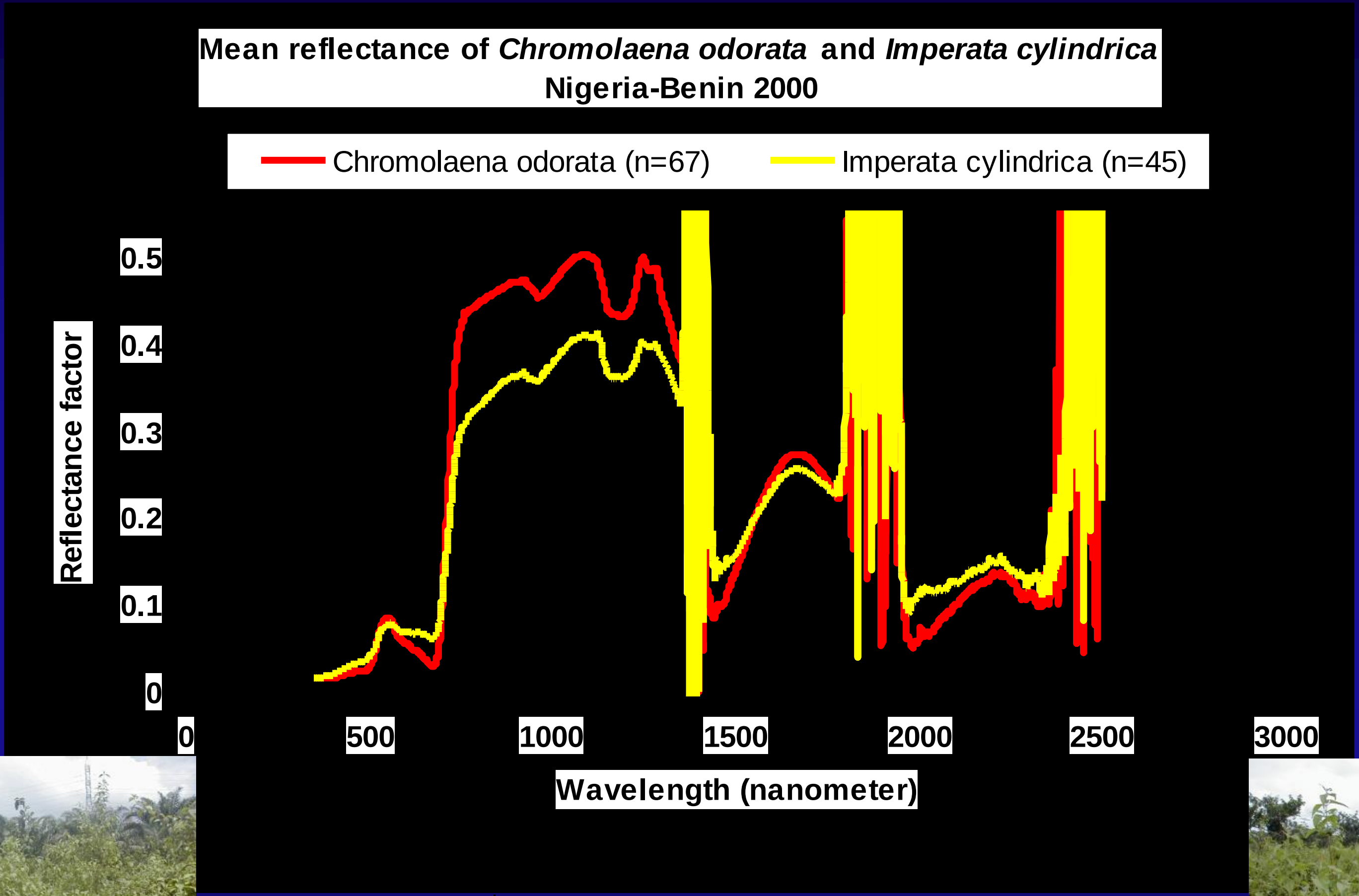

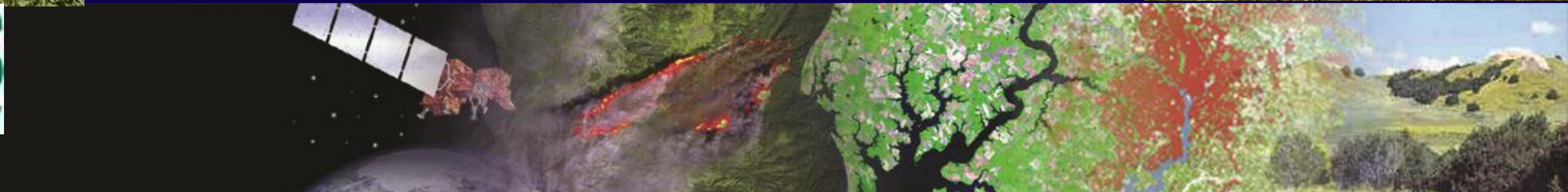

Hyperspectral Data of Vegetation Species and Agricultural Crops

Illustrations for Numerous Vegetation Species from African Savannas

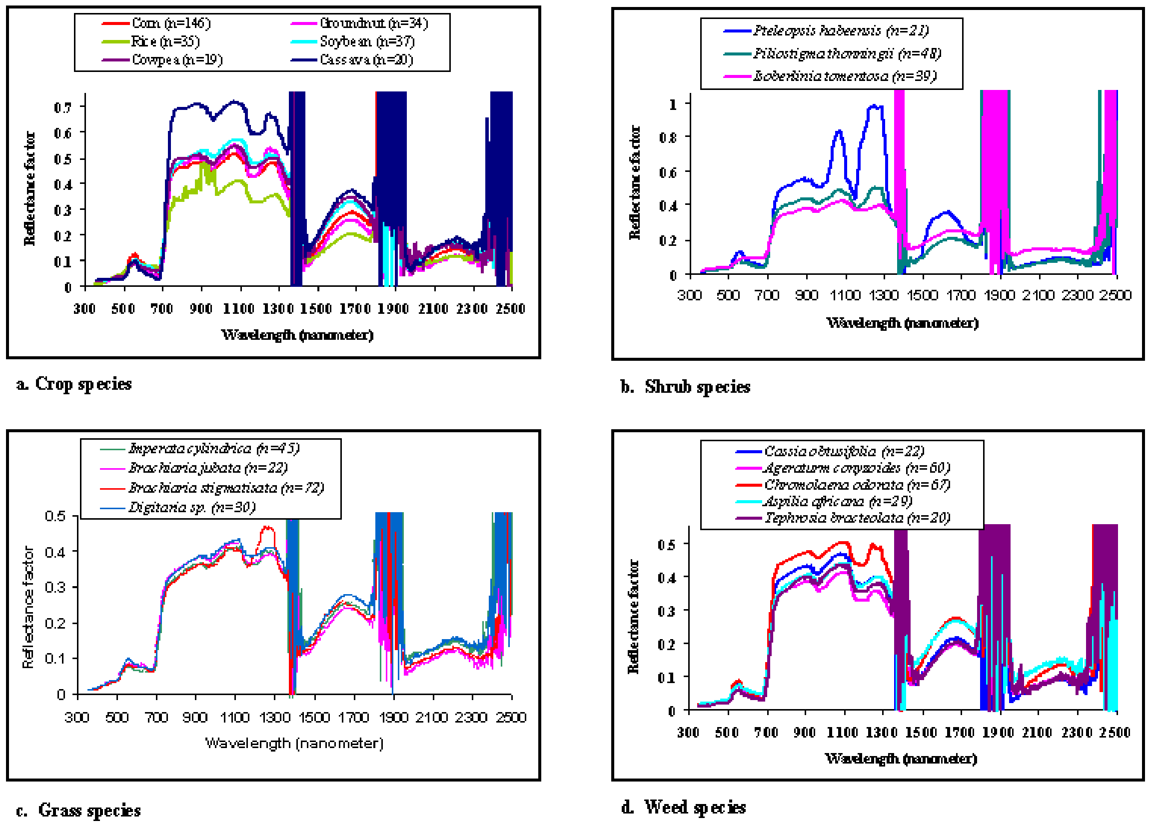

science for a changing world

U.S. Geological Survey
U.S. Department of Interior

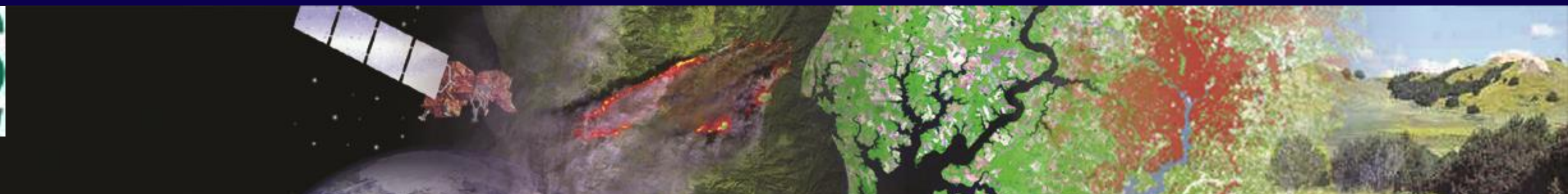

Hyperspectral (imaging spectroscopy) Data on Agricultural Crops

Biophysical and Biochemical Properties

	Property (BB-PAC)	Example crops	Agro-technical management parameter
Biophysical			
	Biomass [kg m^{-1}]	wheat, rice, corn	fertilization
	Leaf Area Index/ Crop cover [No units / %]	wheat, soybean, corn, cotton	fertilization
	Crop height [m]	cotton, wheat	irrigation, application of growth regulators
	Canopy volume [m^3]	orchards, wheat	irrigation, fertilization
	Yield [kg m^{-1}]	wheat, corn, cotton	-
	Stomata conductance [mmol sec^{-1}]	vineyards	irrigation
	Leaf/Stem water potential [MPa]	cotton, orchards, vineyards	irrigation
	Flowering intensity [Relative units]	orchards	growth regulators, mechanical thinning
Biochemical			
	Nitrogen content [%N]	corn, wheat, potatoes	fertilization
	Chlorophyll content [μg cm^{-2}]	corn, wheat, cotton	fertilization
	Salinity [mg l^{-1}]	cotton	water quality management, not used in practice
	Leaf water content [%]	wheat, potato	irrigation
	Leaf macro-elements like phosphorus (P) and potassium (K) [mg Kg^{-1}]	olives	fertilization, not used in practice

Note: see chapter 13, Alchanatis and Cohen

Hyperspectral Data in Study of Complex Vegetation

e.g., Hyperion EO-1 Data for Biochemical Characteristics of African rainforests

Biochemistry (e.g., plant pigments, water, and structural carbohydrates):
Leaf reflectance in the visible spectrum is dominated by absorption features created by plant pigments, such as:

- **chlorophyll a (chl-a): absorps in 410-430 nm and 600-690 nm;**
- **chlorophyll b (chl-b): absorps in 450-470 nm;**
- **carotenoids (e.g., β-carotene and lutein): peak absorption in wavebands <500 nm; and**
- **anthocyanins.**
- **Lignin, cellulose, protein, Nitrogen: relatively low reflectance and strong absorption in SWIR bands by water that masks other absorption features**

……………However, dry leaves do not have strong water absorption and reveal overlapping absorptions by carbon compounds, such as lignin and cellulose, and other plant biochemicals, including protein nitrogen,starch, and sugars.

Hyperspectral Data on Tropical Forests

Factors Influencing Spectral Variation over Tropical Forests

2. Structure or biophysical (e.g., leaf thickness and air spaces): of leaves, and the scaling of these spectral properties due to volumetric scattering of photons in the canopy;

3. Nonphotosynthetic tissues (e.g., bark, flowers, and seeds); and

4. Other photosynthetic canopy organisms (e.g., vines, epiphytes, and epiphylls) can mix in the photon signal and vary depending on a complex interplay of species, structure, phenology, and site differences,

……………………………..currently, none of which are well understood.

Note: see chapter 18, Clark et al.

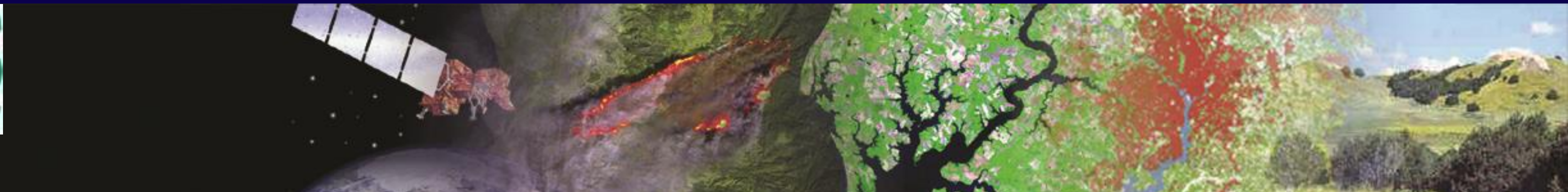

Study of Biophysical Characteristics

1. Biomass: wet and dry; (kg\m^2);
2. Leaf area index (LAI), Green LAI; (m^2\m^2)
3. Plant height; (mm)
4. Vegetation fraction; (%)
5. Fraction of PAR absorbed by photosynthetically active vegetation (fAPAR); (MJ\m^2)
6. Total crop chlorophyll content; (g\m^2) and
7. Gross primary production. (g C\m^2\yr)

Note: see chapter 1, Thenkabail et al.; chapter 6, Gitelson et al.

Hughes Phenomenon

(or Curse of High Dimensionality of Data) and

overcoming data redundancy through Data Mining

Hyperspectral Data (Imaging Spectroscopy data)

Not a Panacea!

For example, hyperspectral systems collect large volumes of data in a short time. Issues include:

- data storage volume;
- data storage rate;
- downlink or transmission bandwidth;
- computing bottle neck in data analysis; and
- new algorithms for data utilization (e.g., atmospheric correction more complicated).

Data Mining Methods and Approaches in Vegetation Studies

Lambda by Lambda R-square Contour Plots: Identifying Least Redundant Bands

Hyperion rainforest vegetation: Least redundant bands

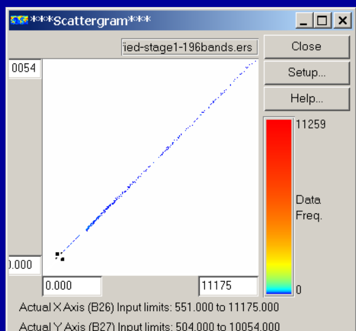

Highly redundant: bands centered at 680 nm and 690 nm

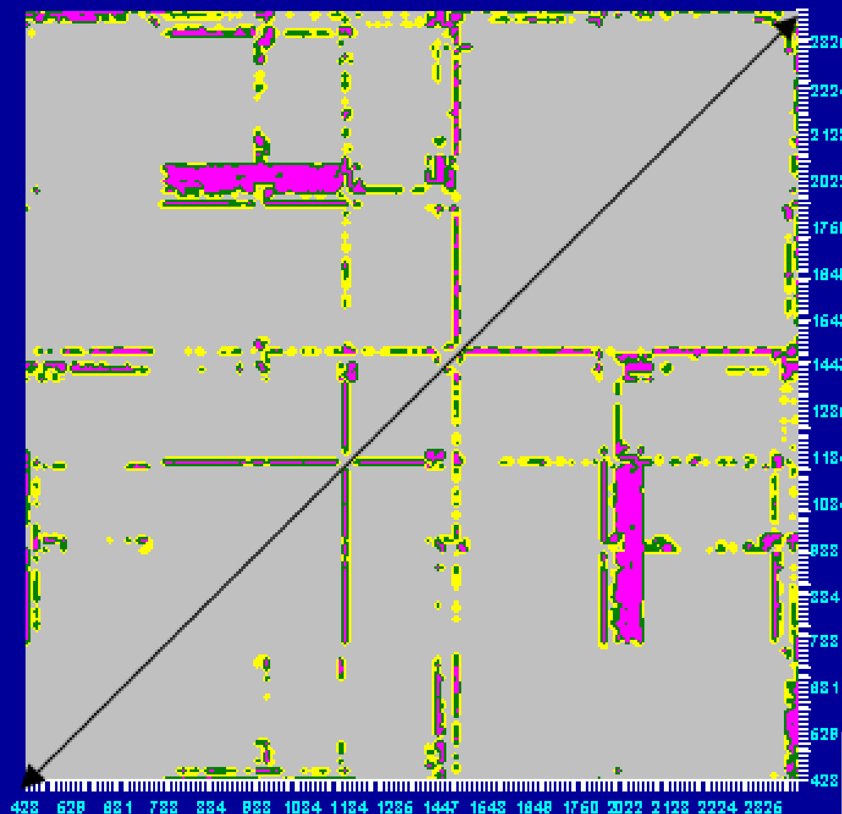

R^2 values between wavebands (lesser the R^2 value lesser the redundancy)

0.009-0.01
0.008-0.009
0.007-0.008
0.006-0.007
0.005-0.006
0.004-0.005
0.003-0.004
0.002-0.003
0.001-0.002
0-0.001

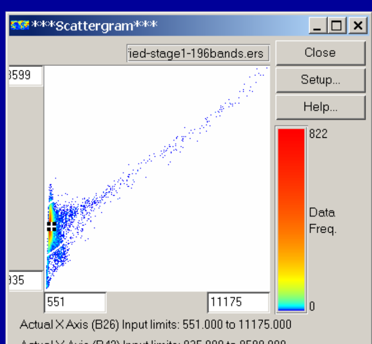

Significantly different: bands centered at 680 nm and 890 nm

Lambda vs. Lambda Correlation plot for African rainforest Vegetation

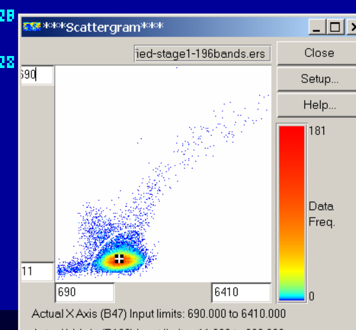

Distinctly different: bands centered at 920 nm and 2050 nm

Data Mining Methods and Approaches in Vegetation Studies
Feature selection\extraction and Information Extraction

Feature selection is necessary in any data mining effort. Feature selection reduces the dimensionality of data by selecting only a subset of measured features (predictor variables). Feature selection methods recommendation based on:

(a)Information Content (e.g., Selection based on Theoretical Knowledge, Band Variance, Information Entropy),
(b)Projection-Based methods (e.g., Principal Component Analysis or PCA, Independent Component Analysis or ICA),
(c)Divergence Measures (e.g., Distance-based measures),
(d)Similarity Measures (e.g., Correlation coefficient, Spectral Derivative Analysis), and
(e)Other Methods (e.g., wavelet Decomposition Method).

Note: see chapter 4

Data Mining Methods and Approaches in Vegetation Studies

Principal Component Analysis: Identifying Most useful Bands

Wavebands with Highest Factor Loadings

Principal component analysis for crop species											
Crops	Band centers (nm) with first 20 highest factor loadings					% variability explained					
	PCA1	PCA2	PCA3	PCA4	PCA5	PCA 1	PCA 2	PCA 3	PCA 4	PCA 5	5 cumulative PCAs
Cassava	1725;1715;1705;1575; 1695;1605;1735;1585; 1555;1595;1565;1685; 1625;1655;1545;1615; 1665;1635;1675;1645	635;625;695;615;645; 605;595;655;585;705; 575;685;665;515;525; 565;535;555;545;715	2002;2342;2322;2282; 2312;2312;2272;1455; 1380;2012;2332;2022; 2222;2292;2262;1465; 1982;2252;1445;2132	2002;1245;1255;1235; 1275;1265;1285;1992; 2042;2032;2262;2062; 2292;1225;2322;1982; 2072;2232;2012;2282	2332;2342;2322;1982; 2312;2312;1445;2292; 2022;1992;2262;865; 875;855;775;885;785; 845;795;805	63.9	18.9	5.6	2.6	1.9	92.7
Dominating bands	EMIR	Green; Red	MIR; MMIR; FMI	R;EMIR;MMIR;FN	; EMIR; MMIR; FMIR						
Corn	1675;1665; 1645;1655; 1685;1695;1635;1705; 1625;1715;1725;1615; 1735;1605;1745;1595; 1755;1585;1765;1575	2032;2052;2042;2082; 2072;2062;2092;2102; 1982;2112;1465;2122; 2022;1455;2132;1992; 1475;2142;1485;2252	2002;2012;2342;1992; 2022;1982;2332;2322; 2032;2072;1255;1245; 2042;1275;1285;1265; 2062;1235;2052;1380	355;365;375;385;395; 405;415;425;435;1445; 1245;445;1255;1235; 1275;1265;1285;1225; 1135;1455	2342;2002;2012;1992; 1982;2332;2022;355; 375;2052;365;2322; 385;395;405;2042; 2062; 2312;2312;415	67.0	16.1	7.8	2.2	1.9	94.9
Dominating bands	EMIR	MIR; MMIR; FMI	FNIR; EMIR; MMIR; FMIR	UV; Blue; FNIR; EMIR	UV; Blue; EMIR; MMIR; FMIR						

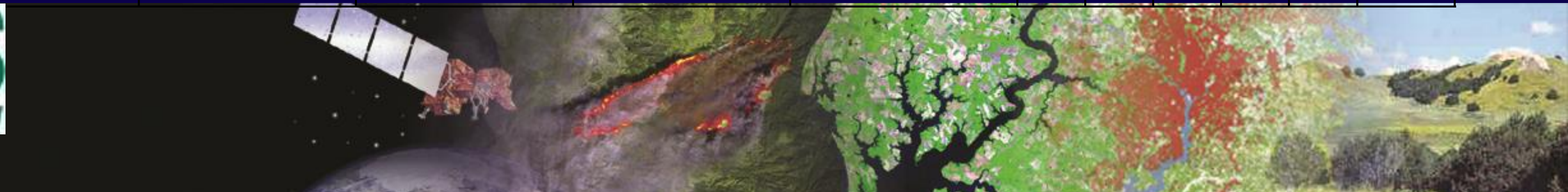

Hyperspectral Data
Characteristics in Study of Agriculture and Vegetation

science for a changing world

U.S. Geological Survey
U.S. Department of Interior

Hyperspectral Remote Sensing (Imaging Spectroscopy) of Vegetation
~64,000 Hyperspectral Hyperion Images of the World (2001-2013)

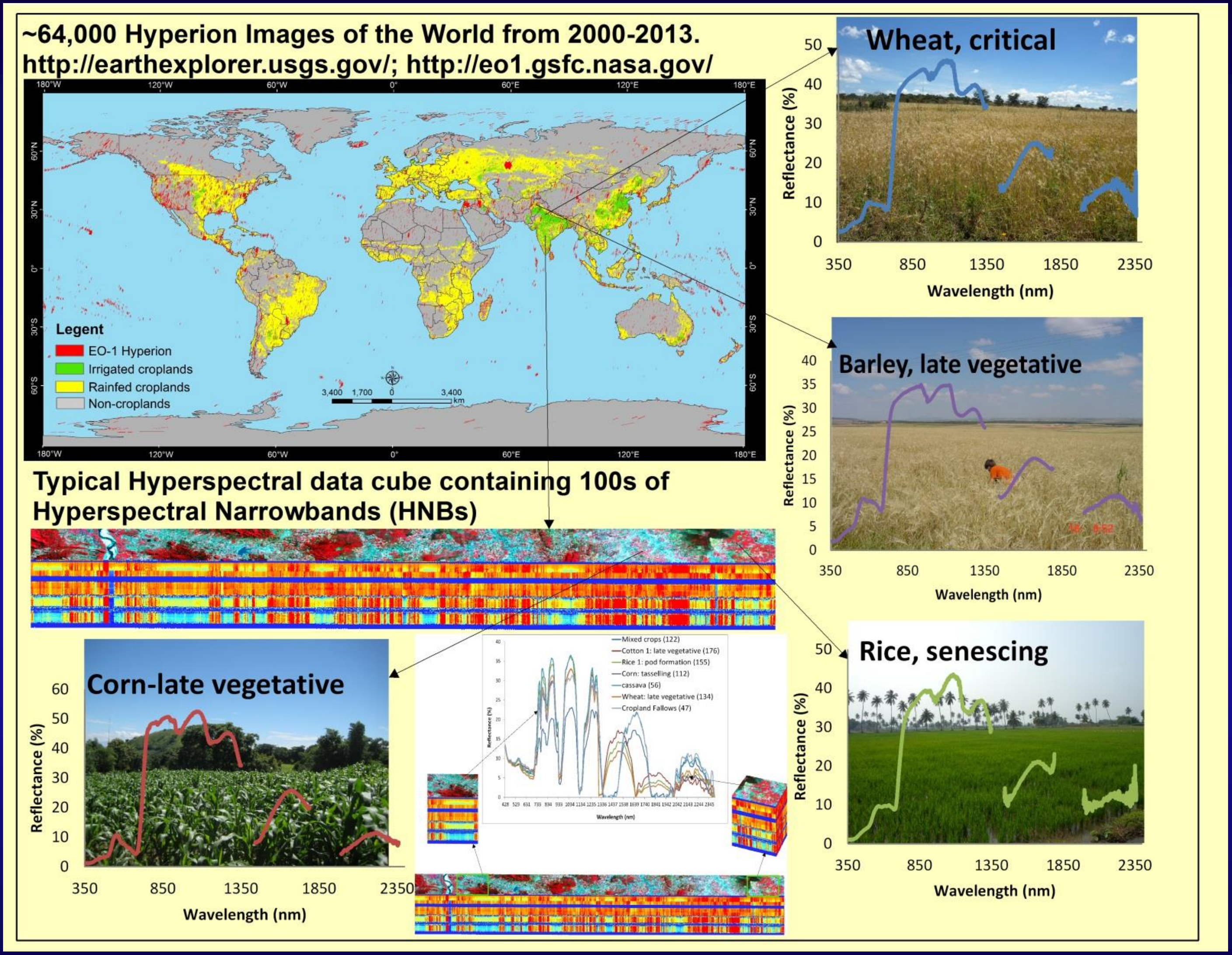

U.S. Geological Survey
U.S. Department of Interior

Hyperspectral Remote Sensing (Imaging Spectroscopy) of Vegetation
~64,000 Hyperspectral Hyperion Images of the World (2001-2013)

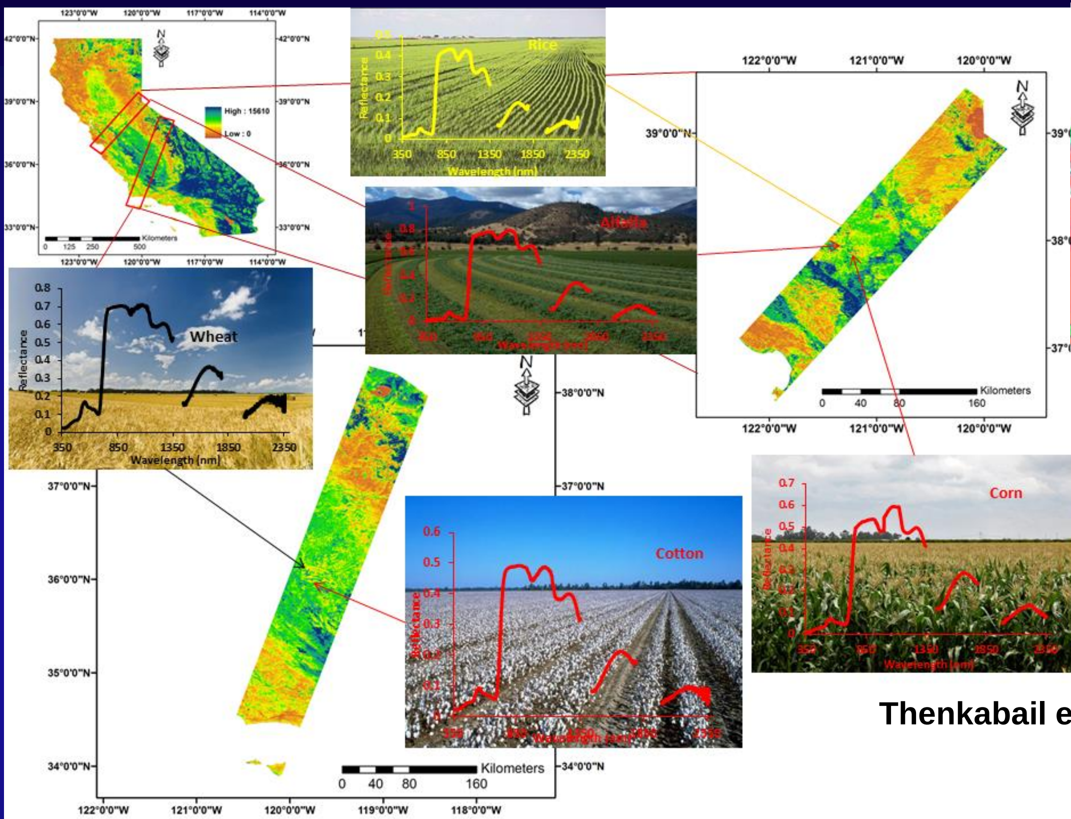

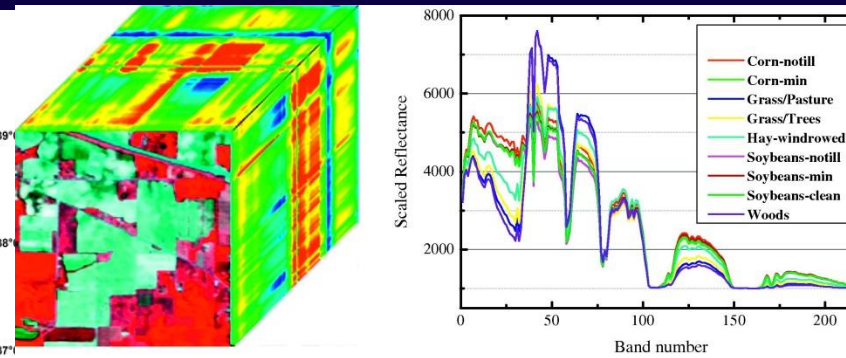

(a) Guo, X. et al., 2013 (b)

Thenkabail et al., 2015

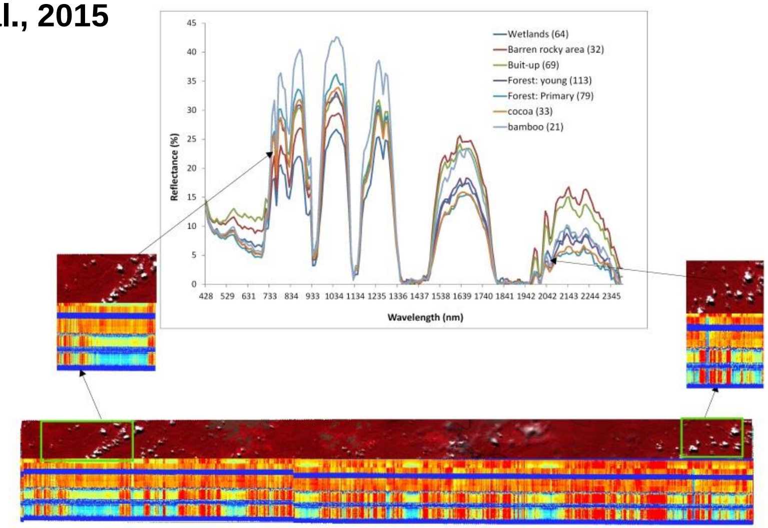

USGS
science for a changing world

U.S. Geological Survey
U.S. Department of Interior

Hyperspectral Study of Agricultural Crops

Hyperspectral Data from Various Benchmark Areas of the World for Leading World Crops

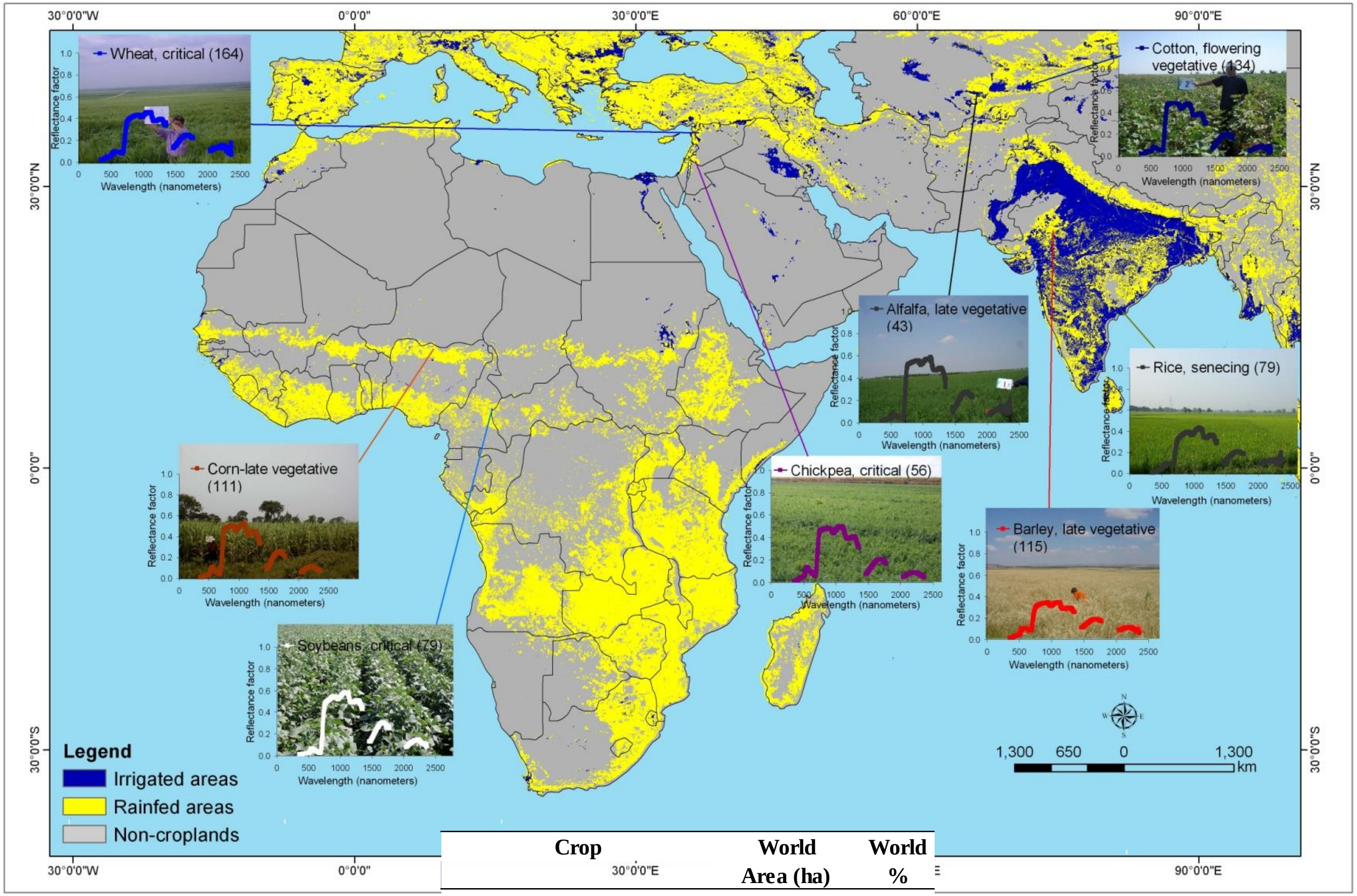

Study areas from where hyperspectral data from spectroradiometer and Hyperion were gathered. The irrigated and rainfed cropland study areas of eight major world crops (Table below) in distinct agroecosystems for which hyperspectral data from spectroradiometer and Hyperion were collected from four study areas (see details in next slide).

Crop	World Area (ha)	World %
Wheat	402,800,000	22.5
Maize	227,100,000	12.7
Rice	195,600,000	10.9
Barley	158,000,000	8.8
Soybeans	92,700,000	5.2
Pulses	79,400,000	4.4
Cotton	53,400,000	3.0
Alfalfa	30,000,000	1.7
Total of major 8 crops (ha)	**1,239,000,000**	69.1
Others (ha)	553,000,000	30.9
Total cropland (ha)	1,792,000,000	100.0

Hyperspectral Study of Agricultural Crops

Hyperspectral Data from Various Benchmark Areas of the World for Leading World Crops

Study area (#)	Study areas (name)	Major crops Studied (crop types)	Major crop characteristics for which data gathered (crop parameters)	Hyperspectral data (sensor types)	number of data points (#)
1	Africa (sudan savanna, N. guinea savanna, S. guinea savanna, derived savanna, humid forests)	corn, soybeans rice	biomass plant height, plant density, crop types	Hyperion spectroradiometer	532
2	Syria (supplemental irrigated areas)	Barley, corn, soybeans, wheat, pulses (chickpea)	biomass, LAI, Yield, plant height, plant density, nitrogen, crop types	spectroradiometer,	467
3	Uzbekistan (irrigated areas)	wheat, rice, cotton, alfalfa, corn	biomass, Yield, plant height, plant density, crop types	Hyperion spectroradiometer	372
4	India (rainfed areas)	barley, soybeans, pulses (chickpea)	biomass plant height, plant density, crop types	Hyperion spectroradiometer	182

Cross-site hyperspectral spectroradiometer data. Cross-site mean (regardless of which study site (1-4, Table)) spectral plots of eight leading world crops in various growth stages. (A) Four crops at different growth stages; (B) same four crops as in A but in different growth stages; (C) four more crops at early growth stages; and (D) same four crops as C, but at different growth stages. Note: numbers in bracket are sample sizes.

Hyperion Hyperspectral Study of Agricultural Crops

Hyperspectral Data from Various Benchmark Areas of the World for Leading World Crops

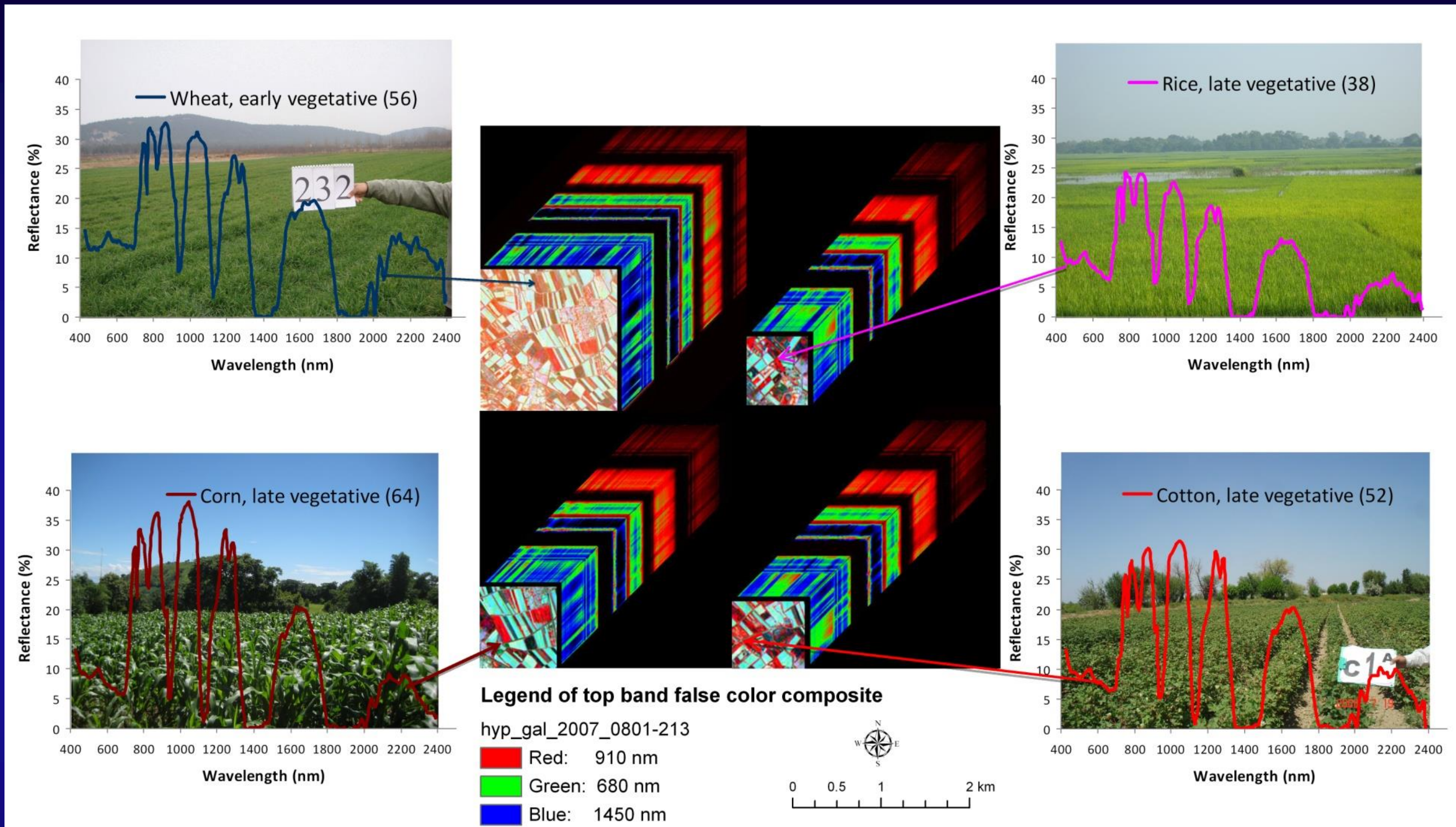

Hyperion data of crops illustrated for typical growth stages in the Uzbekistan study area. The Hyperion data cube shown here is from a small portion of one of the two Hyperion images. The Hyperion spectra of crops are gathered from different farm fields in the two images and their average spectra illustrated here along with the sample sizes indicated within the bracket. The field data was collected within two days of the image acquisition.

Hyperspectral Study of Agricultural Crops

Hyperspectral Data from Various Benchmark Areas of the World for Leading World Crops

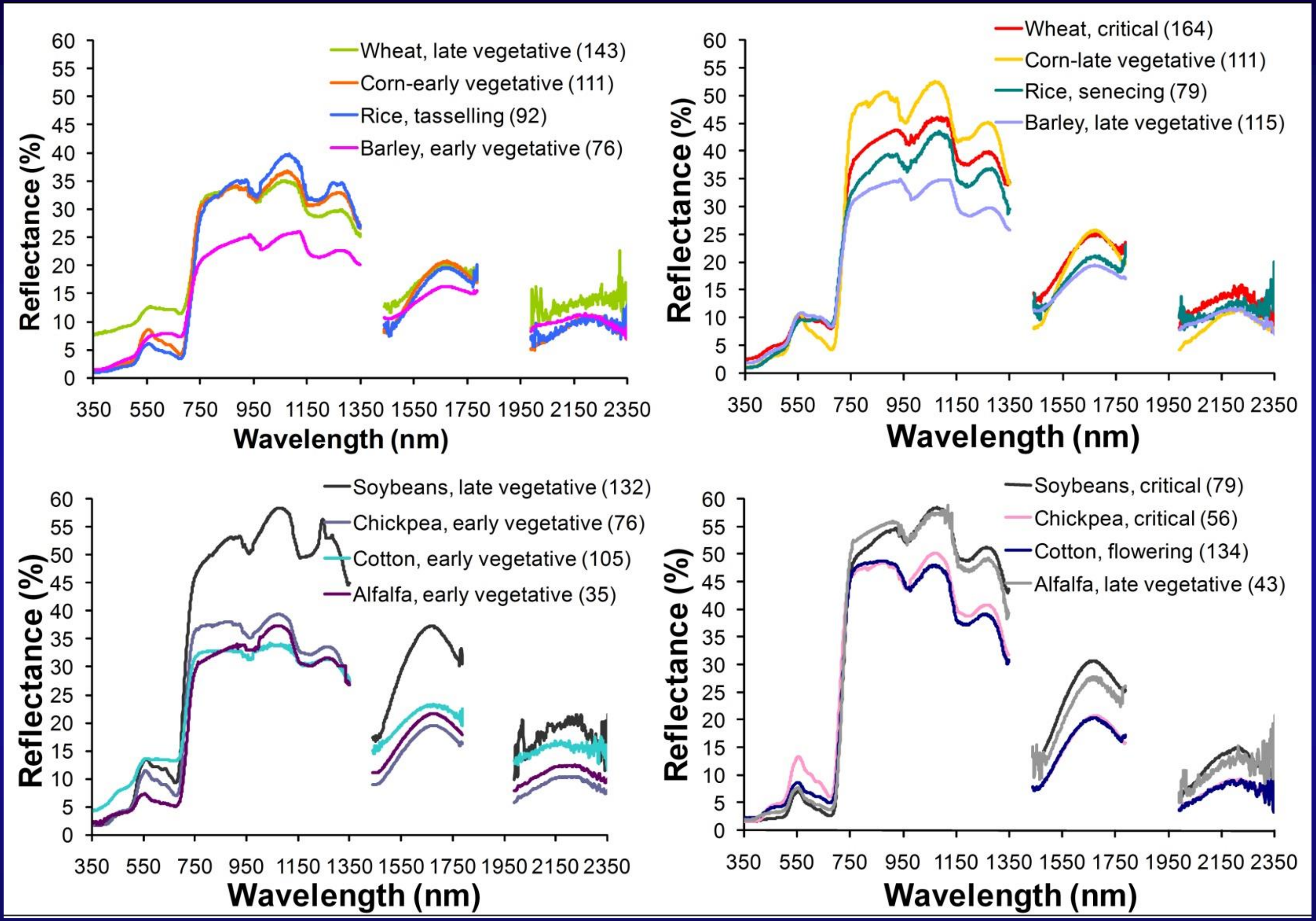

Cross-site hyperspectral spectroradiometer data. Cross-site mean (regardless of which study site (1-4, Table 2)) spectral plots of eight leading world crops in various growth stages. (A) Four crops at different growth stages; (B) same four crops as in A but in different growth stages; (C) four more crops at early growth stages; and (D) same four crops as C, but at different growth stages. Note: numbers in bracket are sample sizes.

Hyperspectral Remote Sensing of Vegetation

Spectral Wavelengths and their Importance in the Study of Vegetation in different Growth Stages

Figure 3a. Cotton in critical growth stage.

(a) Cotton (critical)

Figure 3c. Soybeans in critical growth stage.

(b) Soybeans (early)

Figure 3e. Potato in early growth stage.

(c) Potato (early)

Figure 3b. Cotton in yielding/harvest

(a) Cotton (flowering/senescing)

Figure 3d. Soybeans in flowering growth stage.

(b) Soybeans (critical)

Figure 3f. Potato in late growth stage.

(c) Potato (mid-vegetative)

Data was Gathered at Various Growth Stages

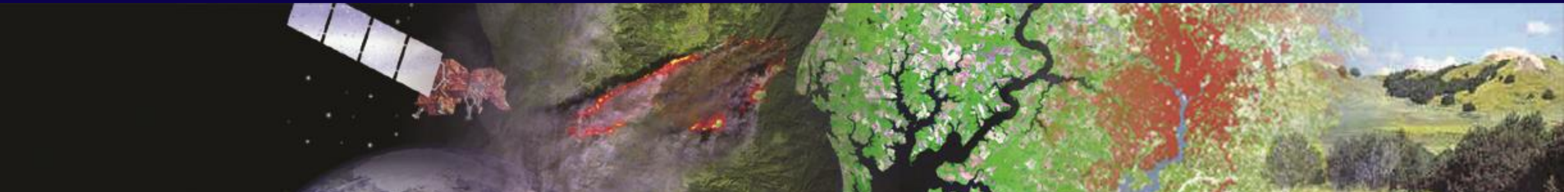

Hyperspectral Remote Sensing of Vegetation

Spectral Wavelengths and their Importance in the Study of Vegetation in different Growth Stages

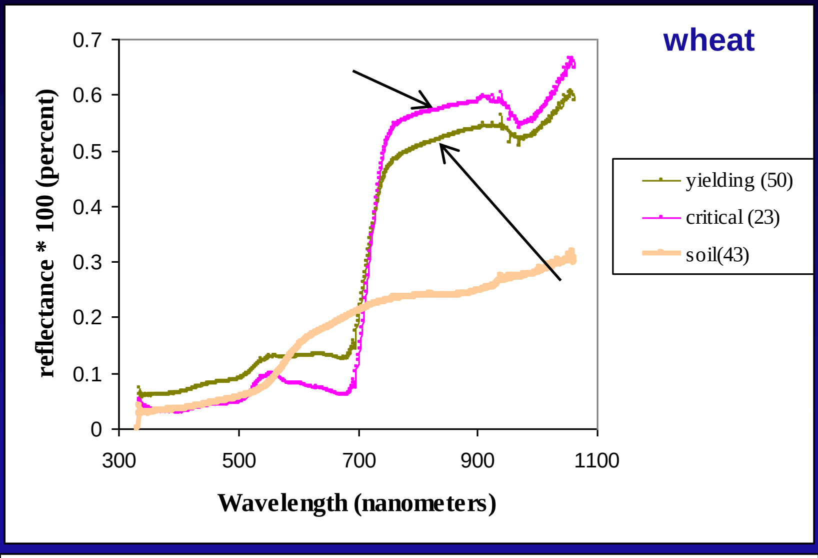

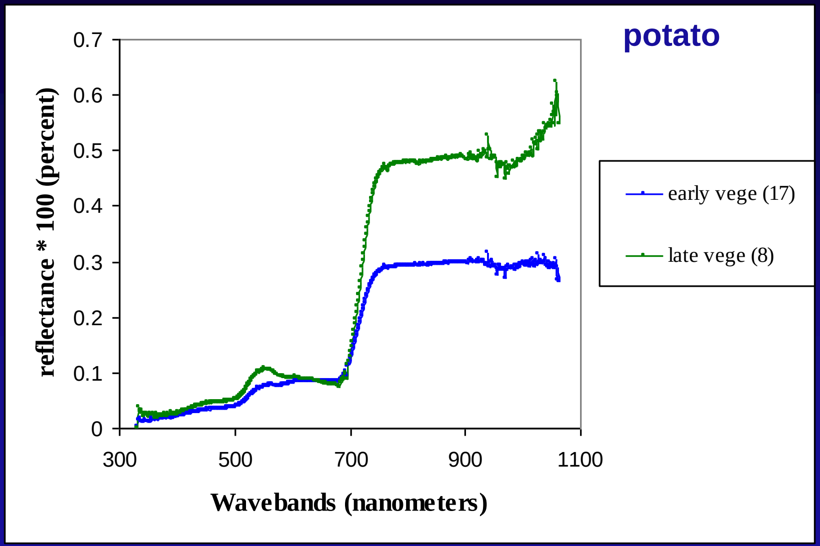

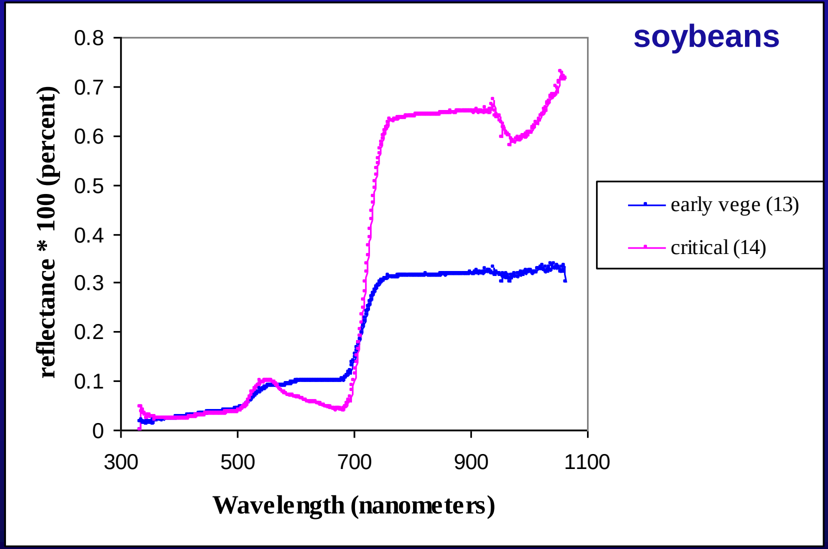

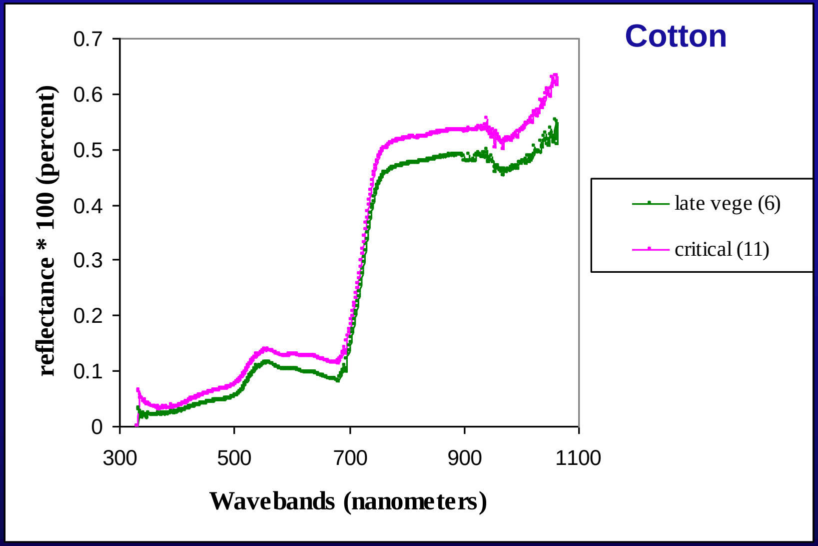

Hyperspectral Remote Sensing of Vegetation

Spectral Wavelengths and their Importance in the Study of Vegetation over Time

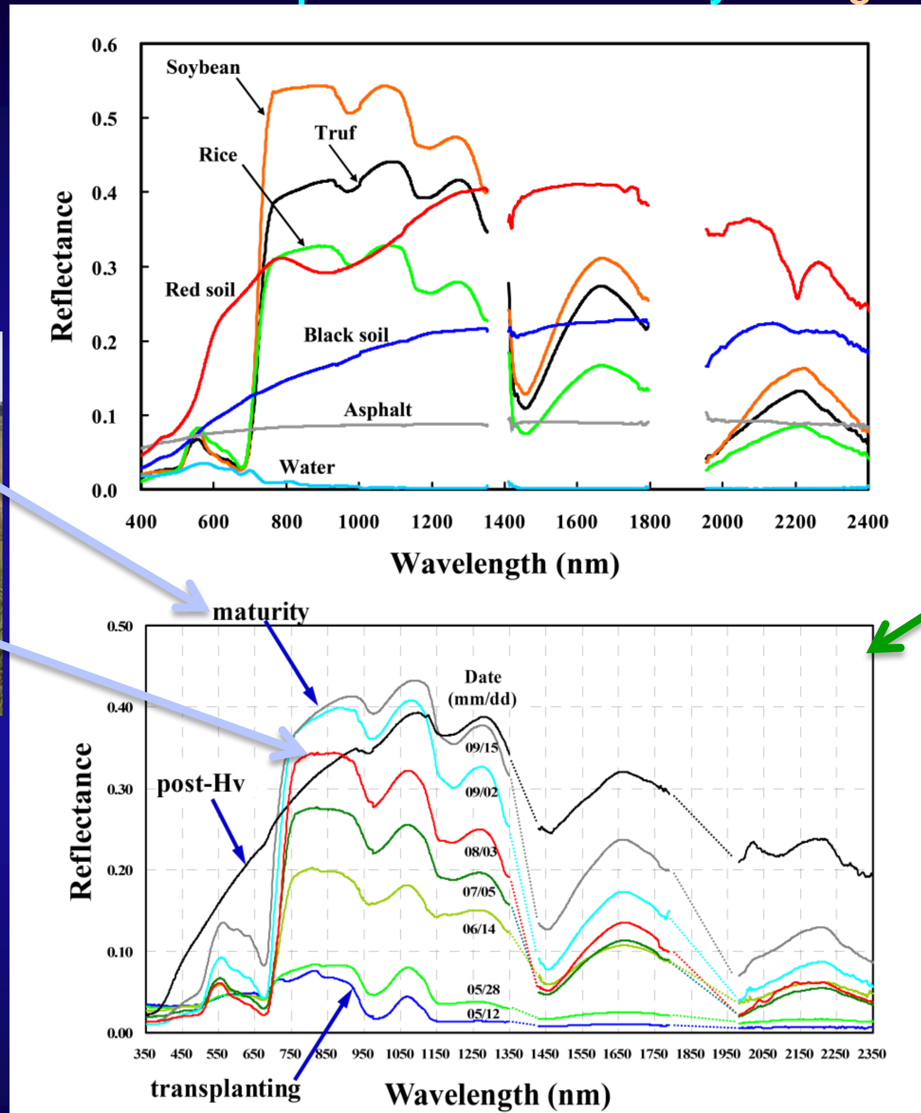

Typical reflectance spectra in agro-ecosystem surfaces (upper), and <u>seasonal changes</u> of spectra in a paddy rice field (lower).

Hyperspectral Remote Sensing of Vegetation

Study of Pigments: chlorophyll

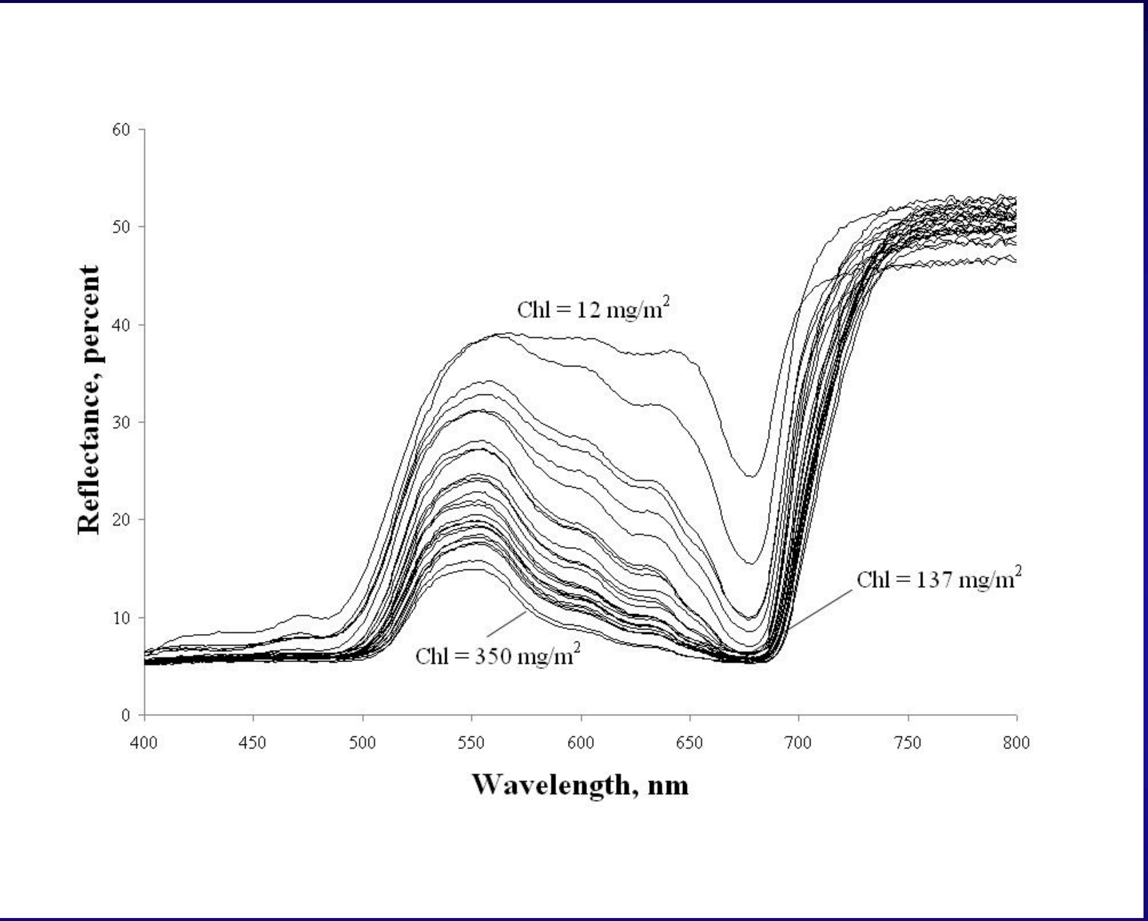

e.g., Reflectance spectra of beech leaves…red-edge (700-740 nm) one of the best.

Note: see chapter 6; Gitelson et al.

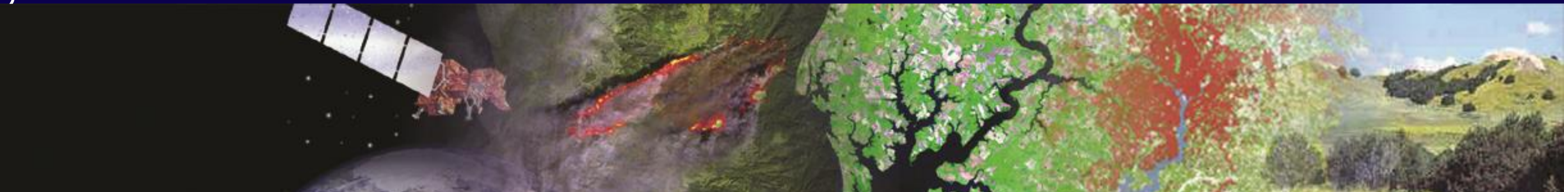

Hyperspectral Remote Sensing of Vegetation

Study of Pigments: carotenoids/chlorophyll

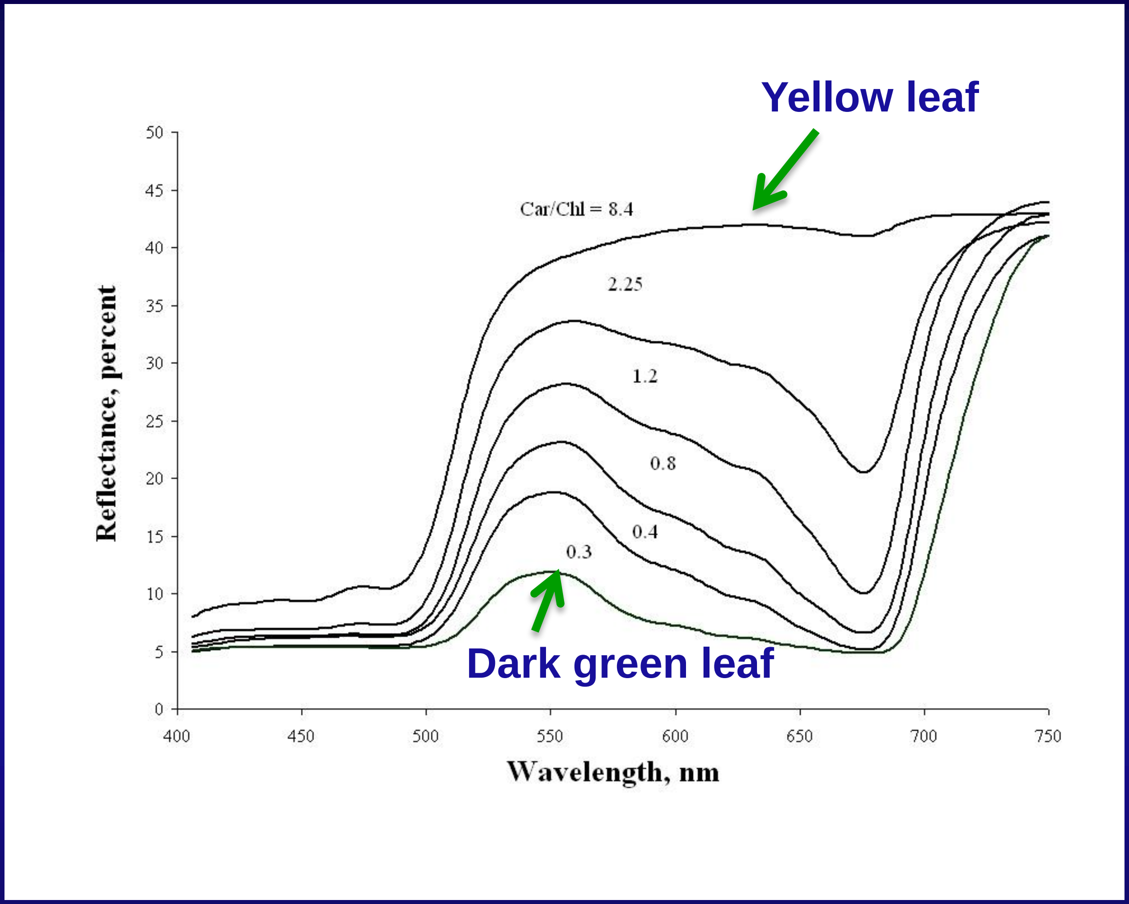

e.g., Reflectance spectra of chestnut leaves…difference reflectance of (680-500 nm)/750 nm quantitative measurement of plant senescence

Note: see chapter 6; Gitelson et al.

Wheat Crop Versus Barley Crop Versus Fallow Farm

Hyperspectral narrow-band Data for an Erectophile (65 degrees) canopy Structure

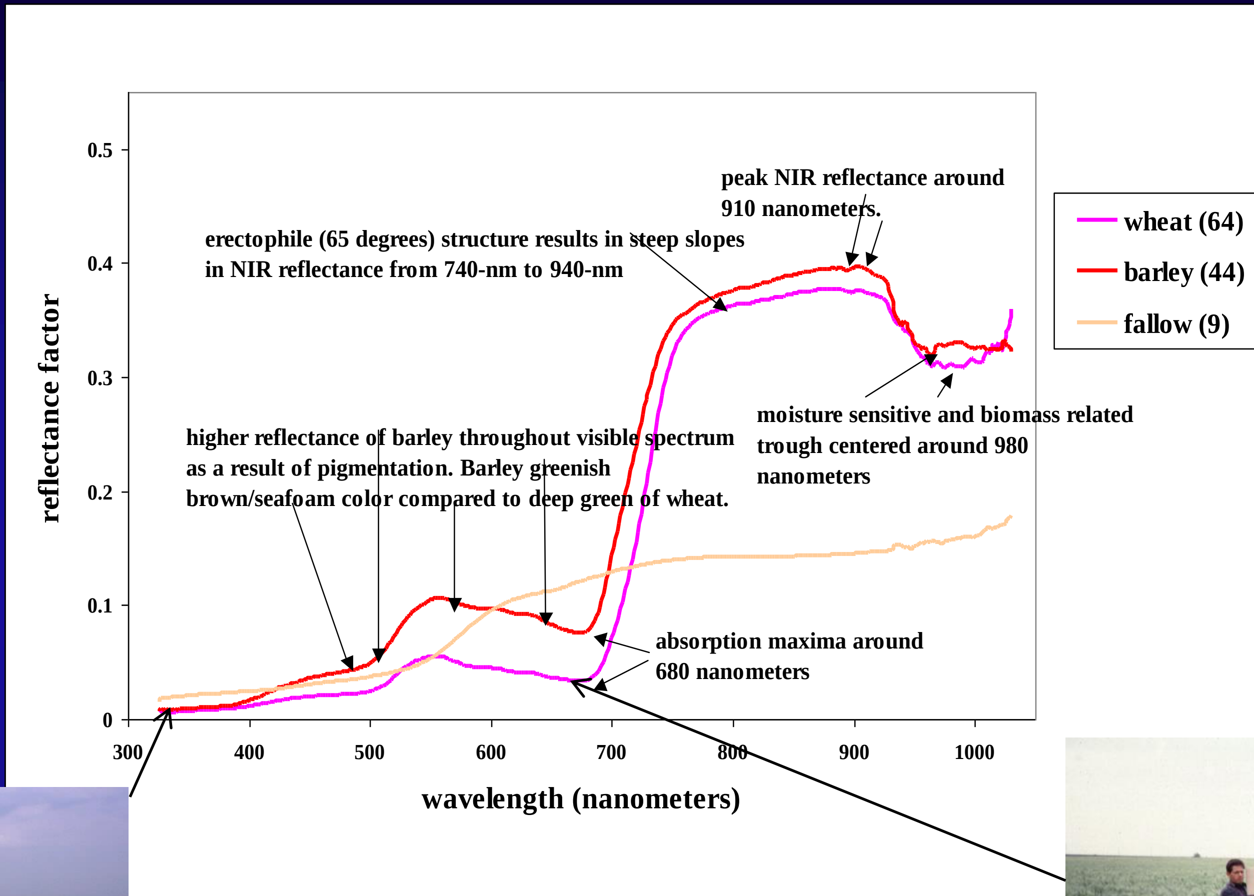

USGS
science for a changing world

U.S. Geological Survey
U.S. Department of Interior

Hyperspectral Remote Sensing of Vegetation

Spectral Wavelengths and their Importance in the Study of Vegetation Structure

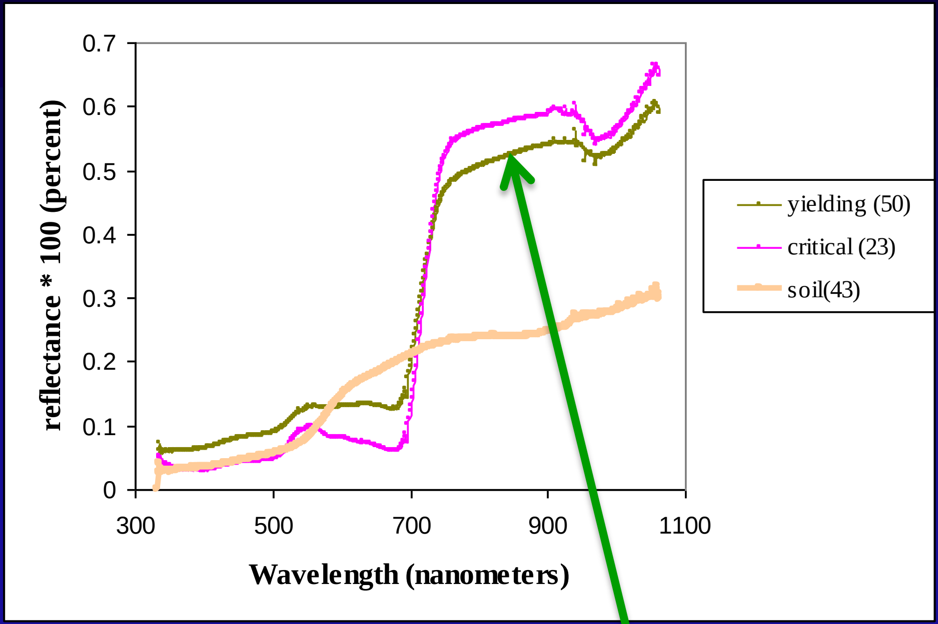

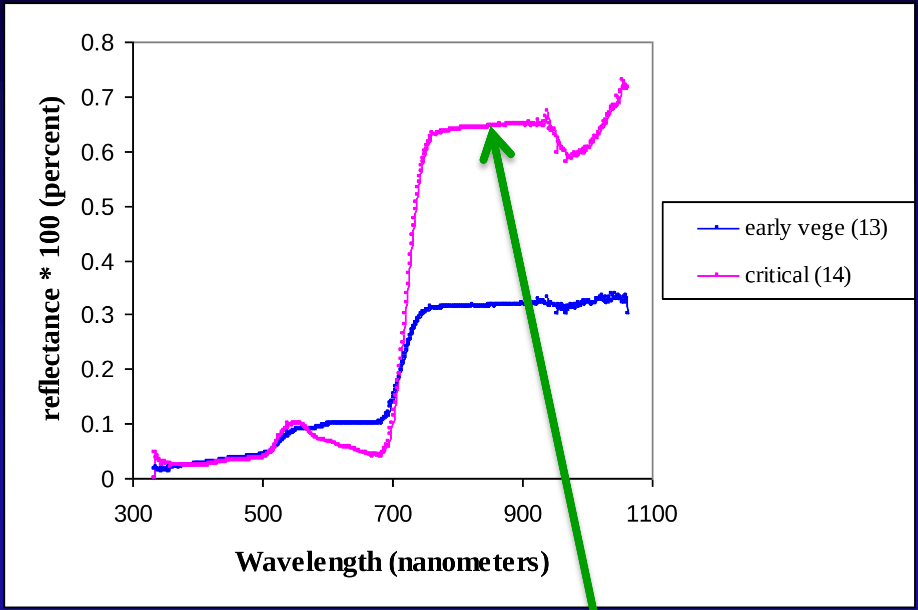

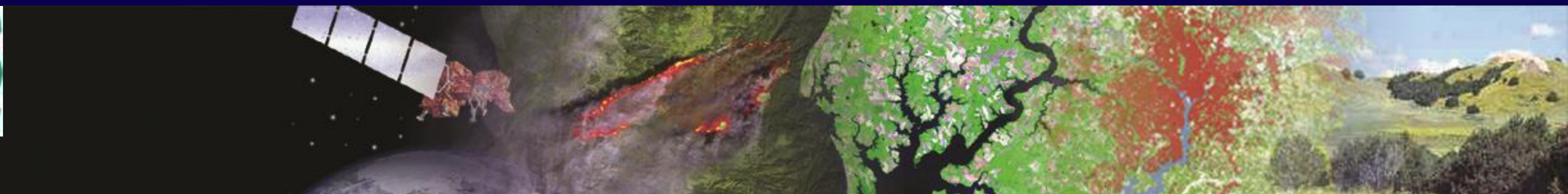

USGS
science for a changing world
U.S. Geological Survey
U.S. Department of Interior

Rainforest Vegetation Studies: biomass, tree height, land cover, species
in African Rainforests


Fallows biomass


dbh


Tree height


LULC


Road network and logging

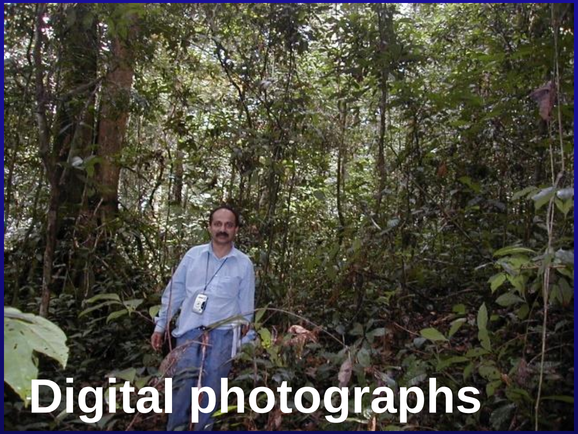
Digital photographs

Methods of Hyperspectral Data Analysis
Hyperspectral Vegetation Indices (HVIs)
Agriculture and Vegetation

Methods of Modeling Vegetation Characteristics using Hyperspectral Indices

Hyperspectral Two-band Vegetation Indices (TBVIs) = 12246 unique indices for 157 useful Hyperion bands of data

$$HTBVI_{ij} = \frac{(R_j - R_i)}{(R_j + R_i)}$$

- **Hyperion**:
- A. acquired over 400-2500 nm in 220 narrow-bands each of 10-nm wide bands. Of these there are 196 bands that are calibrated. These are: (i) bands 8 (427.55 nm) to 57 (925.85 nm) in the visible and near-infrared; and (ii) bands 79 (932.72 nm) to band 224 (2395.53 nm) in the short wave infrared.
- B. However, there was significant noise in the data over the 1206–1437 nm, 1790– 1992 nm, and 2365–2396 nm spectral ranges. When the Hyperion bands in this region were dropped, 157 useful bands remained.

- **Spectroradiometer**:
- A. acquired over 400-2500 nm in 2100 narrow-bands each of 1-nm wide. However, 1-nm wide data were aggregated to 10-nm wide to coincide with Hyperion bands.
- B. However, there was significant noise in the data over the 1350-1440 nm, 1790-1990 nm, and 2360-2500 nm spectral ranges. was seriously affected by atmospheric absorption and noise. The remaining good noise free data were in 400-1350 nm, and 1440-1790 nm, 1990-2360 nm.

- ……..So, for both Hyperion and Spectroradiometer we had 157 useful bands, each of 10-nm wide, over the same spectral range.

- where, i,j = 1, N, with N=number of narrow-bands= 157 (each band of 1 nm-wide spread over 400 nm to 2500 nm), R=reflectance of narrow-bands.

Model algorithm: two band NDVI algorithm in Statistical Analysis System (SAS). Computations are performed for all possible combinations of λ_1 (wavelength 1 = 157 bands) and λ_2 (wavelength 2 = 157 bands) - a total of 24,649 possible indices. It will suffice to calculate Narrow-waveband NDVI's on one side (either above or below) the diagonal of the 157 by 157 matrix as values on either side of the diagonal are the transpose of one another.

Hyperspectral Data (Imaging Spectroscopy data)

Hyperspectral Vegetation Indices (HVIs)

Unique Features and Strengths of HVIs

1. **Eliminates redundant bands**
   - removes highly correlated bands
2. **Physically meaningful HVIs**
   - e.g., Photochemical reflective index (PRI) as proxy for light use efficiency (LUE)
3. **Significant improvement over broadband indices**
   - e.g., reducing saturation of broadbands, providing greater sensitivity (e.g., an index involving NIR reflective maxima @ 900 nm and red absorption maxima @680 nm
4. **New indices not sampled by broadbands**
   - e.g., water-based indices (e.g., involving 970 nm or 1240 nm along with a nonabsorption band)
5. **multi-linear indices**
   - indices involving more than 2 bands

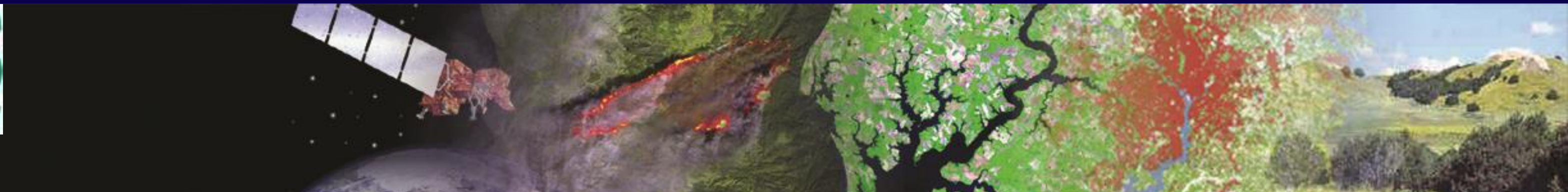

Methods of Modeling Vegetation Characteristics using Hyperspectral Indices

Non-linear biophysical quantities (e.g., biomass, LAI) vs.:(a)Broadband models (top two), & (b)Narrowband HTBVI models (bottom two)

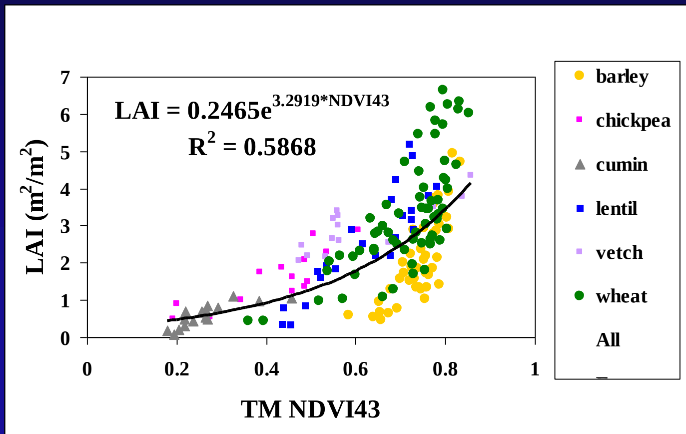

broad-band NDVI43 vs. LAI

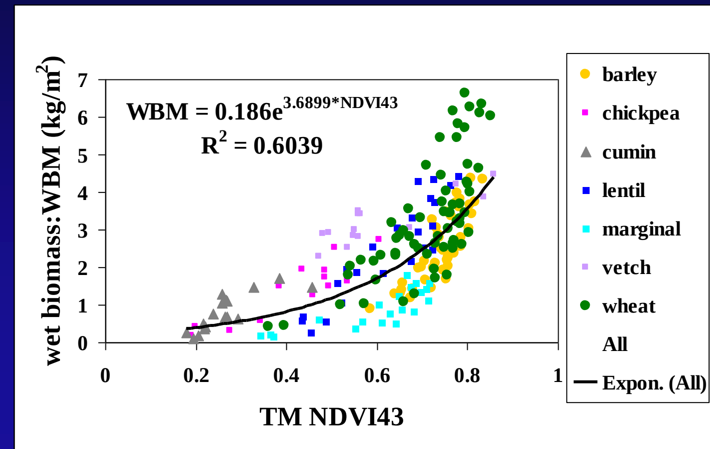

broad-band NDVI43 vs. WBM

HTBVIs explain about 13 percent Greater Variability than Broad-band TM indices in modeling LAI and biomass

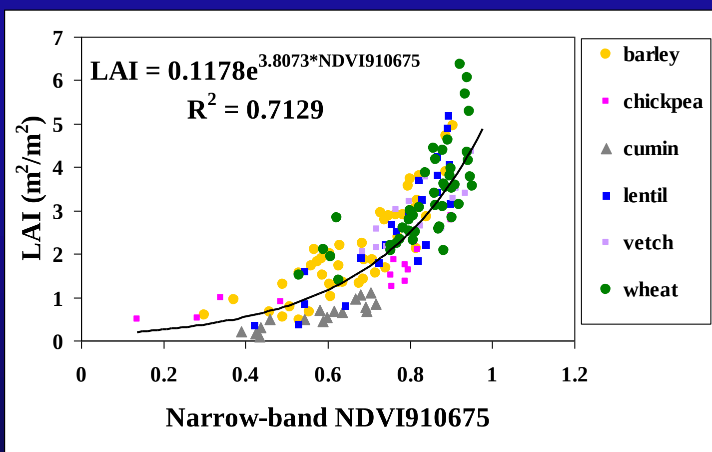

narrow-band NDVI43 vs. LAI

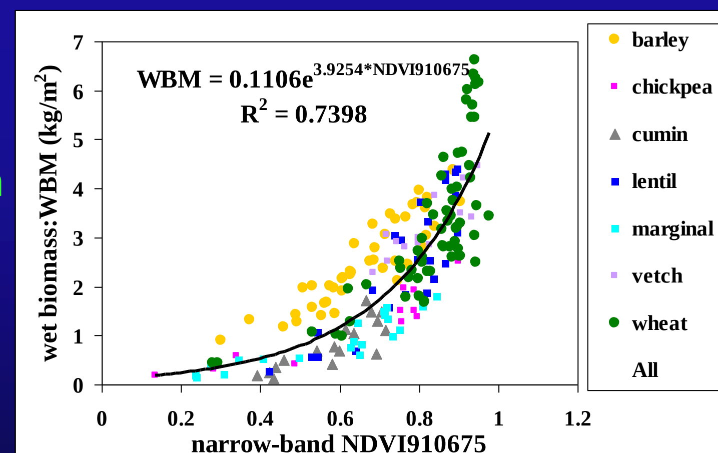

narrow-band NDVI43 vs. WBM

USGS
science for a changing world

U.S. Geological Survey
U.S. Department of Interior

Methods of Modeling Vegetation Characteristics using Hyperspectral Indices

Lambda vs. Lambda R-square contour plot on non-linear biophysical quantity (e.g., biomass) vs. HTBVI models

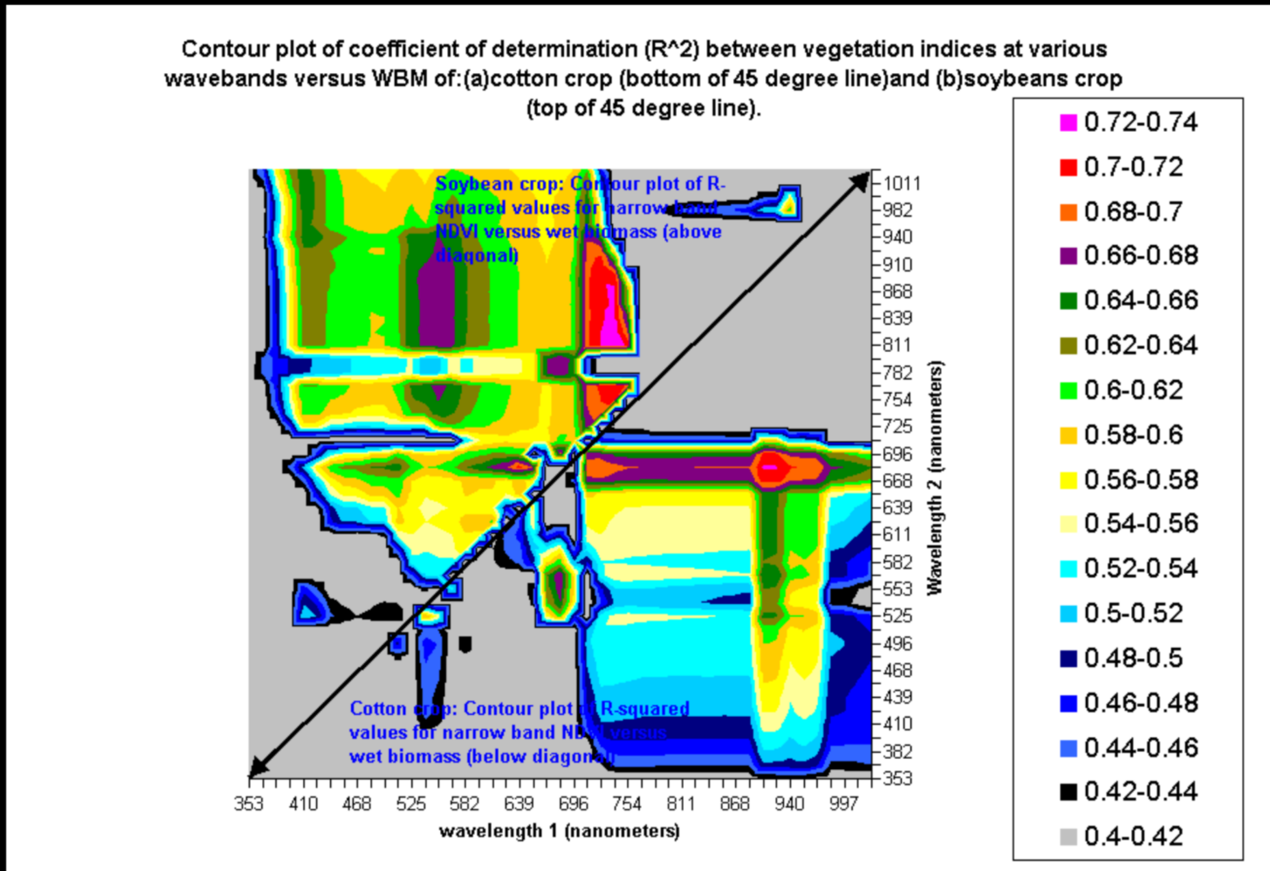

Illustrated for 2 crops here

Hyperion Hyperspectral Data on Agricultural Crops from

Lambda versus Lambda R-square Contour plots of 2 Major Crops

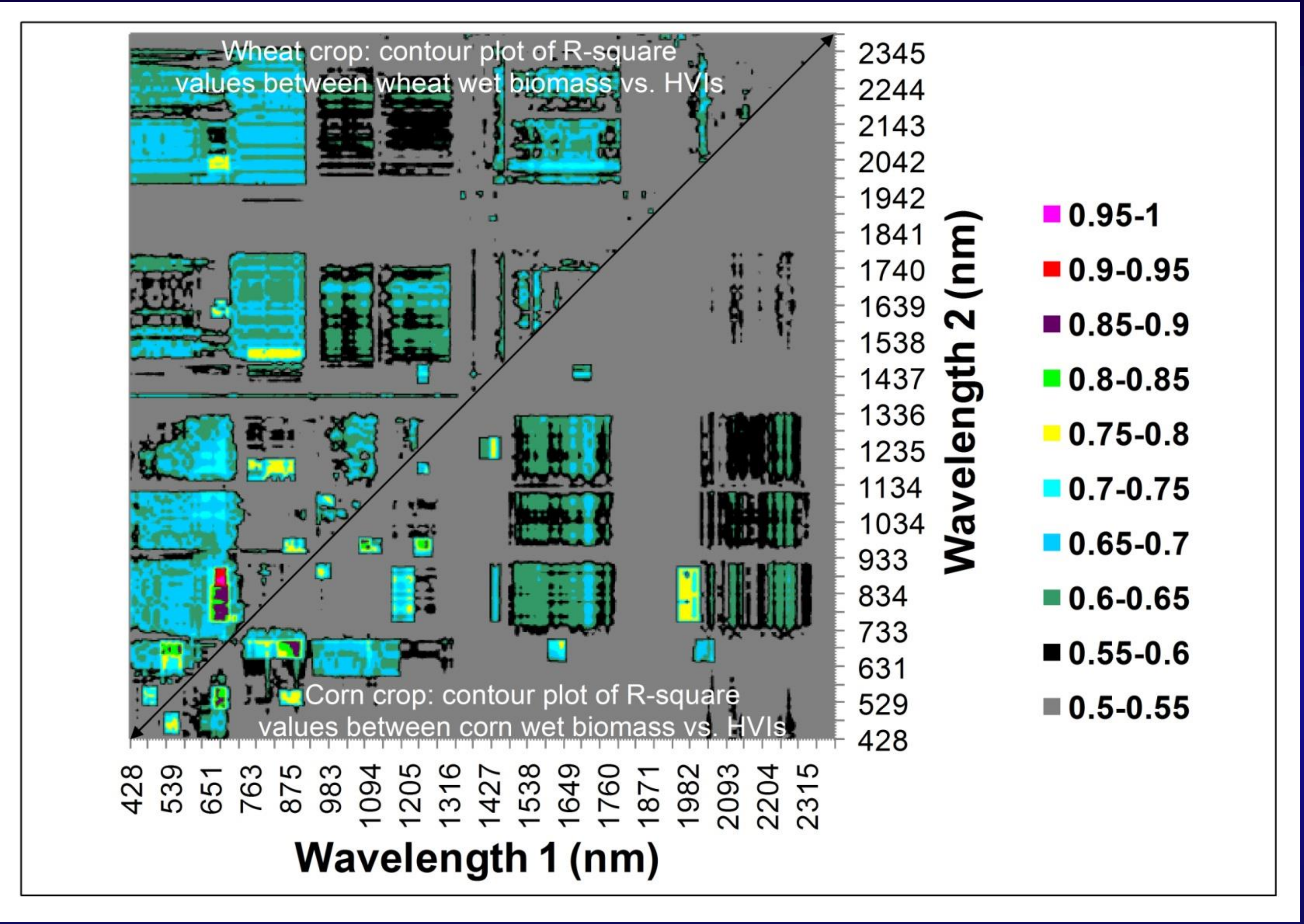

Contour plot of λ versus λ R^2- values for wavelength bands between two-band hyperspectral vegetation indices (HVIs) and wet biomass of wheat crop (above diagonal) and corn crop (below diagonal). The 242 Hyperion bands were reduced to 157 bands after eliminating uncalibrated bands and the bands in atmospheric window. HVIs were then computed using the 157 bands leading to 12,246 unique two-band normalized difference HVIs each of which were then related to biomass to obtain R-square values. These R^2-values were then plotted in a λ versus λ R^2-contour plot as shown above.

Hyperion Hyperspectral Data on Agricultural Crops from

Lambda versus Lambda R-square Contour plots of 2 Major Crops

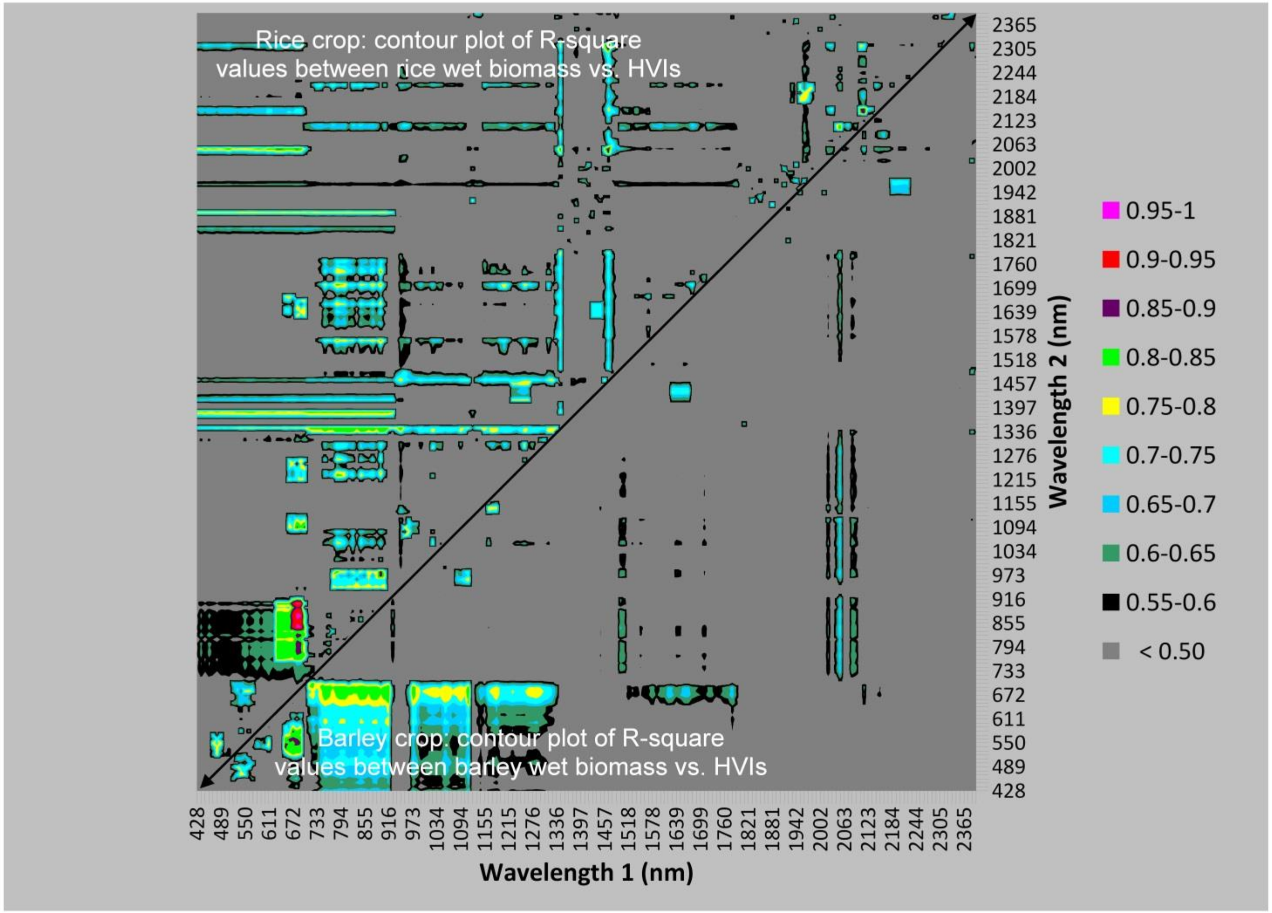

Contour plot of λ versus λ R^2- values for wavelength bands between two-band hyperspectral vegetation indices (HVIs) and wet biomass of wheat crop (above diagonal) and corn crop (below diagonal). The 242 Hyperion bands were reduced to 157 bands after eliminating uncalibrated bands and the bands in atmospheric window. HVIs were then computed using the 157 bands leading to 12,246 unique two-band normalized difference HVIs each of which were then related to biomass to obtain R-square values. These R^2-values were then plotted in a λ versus λ R^2-contour plot as shown above.

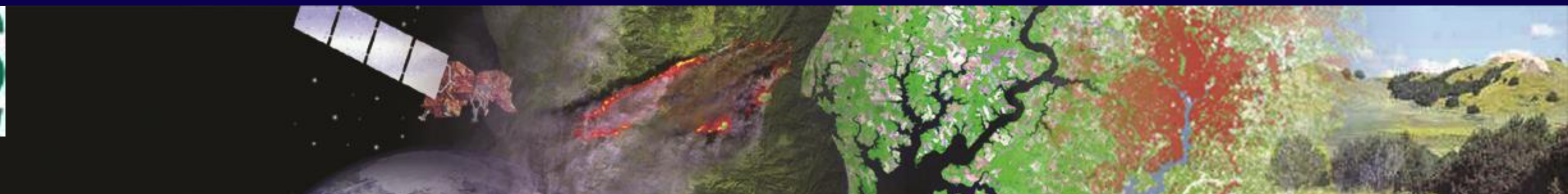

Methods of Modeling Vegetation Characteristics using Hyperspectral Indices

Lambda vs. Lambda R-square contour plot on non-linear biophysical quantity (e.g., biomass) vs. HTBVI models

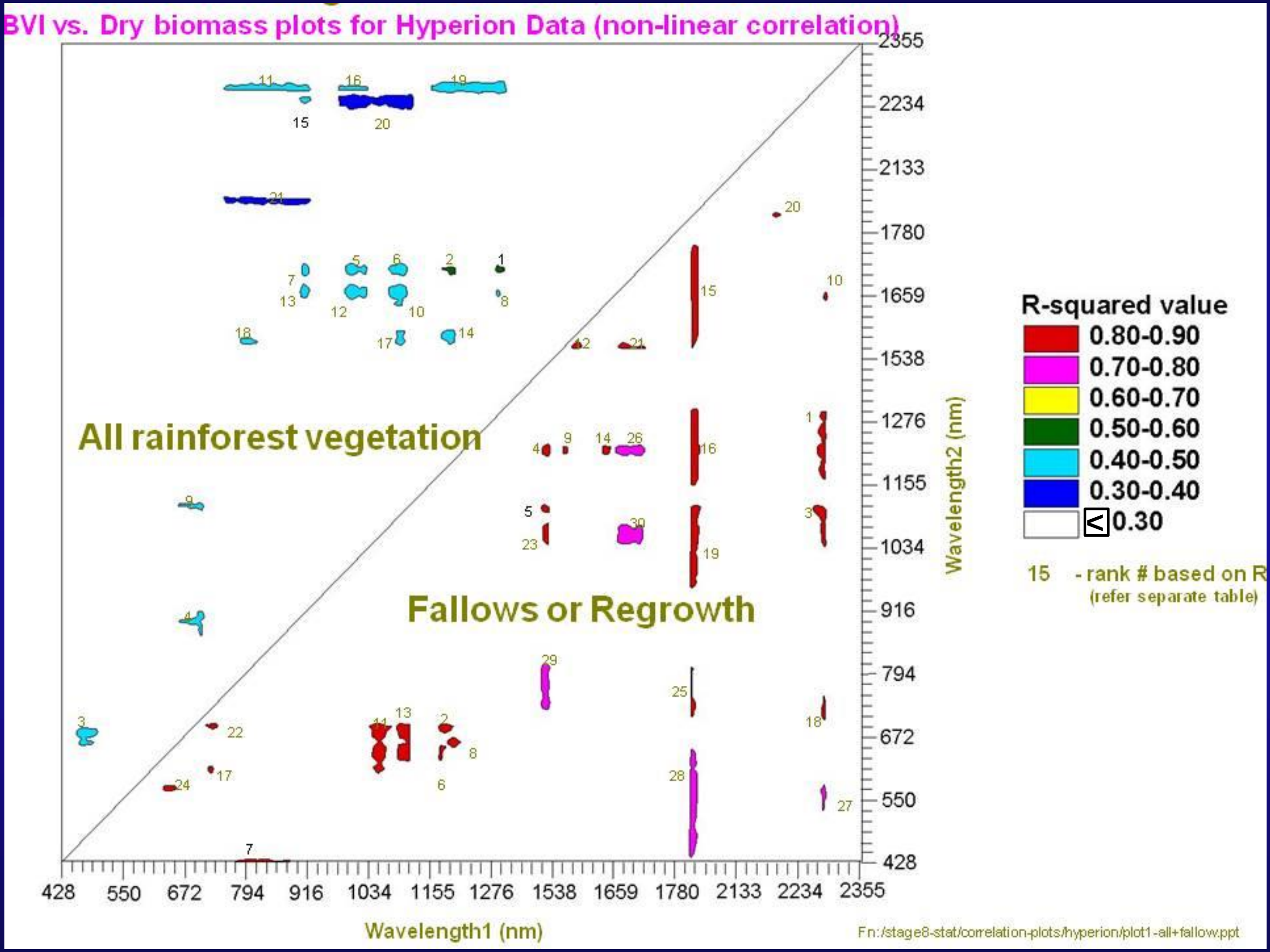

Waveband combinations with greatest R^2 values Greater are ranked…….bandwidths can also be determined.

Methods of Hyperspectral Data Analysis

HVIs involving Multiple Hyperspectral Narrowbands (HNBs)

Agriculture and Vegetation

Methods of Modeling Vegetation Characteristics using Hyperspectral Indices

Hyperspectral Multi-band Vegetation Indices (HMBVIs)

$$HMBVI_i = \sum_{J=1}^{N} a_{ij} R_j$$

where, OMBVI = crop variable i, R = reflectance in bands j (j= 1 to N with N=157; N is number of narrow wavebands); a = the coefficient for reflectance in band j for i th variable.

<u>Model algorithm</u>: MAXR procedure of SAS (SAS, 1997) is used in this study. The MAXR method begins by finding the variable (R_j) producing the highest coefficient of determination (R^2) value. Then another variable, the one that yields the greatest increase in R^2 value, is added……………and so on…….so we will get the best 1-variable model, best 2-variable model, and so on to best n-variable model………………..when there is no significant increase in R^2-value when an additional variable is added, the model can stop.

Methods of Modeling Vegetation Characteristics using Hyperspectral Indices

Multiband HVIs for Winter Wheat in China

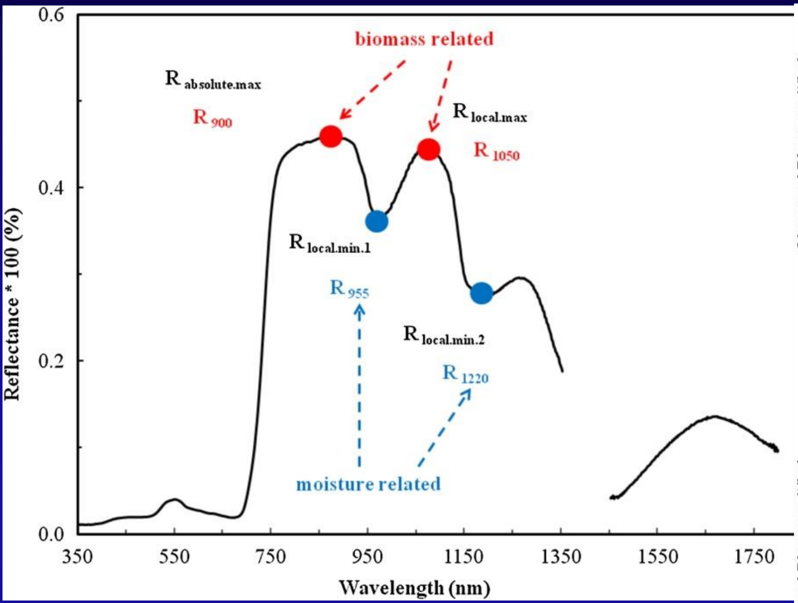

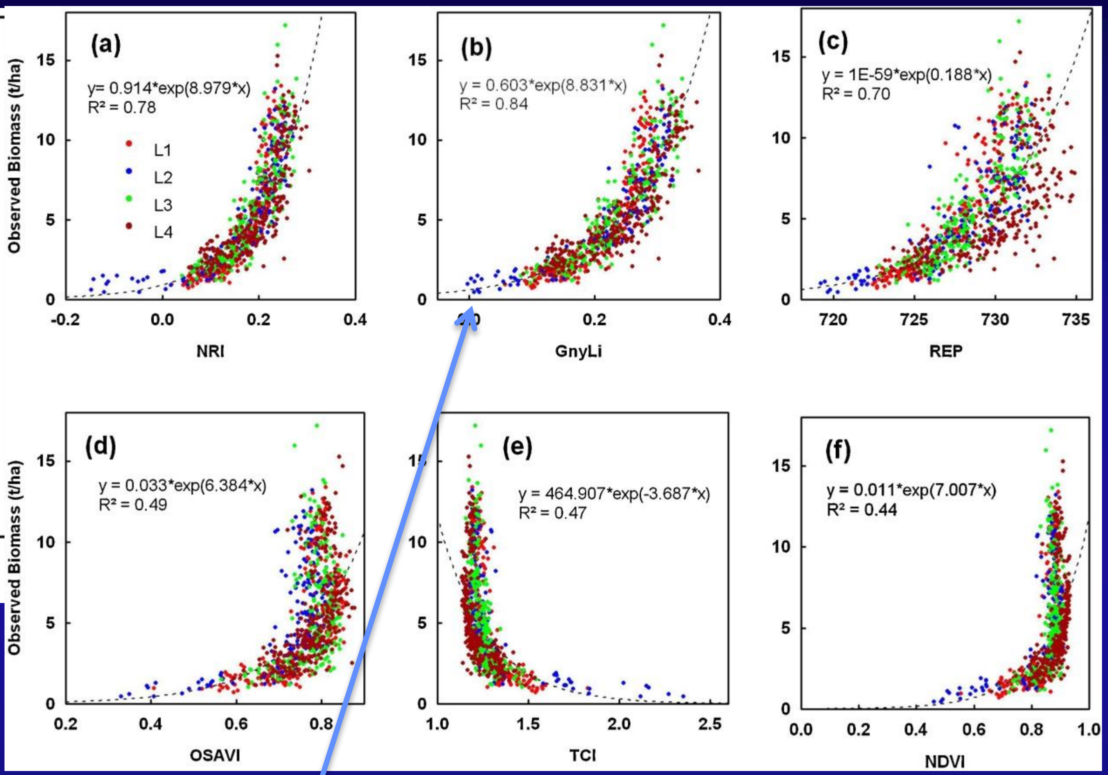

Gnyp, M.L. et al., 2014

$$\text{GnyLi} = \frac{R_{900} \times R_{1050} - R_{955} \times R_{1220}}{R_{900} \times R_{1050} + R_{955} \times R_{1220}}$$

USGS
science for a changing world

U.S. Geological Survey
U.S. Department of Interior

Methods of Modeling Vegetation Characteristics using Hyperspectral Indices

Predicted biomass derived using MBVI's involving various narrowbands in African Rainforests

Note: Increase in R^2 values beyond 6 bands is negligible

Note: Increase in R^2 values beyond 11 bands is negligible

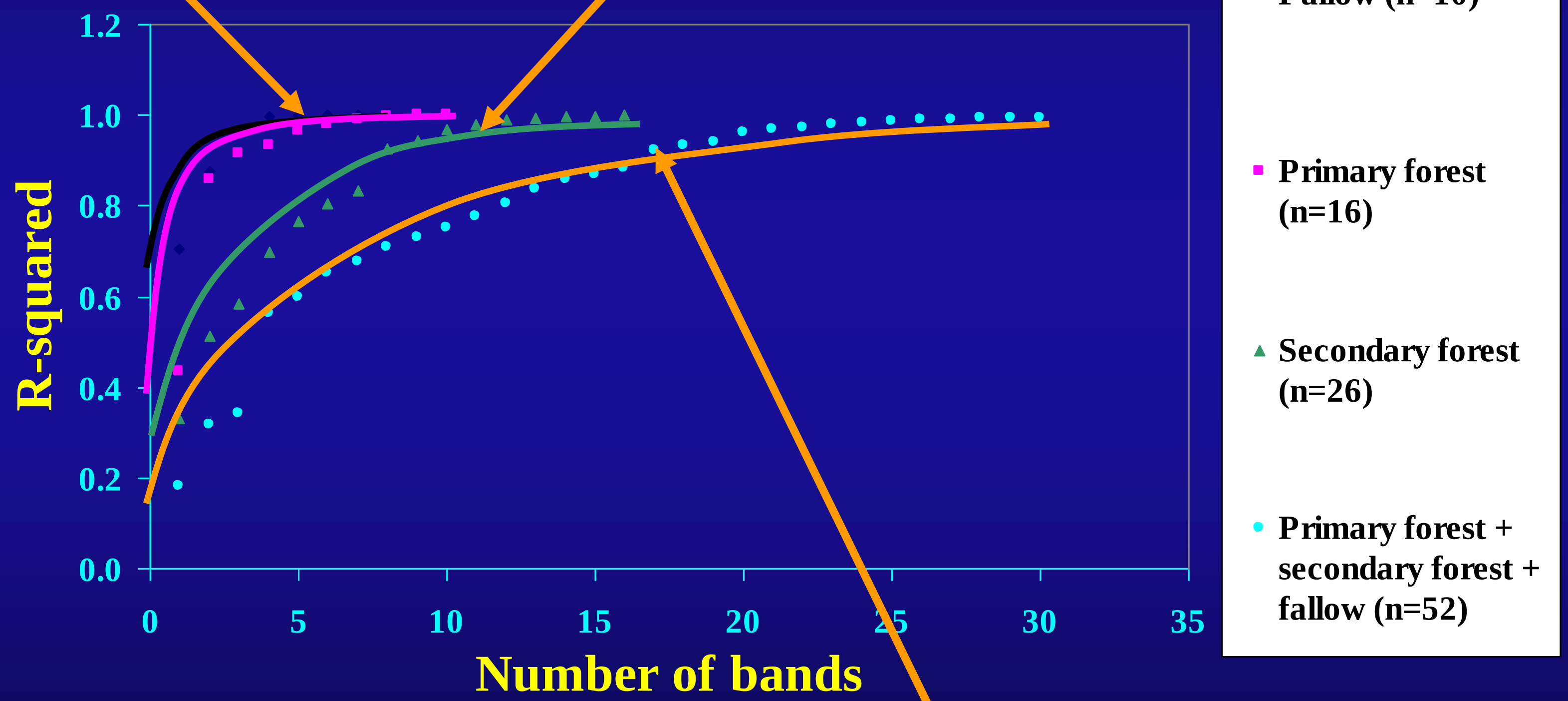

Note: Increase in R^2 values beyond 17 bands is negligible

Methods of Classifying Vegetation Classes or Categories

Discriminant Model or Classification Criterion (DM) to Test

How Well <u>12 different Vegetation</u> are Discriminated <u>using different Combinations of Broadbands vs. Narrowbands</u>?

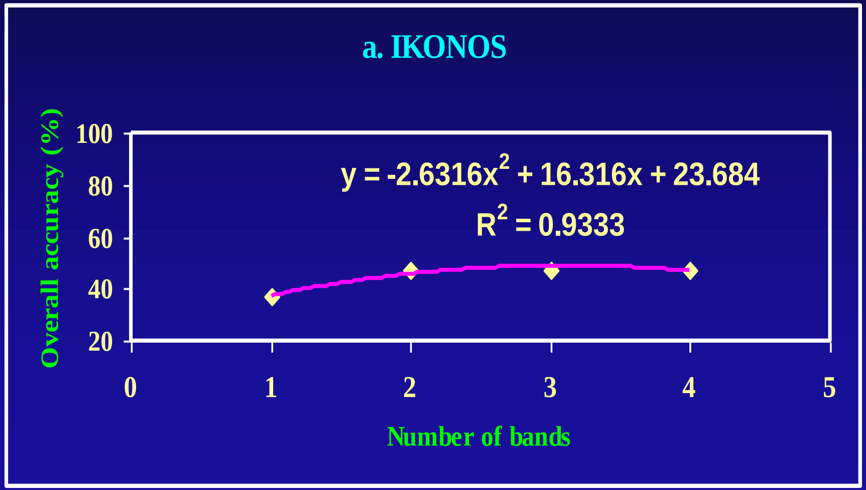

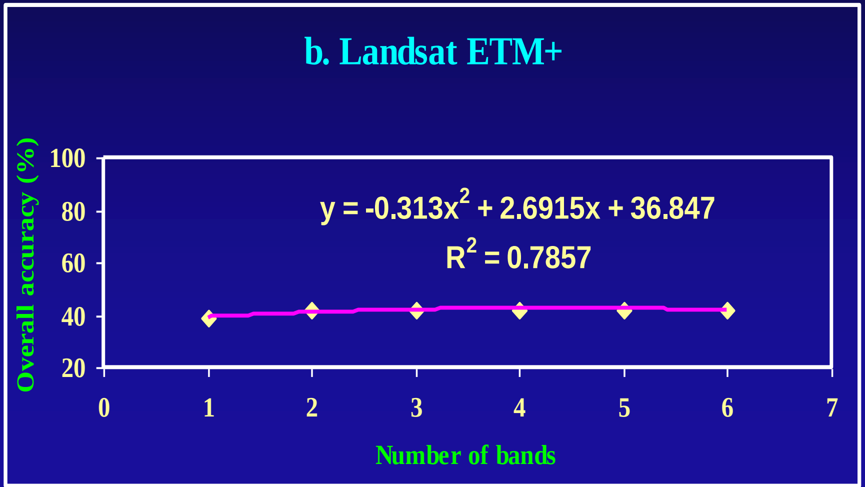

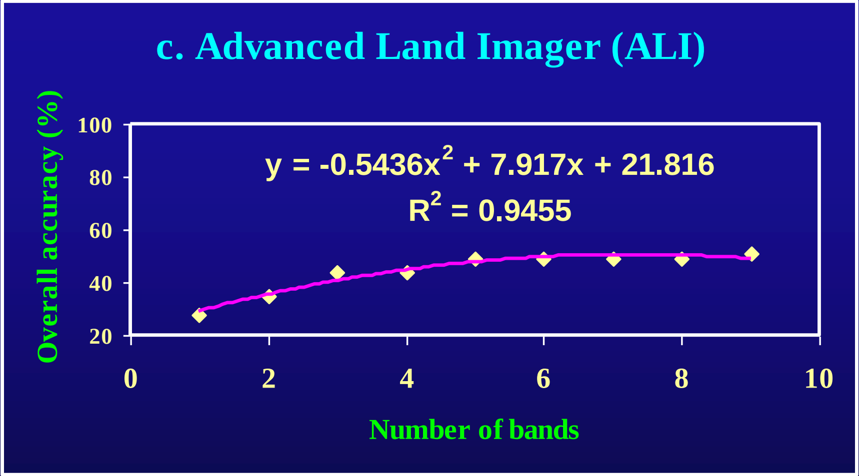

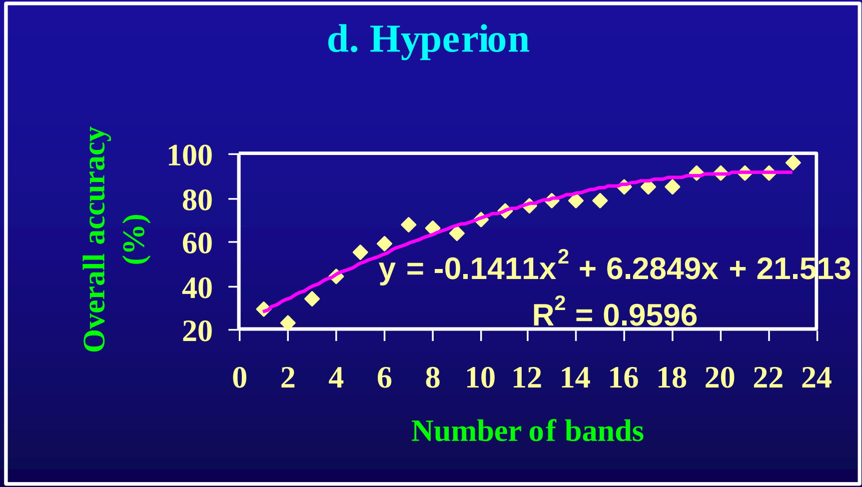

USGS
science for a changing world

U.S. Geological Survey
U.S. Department of Interior

Methods of Hyperspectral Data Analysis

Derivative Greeness Vegetation Indices (DGVIs)

Agriculture and Vegetation

Methods of Modeling Vegetation Characteristics using Hyperspectral Indices

Hyperspectral Derivative Greenness Vegetation Indices (DGVIs)

First Order Hyperspectral Derivative Greenness Vegetation Index (HDGVI) (Elvidge and Chen, 1995): These indices are integrated across the (a) chlorophyll red edge:.626-795 nm, (b) Red-edge more appropriately 690-740 nm……and other wavelengths.

$$DGVI1 = \sum_{\lambda_1}^{\lambda_n} \frac{(\rho'(\lambda_i) - (\rho'(\lambda j)}{\Delta\lambda_I}$$

Where, I and j are band numbers,

λ = center of wavelength,

$\lambda_1 = 0.626\ \mu m$,

$\lambda_n = 0.795\ \mu m$,

ρ' = first derivative reflectance.

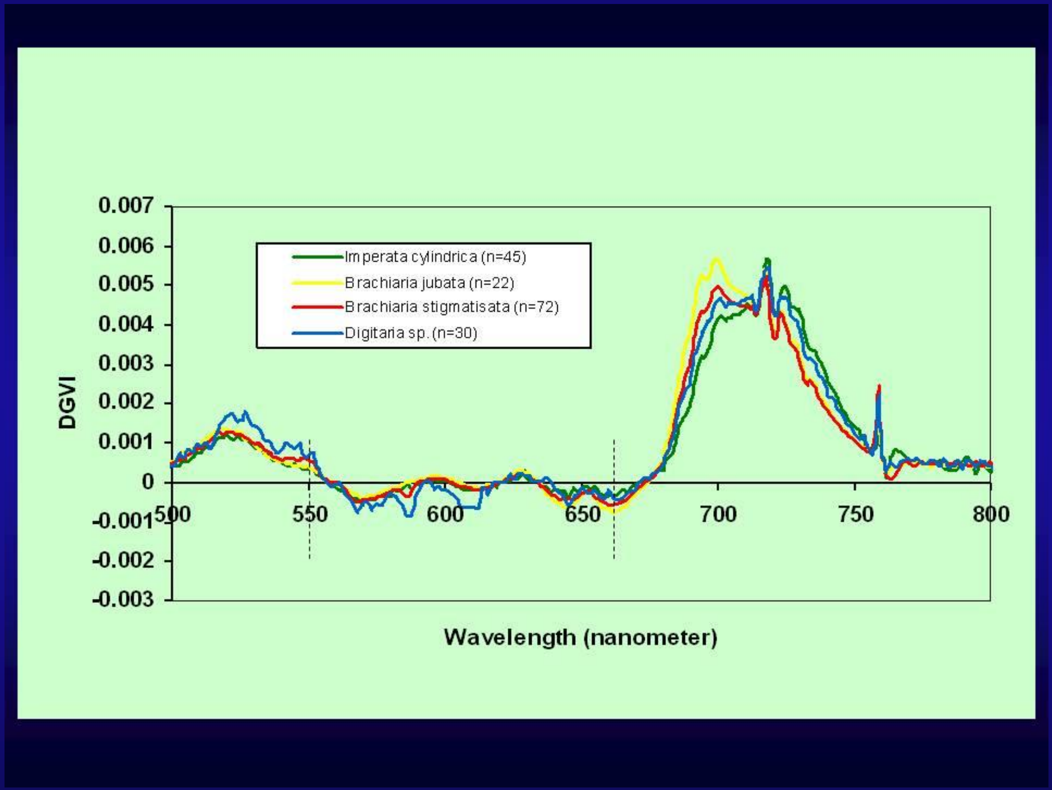

Note: HDGVIs are near-continuous narrow-band spectra integrated over certain wavelengths

Methods of Hyperspectral Data Analysis

Class Separability

Agriculture and Vegetation

Hyperspectral Narrowband Study of Agricultural Crops

Methods of Hyperspectral Data Analysis

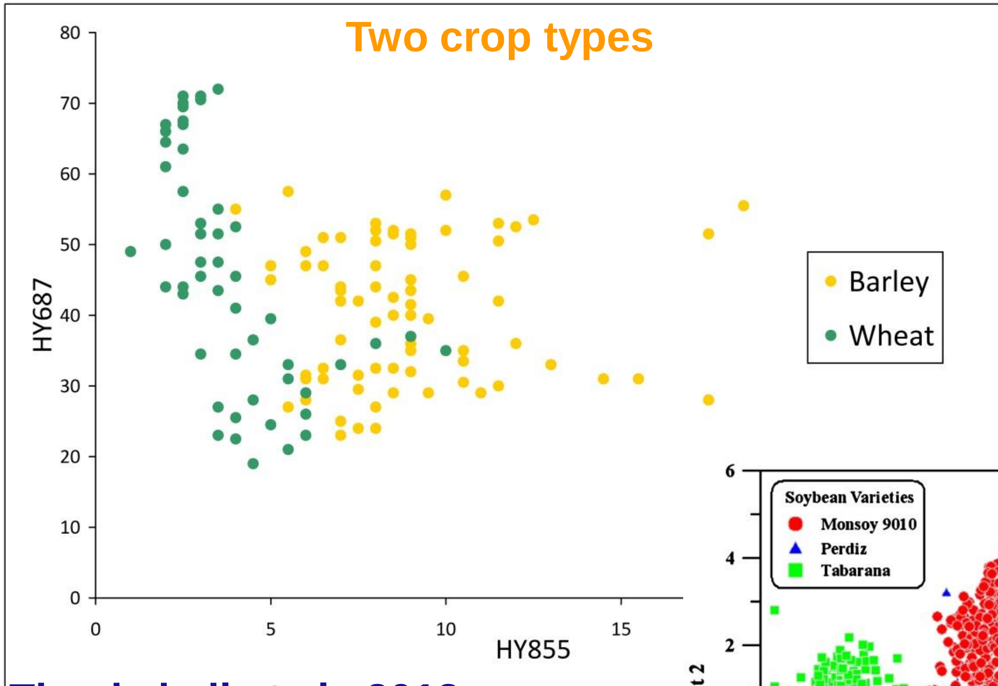

Thenkabail et al., 2012

Three soybean varieties

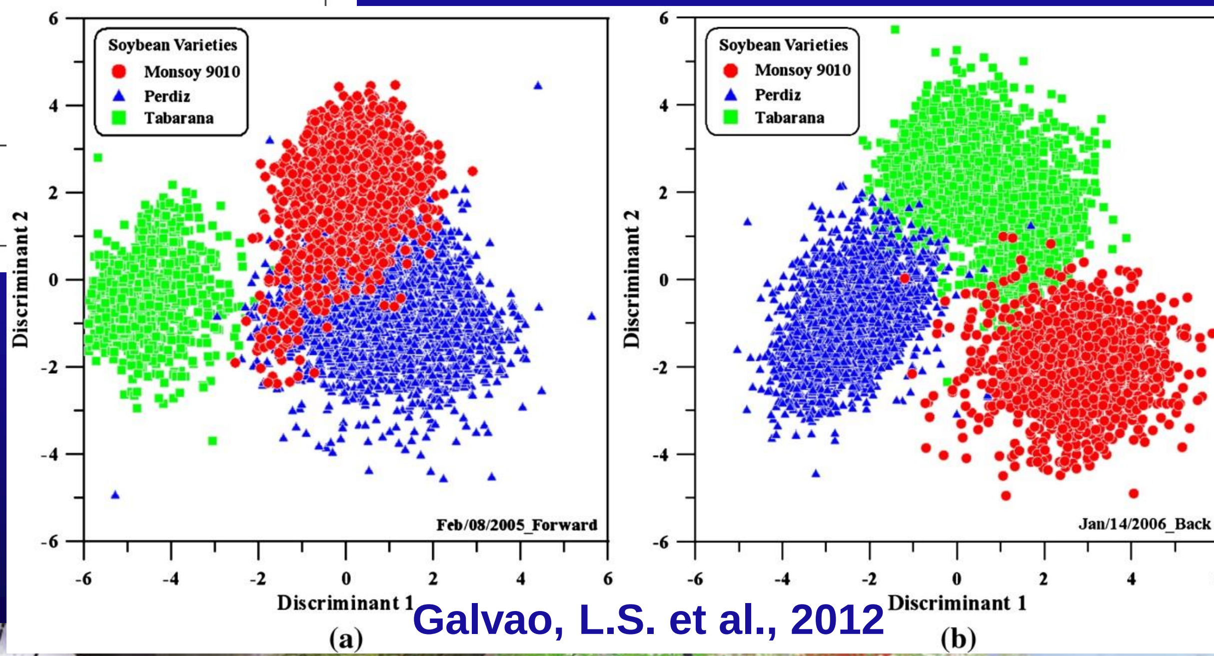

Galvao, L.S. et al., 2012

science for a changing world

U.S. Geological Survey
U.S. Department of Interior

Discriminating\Separating Vegetation Types

Note: Distinct separation of vegetation or crop types or species using distinct narrowbands

Broad-band (Landsat-5 TM) NIR vs. Red

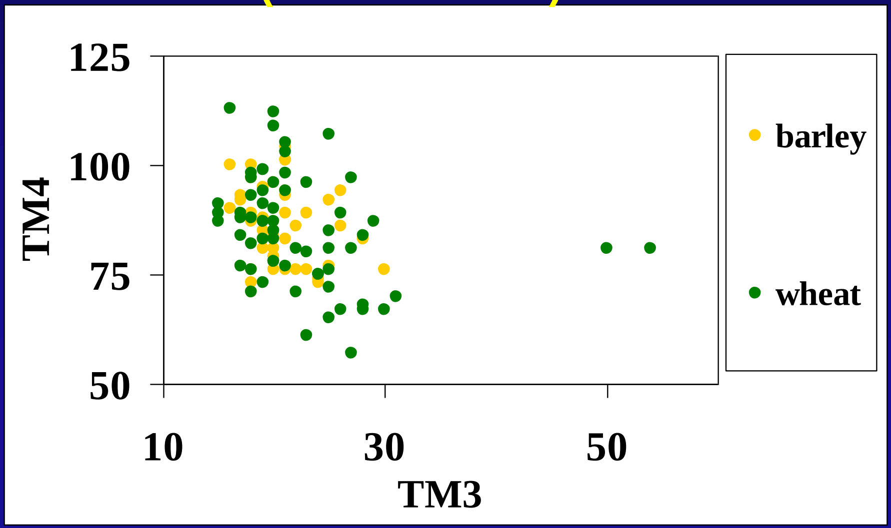

Narrow-band NIR vs. Red

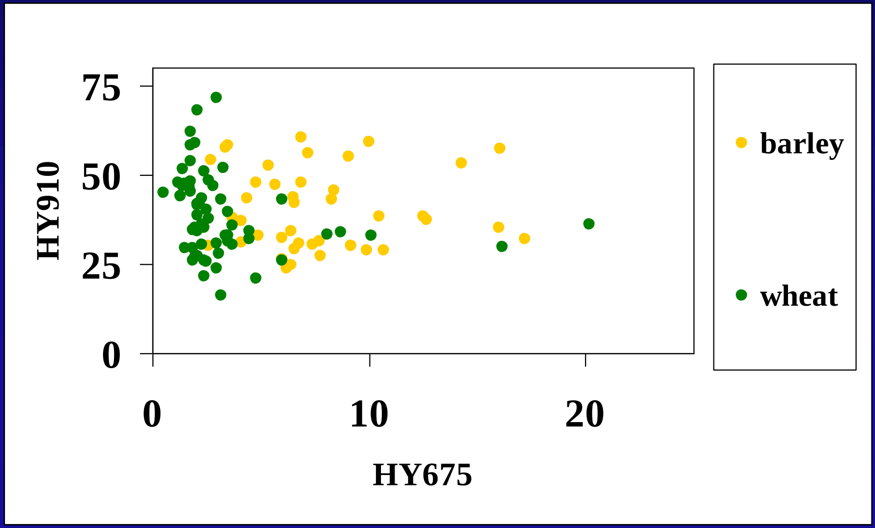

Barley

Wheat

Numerous narrow-bands provide unique opportunity to discriminate different crops and vegetation.

Improved Classification Accuracies (and reduced Errors and uncertainties)

Stepwise Discriminant Analysis (SDA)- Wilks' Lambda to Test : How Well Different Forest Vegetation are Discriminated from One Another

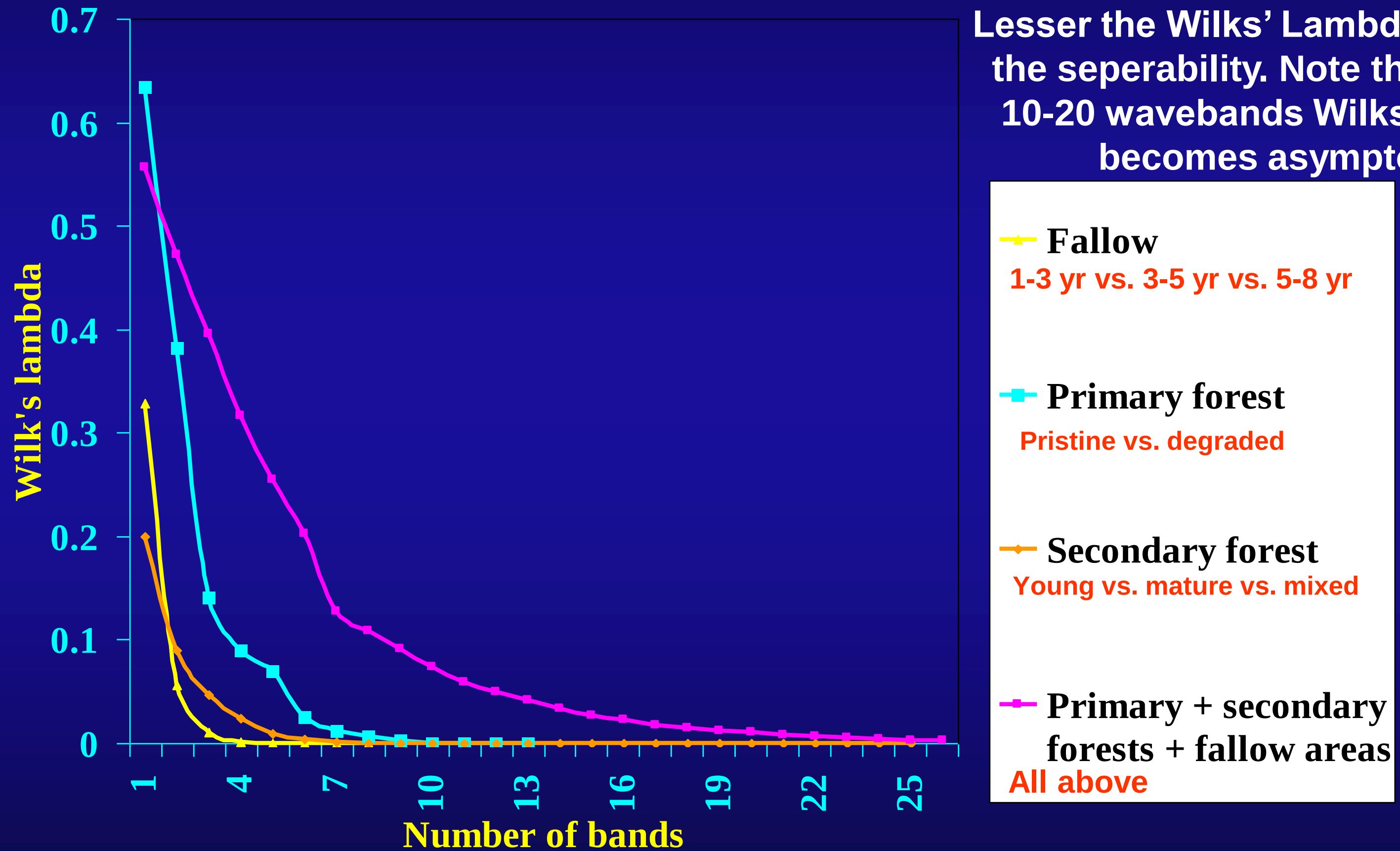

Lesser the Wilks' Lambda greater is the seperability. Note that beyond 10-20 wavebands Wilks' Lambda becomes asymptotic.

Hyperion Hyperspectral Narrowband Data versus Landsat ETM+ Broadband Data on Agricultural Crops

Wilk's Lambda of Broadband vs. Hyperspectral Narrowband data

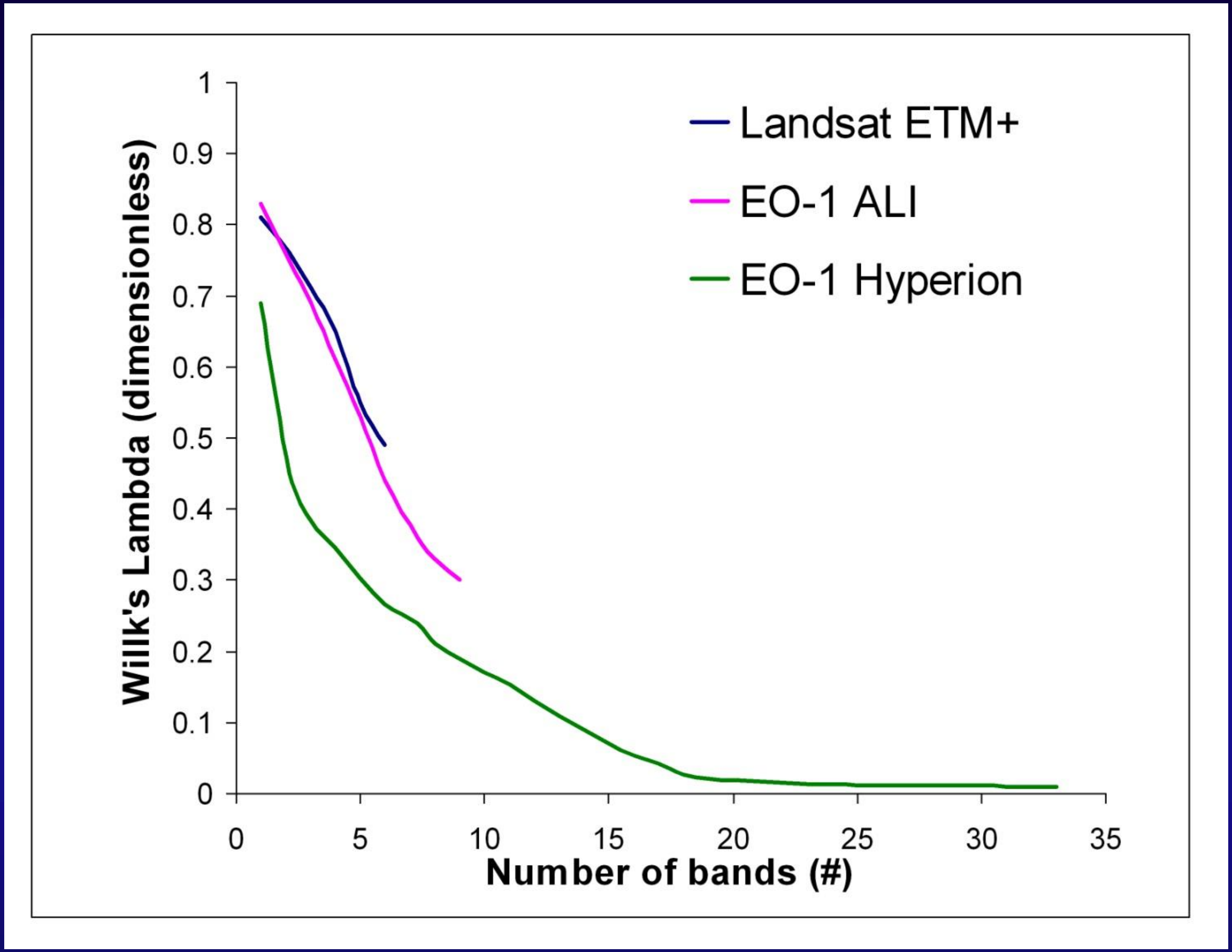

Separating eight major crops of the world based on Wilks' Lambda stepwise discriminant analysis (SDA) method using: (a) broadband data of Landsat ETM+ and EO-1 ALI, and (b) hyperspectral narrowband (HNB) data of EO-1 Hyperion using some of the data of three study areas. Note: the smaller the Wilks' Lambda the greater the separability. A Wilks' Lambda of 1 means perfect separability. It took about 25 HNBs to achieve near perfect separability between eight crops.

Methods of Hyperspectral Data Analysis
Spectral Matching Techniques (SMTs)
Agriculture and Vegetation

Quantitative Spectral Matching Techniques (SMTs)

Methods and Concepts of Quantitative SMTs

Quantitative SMTs compare class spectra of one class with class spectra of every other class & determine, quantitatively, similarities and dissimilarities between classes through automated process; facilitates rapid identification of classes.

1. Spectral Correlation Similarity (SCS)

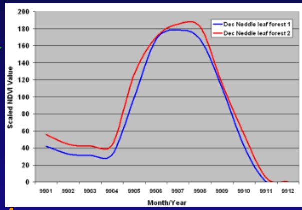

a. shape measure

b. Values vary between 0 to 1 (theoretically between -1 and +1).

Negative values have no meaning here. Ignore.

Note: Greater the SCS greater is the similarity between class spectra and target spectra

2. Spectral Similarity Value (SSV)

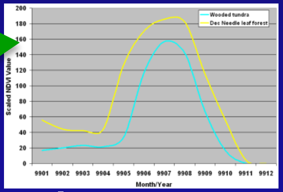

a. Shape and magnitude measure

b. Values vary between 0 to 1.415

Note: Smaller the SSV value greater the similarity between class spectra and target spectra

3. Modified Spectral Angle similarity (MSAS)

a. hyper-angle measure

b. practical implementation was difficult, hence dropped.

Note: Euclidian distance was a distance measure. We dropped it since SSV and SCS perform better.

Reference: Thenkabail, P.S., GangadharaRao, P., Biggs, T., Krishna, M., and Turral, H., 2007. Spectral Matching Techniques to Determine Historical Land use/Land cover (LULC) and Irrigated Areas using Time-series AVHRR Pathfinder Datasets in the Krishna River Basin, India. Photogrammetric Engineering and Remote Sensing. 73(9): 1029-1040. (Second Place Recipients of the 2008 John I. Davidson ASPRS President's Award for Practical papers).

Hyperspectral Narrowband Study of Agricultural Crops

Methods of Hyperspectral Data Analysis: Spectral Matching Techniques

In spectral matching techniques you

match

class spectra with

ideal spectra or target spectra

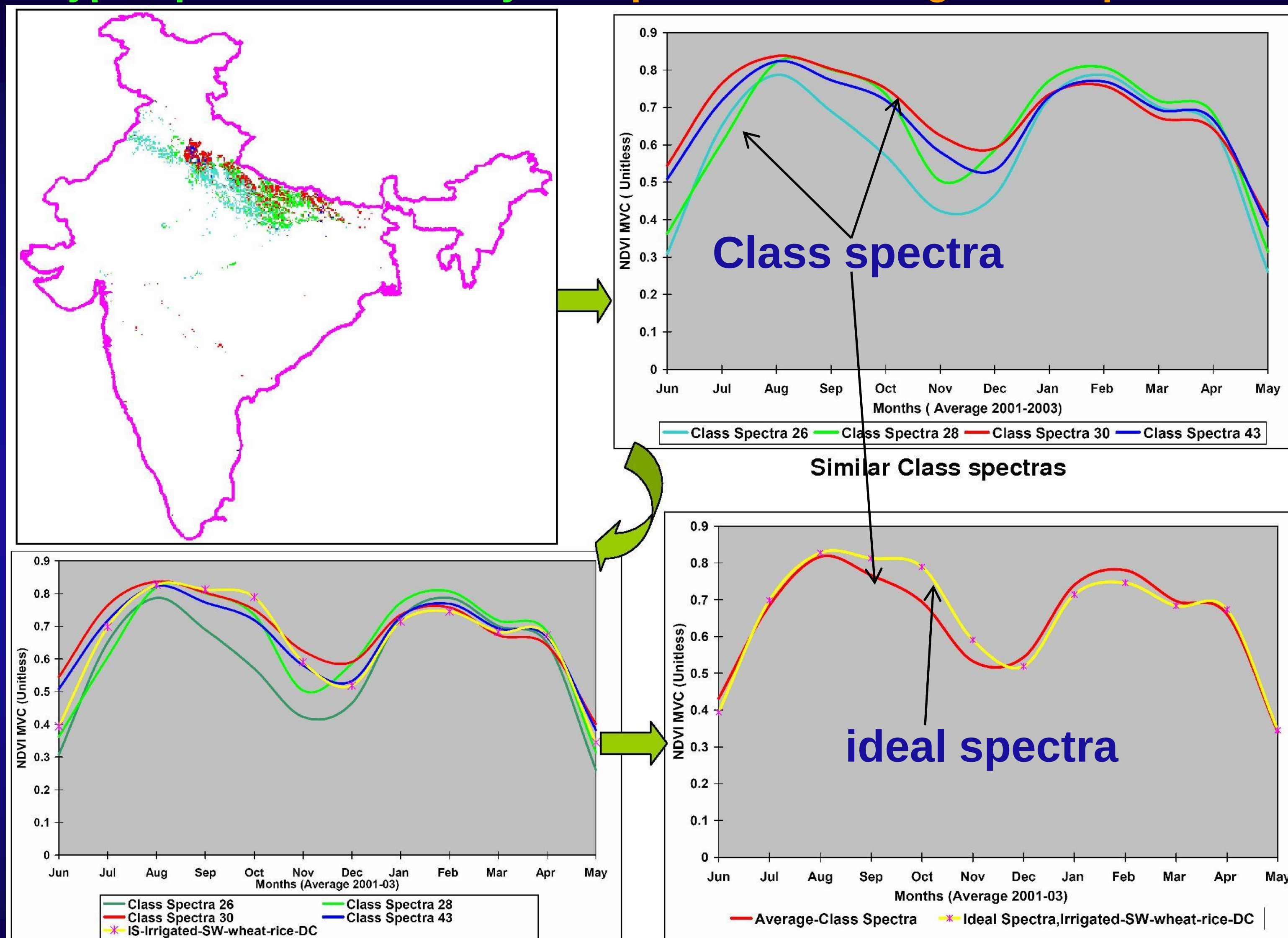

Matching Ideal Spectra with similar class spectras

Ideal Spectra Matches with class spectras

USGS
science for a changing world

U.S. Geological Survey
U.S. Department of Interior

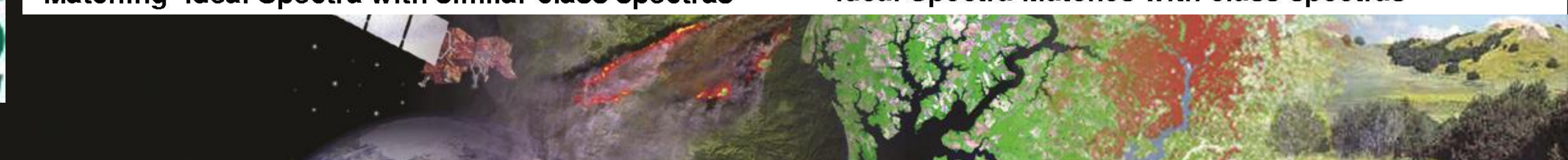

Methods of Hyperspectral Data Analysis
Classification Accuracies
Agriculture and Vegetation

Hyperspectral Narrowband Study of Agricultural Crops

Methods of Hyperspectral Data Analysis

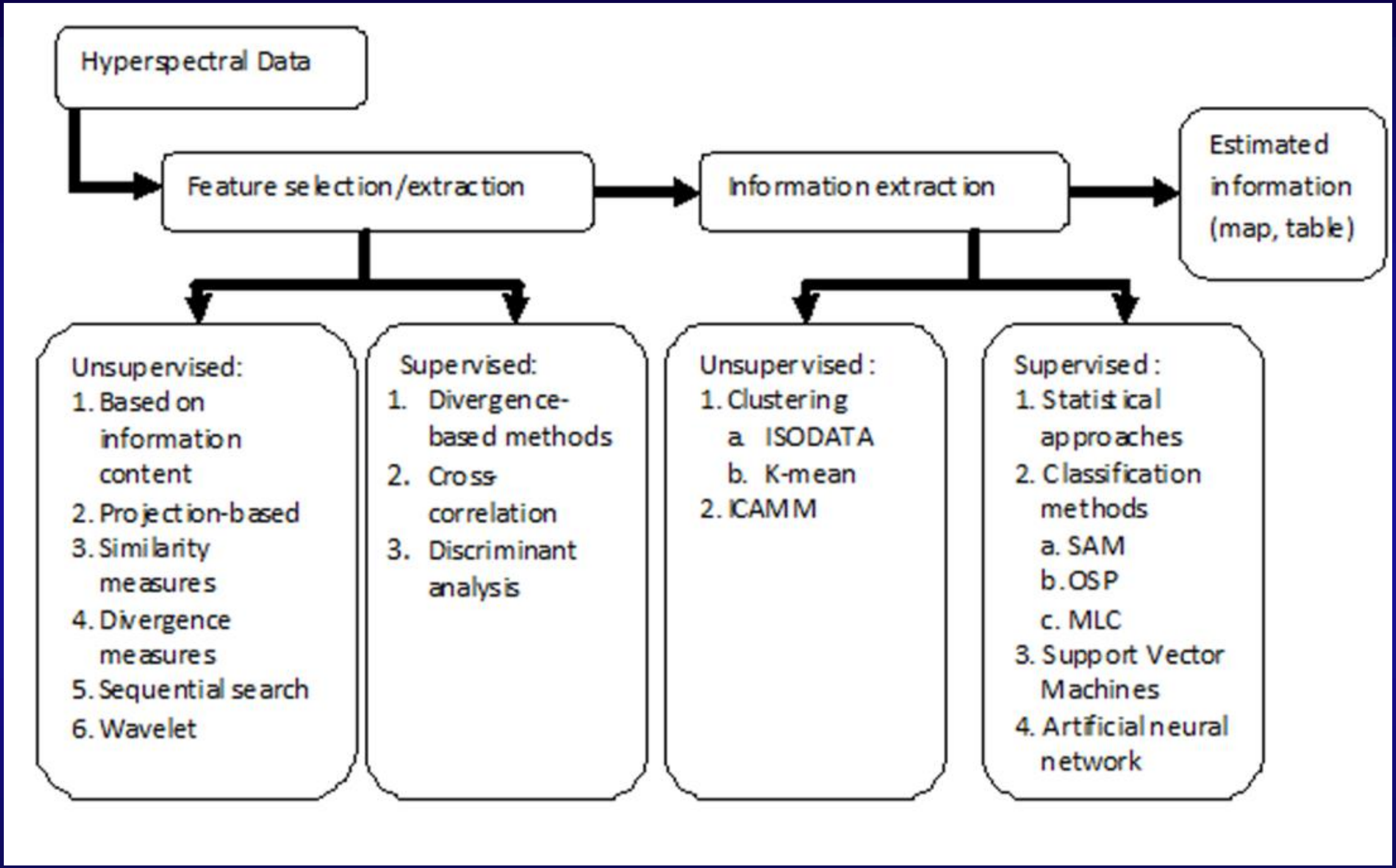

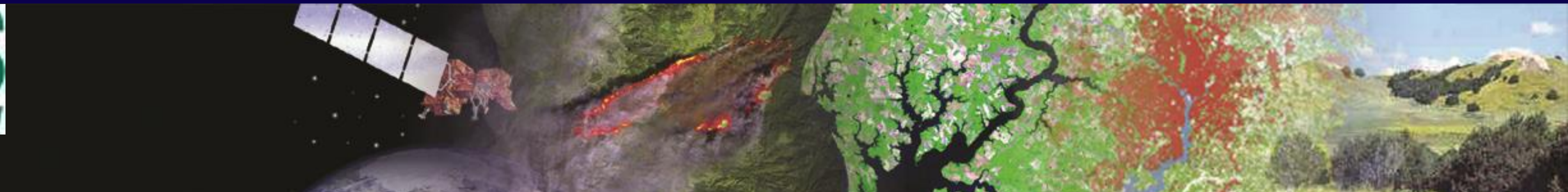

Improved Classification Accuracies (and reduced Errors and uncertainties)

Note: Overall Accuracies and K_{hat} Increase by about 30 % using 20 narrow-bands compared 6 non-thermal TM broad-bands in classifying 12 classes

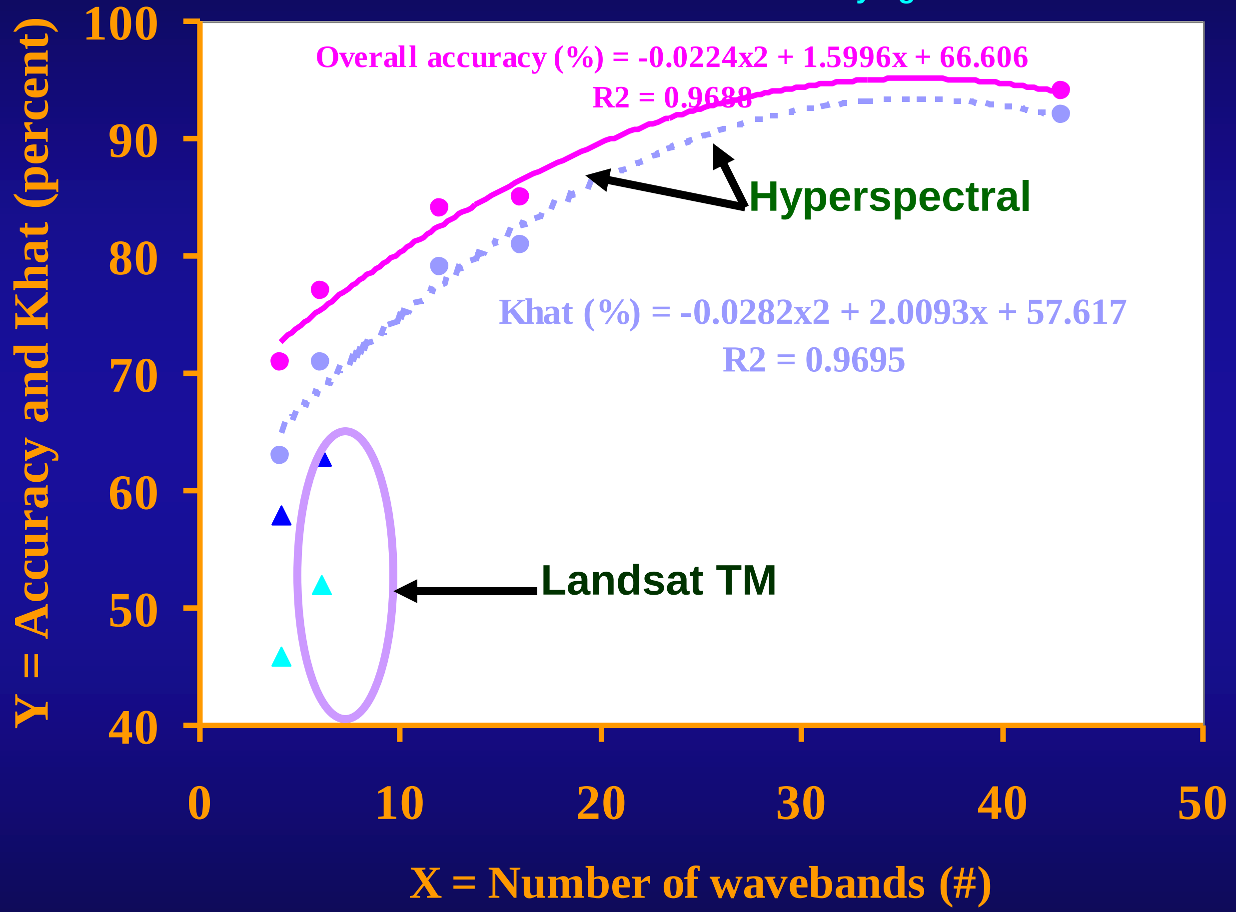

Note: Improved accuracies in vegetation type or species classification: Combination of these wavebands in Table 28.1 help provide significantly improved accuracies (10-30 %) in classifying vegetation types or species types compared to broadband data;

USGS
science for a changing world

U.S. Geological Survey
U.S. Department of Interior

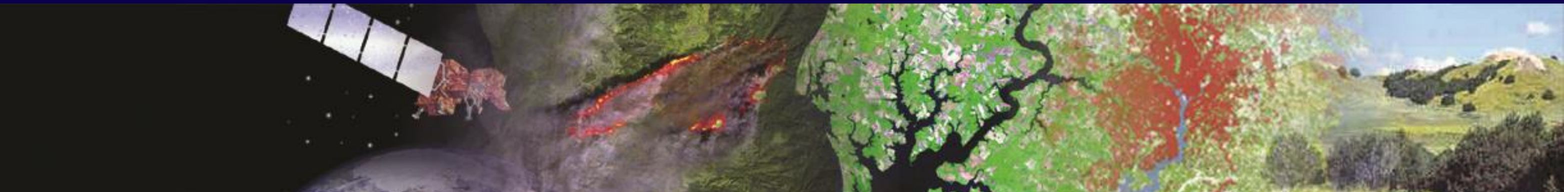

Methods of Classifying Vegetation Classes or Categories

Discriminant Model or Classification Criterion (DM) to Test

How Well 5 different Crops are Discriminated using 9 Narrowbands?

Generalized Squared Distance Function:

$$D_j^2(X) = (X-\bar{X}_j)' \, COV^{-1} \, (X-\bar{X}_j)$$

Posterior Probability of Membership in each CROPTY:

$$Pr(j|X) = \exp(-.5 \, D_j^2(X)) \; / \; SUM_k \exp(-.5 \, D_k^2(X))$$

Number of Observations and Percent Classified into weed

From weed	ag	as	cao	cho	te	total	Errors of commission
ag	51 85.00	2 3.33	5 8.33	2 3.33	0 0.00	60	15
as	0 0.00	22 75.86	0 0.00	0 0.00	7 24.14	29	24
cao	2 9.09	0 0.00	20 90.91	0 0.00	0 0.00	22	9
cho	0 0.00	0 0.00	0 0.00	67 100.00	0 0.00	67	0
te	0 0.00	1 5.00	1 5.00	0 0.00	18 90.00	20	11
total	53	25	26	69	25	198	
Errors of omission	4	12	6	3	28		

178

Overall accuracy = 89.9 %

(i.e., 178/198)

$$K_{hat} = \left(N \sum_{i=1}^{R} X_{ii} - \sum_{i=1}^{r} X_{+i} * X_{i+}\right) / \left(N^2 - \sum_{i=1}^{r} X_{i+} * X_{+i}\right)$$

where, r is the number of rows in the matrix, X_{ii} is the number of observations in row i and column i, X_{i+} and X_{+i} are the marginal totals of i and column i respectively and N is the total number of observations (Bishop et al. 1975).

Thereby,

K_{hat} = ((198)* (178) - (9,600)) / ((198)^2 - (9,600))

Where, (53*60) + (25*29) + (26*22) + (69*67) + (25*20) = 9,600

K_{hat} = 0.87

Methods of Classifying Vegetation Classes or Categories
Using hyperspectral narrowband data

1. Multivariate and Partial Least Square Regression,
2. Discriminant analysis
3. unsupervised classification (e.g., Clustering),
4. supervised approaches
   - A. Spectral-angle mapping or SAM,
   - B. Maximum likelihood classification or MLC,
   - C. Artificial Neural Network or ANN,
   - D. Support Vector Machines or SVM,
4. Spectral Matching Technique (SMT)

Excellent for full spectral analysis…..but needs good spectral library

………All these methods have merit; it remains for the user to apply them to the situation of interest.

Hyperion Hyperspectral Narrowband Data versus Landsat ETM+ Broadband Data on Agricultural Crops

Wilk's Lambda of Broadband vs. Hyperspectral Narrowband data

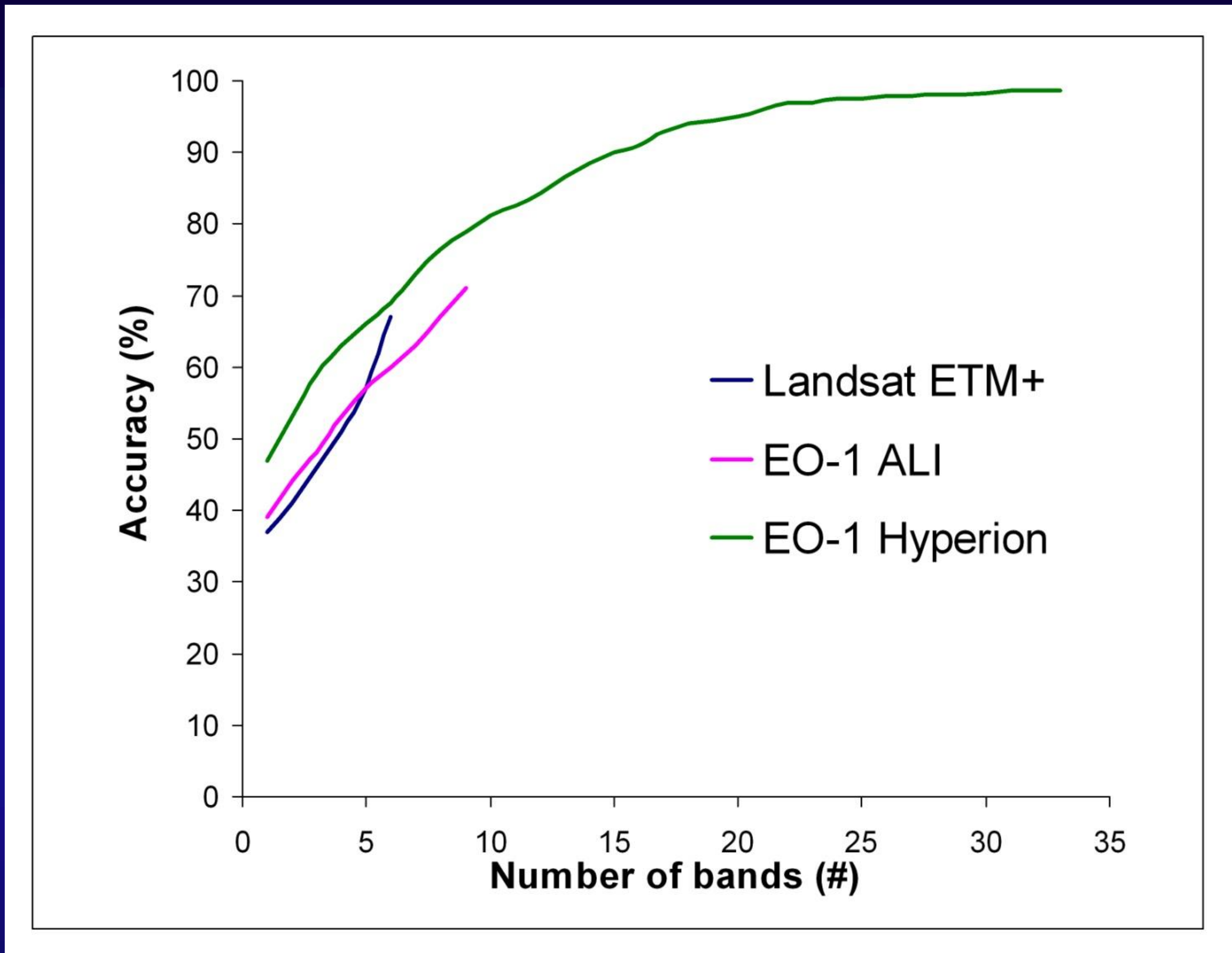

Crop classification performance of hyperspectral narrowbands (HNBs) versus multispectral broadbands (MBBs). Overall accuracies in classifying five agricultural crops using simulated reflectance field spectra of Landsat ETM+ and EO-1 ALI broadband Landsat broadbands vs. Hyperion hyperspectral narrowbands. Overall accuracies attained using six non-thermal Landsat bands was about 60% whereas about 20 hyperspectral narrow bands provided about 90% overall accuracy. Beyond 20 bands, any increase in accuracy with increase in additional bands is very minor.

Key Knowledge Gains and Knowledge Gaps
Hyperspectral Study of Crops and Vegetation

Overcoming Hughes' Phenomenon

1. Overcoming the Hughes phenomenon (or the curse of high dimensionality of hyperspectral data)

Reduce data volumes significantly by eliminating redundant bands and focusing on the most valuable hyperspectral narrowbands to study agricultural crops and vegetation.

Note:

A. Optimal hyperspectral narrowbands (HNBs) Table (next 3 slides). Leave out redundant bands;

B. Overcoming Hughes' Phenomenon: If the number of bands remained high, the number of observations required to train a classifier increases exponentially to maintain classification accuracies. Data volumes are reduced through data mining methods such as feature selection (e.g., principal component analysis, derivative analysis, wavelets), lambda by lambda correlation plots, and vegetation indices. Data mining methods lead to: (a) reduction in data dimensionality, (b) reduction in data redundancy, and (c) extraction of unique information.

Optimal Hyperspectral Narrowbands (HNBs) for Agriculture and Vegetation

Waveband Centers, Waveband Widths, and Targeted Application in 400-2500 nm

Table 2. Optimal (non-redundant) hyperspectral narrowbands to study vegetation and agricultural crops[1,2,3] [modified and adopted from Thenkabail et al., 2014, 2013, 2011, 2004a, 2004b, 2002, 2000].

Waveband number #	Waveband range λ	Waveband center λ	Waveband width Δλ	Importance and physical significance of waveband in vegetation and cropland studies
A. Ultrviolet				
1	373-377	375	5	fPAR, leaf water: fraction of photosynthetically active radiation (fPAR), leaf water content
B. Blue bands				
2	403-407	405	5	Nitrogen, Senescing: sensitivity to changes in leaf nitrogen. reflectance changes due to pigments is moderate to low. Sensitive to senescing (yellow and yellow green leaves).
3	491-500	495	10	Carotenoid, Light use efficiency (LUE), Stress in vegetation: Sensitive to senescing and loss of chlorophyll\browning, ripening, crop yield, and soil background effects
C. Green bands				
4	513-517	515	5	Pigments (Carotenoid, Chlorophyll, anthocyanins), Nitrogen, Vigor: positive change in reflectance per unit change in wavelength of this visible spectrum is maximum around this green waveband
5	530.5-531.5	531	1	Light use efficiency (LUE), Xanophyll cycle, Stress in vegetation, pest and disease: Senescing and loss of chlorophyll\browning, ripening, crop yield, and soil background effects
6	546-555	550	10	Chlorophyll: Total chlorophyll; Chlorophyll/carotenoid ratio, vegetation nutritional and fertility level; vegetation discrimination; vegetation classification
7	566-575	570	10	Pigments (Anthrocyanins, Chlorophyll), Nitrogen: negative change in reflectance per unit change in wavelength is maximum as a result of sensitivity to vegetation vigor, pigment, and N.
D. Red bands				
8	676-685	680	10	Biophysical quantities and yield: leaf area index, wet and dry biomass, plant height, grain yield, crop type, crop discrimination
E. Red-edge bands				
9	703-707	705	5	Stress and chlorophyll: Nitrogen stress, crop stress, crop growth stage studies
10	718-722	720	5	Stress and chlorophyll: Nitrogen stress, crop stress, crop growth stage studies
11	700-740	700-740	700-740	Chlorophyll, senescing, stress, drought: first-order derivative index over 700-740 nm has applications in vegetation studies (e.g., blue-shift during stress and red-shift during healthy growth)
F. Near infrared (NIR) bands				
12	841-860	850	20	Biophysical quantities and yield: LAI, wet and dry biomass, plant height, grain yield, crop type, crop discrimination, total chlorophyll
13	886-915	900	20	Biophysical quantities, Yield, Moisture index: peak NIR reflectance. Useful for computing crop moisture sensitivity index, NDVI; biomass, LAI, Yield.

Thenkabail et al. 2015

……Continued in next slide

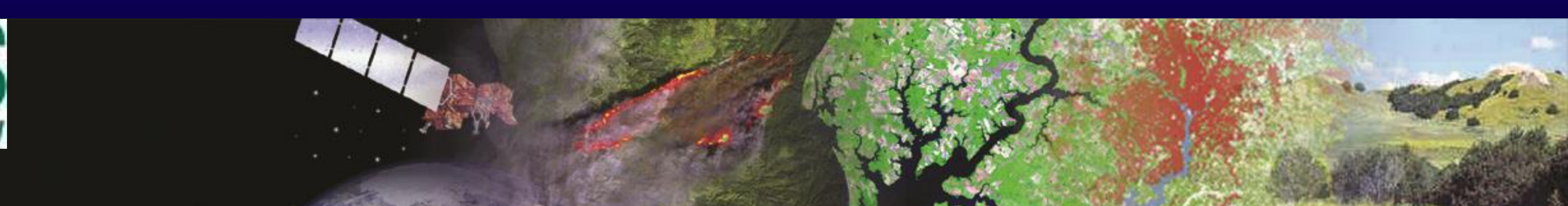

Optimal Hyperspectral Narrowbands (HNBs) for Agriculture and Vegetation
Waveband Centers, Waveband Widths, and Targeted Application in 400-2500 nm

G. Near infrared (NIR) bands				
14	961-980	970	20	Plant moisture content Center of moisture sensitive "trough"; water band index, leaf water, biomass;
H. Far near infrared (FNIR) bands				
15	1073-1077	1075	5	Biophysical and biochemical quantities: leaf area index, wet and dry biomass, plant height, grain yield, crop type, crop discrimination, total chlorophyll, anthocyanin, carotenoids
16	1178-1182	1080	5	Water absorption band
17	1243-1247	1245	5	Water sensitivity: water band index, leaf water, biomass. Reflectance peak in 1050-1300 nm.
I. Early short-wave infrared (ESWIR) bands				
18	1448-1532	1450	5	Vegetation classification and discrimination: ecotype classification; plant moisture sensitivity. Moisture absorption trough inearly short wave infrared (ESWIR)
19	1516-1520	1518	5	Moisture and biomass: A point of most rapid rise in spectra with unit change in wavelength in SWIR. Sensitive to plant moisture.
20	1648-1652	1650	5	Heavy metal stress, Moisture sensitivity: Heavy metal stress due to reduction in Chlorophyll. Sensitivity to plant moisture fluctuations in ESWIR. Use as an index with 1548 or 1620 or 1690 nm..
21	1723-1727	1725	5	Lignin, biomass, starch, moisture: sensitive to lignin, biomass, starch. Discrimiating crops and vegetation.
J. Far short-wave infrared (FSWIR) bands				
22	1948-1952	1950	5	Water absorption band: highest moisture absorption trough in FSWIR. Use as an index with any one of 2025 nm, 2133 nm, and 2213 am. Affected by noise at times.
23	2019-2027	2023	8	Litter (plant litter), lignin, cellulose: litter-soil differentiation: moderate to low moisture absorption trough in FSWIR. Use as an index with any one of 2025 nm, 2133 nm, and 2213 am.
24	2131-2135	2133	5	Litter (plant litter), lignin, cellulose: typically highest refectivity in FSWIR for vegetation. Litter-soil differentiation
25	2203-2207	2205	5	Litter, lignin, cellulose, sugar, startch, protein; Heavy metal stress: typically, second highest reflectivity in FSWIR for vegetation. Heavy metal stress due to reduction in Chlorophyll
26	2258-2266	2262	8	Moisture and biomass: moisture absorption trough in far short-wave infrared (FSWIR). A point of most rapid change in slope of spectra based on land cover, vegetation type, and vigor.
27	2293-2297	2295	5	Stress: sensitive to soil background and plant stress
28	2357-2361	2359	5	Cellulose, protein, nitrogen: sensitive to crop stress, lignin, and starch
Note:				
1 = most hyperspectral narrowbands (HNBs)_ that adjoin one another are highly correlated for a given application. Hence from a large number of HNBs, these non-redundant (optimal) bands are selected				
2 = these optimal HNBs are for studying vegetation and agricultural crops. When we use some or all of these wavebands, we can attain highest possible classification accuracies in classifying vegetation categories or crop types				
3 = wavebands selected here are based on careful evaluation of large number of studies.				

Thenkabail et al. 2015

……Continued from previous slide

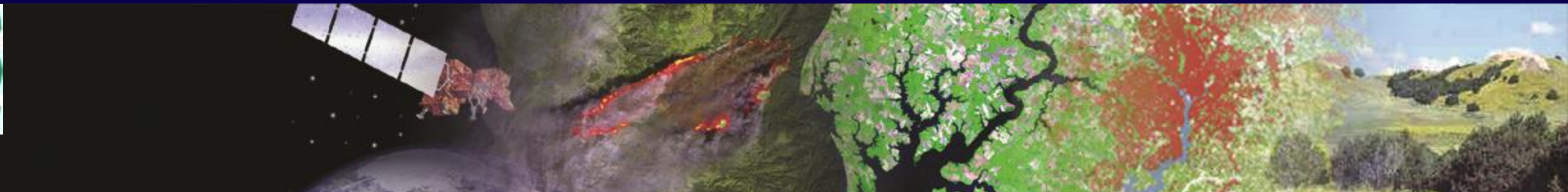

Optimal Hyperspectral Narrowbands (HNBs) for Agriculture and Vegetation

Waveband Centers, Waveband Widths, and Targeted Application in 400-2500 nm

Waveband	Waveband	Waveband	Waveband
number	range	center	width
#	λ	λ	Δλ
A. Ultrviolet			
1	373-377	375	5
B. Blue bands			
2	403-407	405	5
3	491-500	495	10
C. Green bands			
4	513-517	515	5
5	530.5-531.5	531	1
6	546-555	550	10
7	566-575	570	10
D. Red bands			
8	676-685	680	10
E. Red-edge bands			
9	703-707	705	5
10	718-722	720	5
11	700-740	700-740	700-740
F. Near infrared (NIR) bands			
12	841-860	850	20
13	886-915	900	20

Thenkabail et al. 2015

Waveband	Waveband	Waveband	Waveband
number	range	center	width
#	λ	λ	Δλ
G. Near infrared (NIR) bands			
14	961-980	970	20
H. Far near infrared (FNIR) bands			
15	1073-1077	1075	5
16	1178-1182	1080	5
17	1243-1247	1245	5
I. Early short-wave infrared (ESWIR) bands			
18	1448-1532	1450	5
19	1516-1520	1518	5
20	1648-1652	1650	5
21	1723-1727	1725	5
J. Far short-wave infrared (FSWIR) bands			
22	1948-1952	1950	5
23	2019-2027	2023	8
24	2131-2135	2133	5
25	2203-2207	2205	5
26	2258-2266	2262	8
27	2293-2297	2295	5
28	2357-2361	2359	5

Optimal Hyperspectral Narrowbands (HNBs) for Agriculture and Vegetation

Waveband Centers, Waveband Widths, and Targeted Application in 400-2500 nm

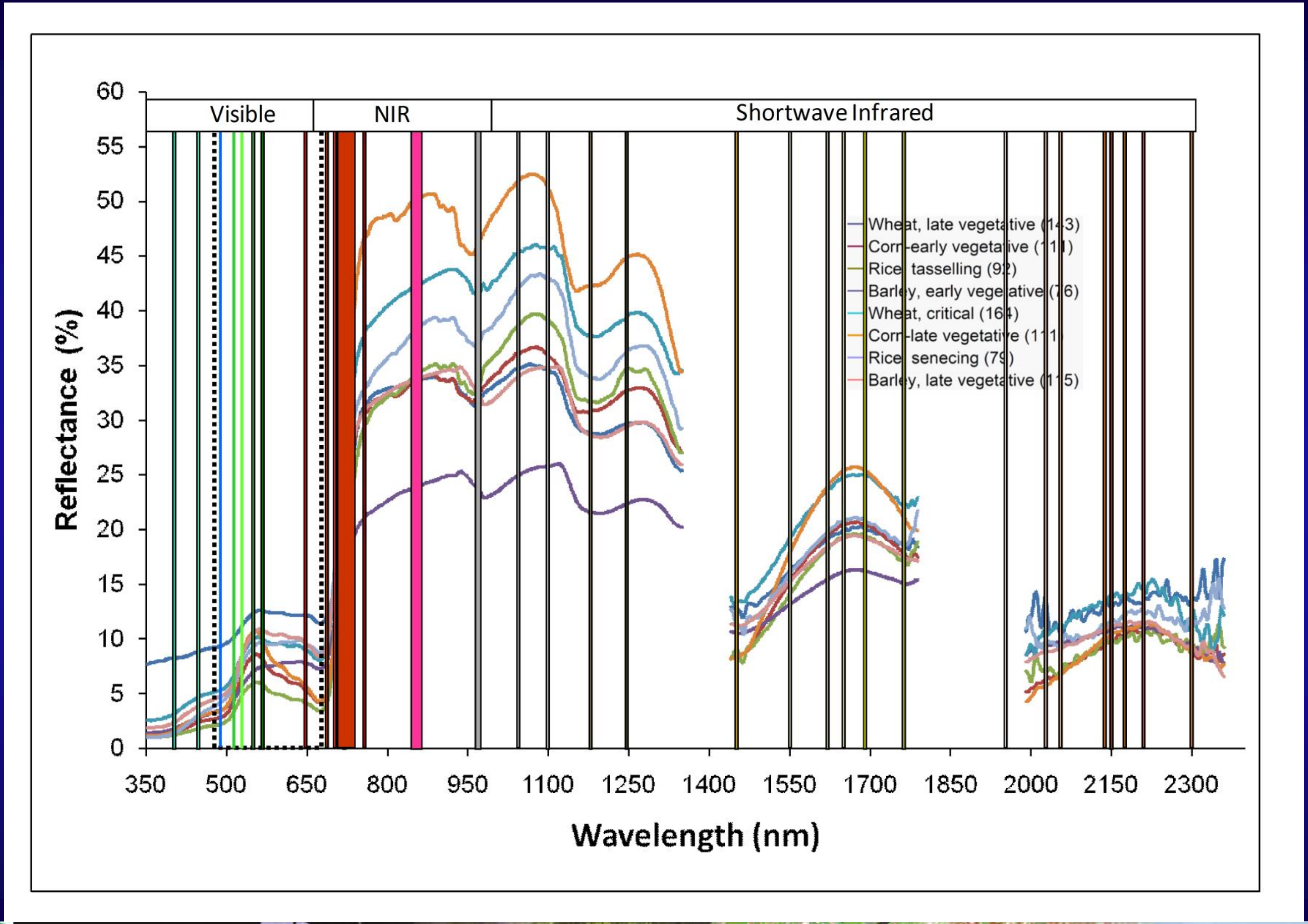

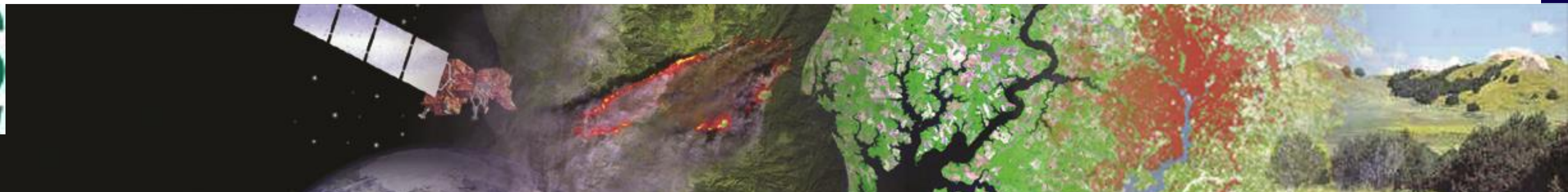

Targeted Hyperspectral Narrowbands (HNBs)

2. Narrowbands targeted to study specific vegetation biophysical and biochemical variable:

Each waveband in Table is uniquely targeted to study specific vegetation biophysical, and biochemical properties and/or captures specific events such as plant stress.

Note:

A. Targeted hyperspectral narrowbands (HNBs) in previous 3 slides: selecting Optimal bands, eliminating redundant bands.

2. Examples of targeted HNBs: For example:

i. waveband centered at 550 nm provided excellent sensitivity to plant nitrogen,
ii. waveband centered at 515 nm is best for pigments (carotenoids, anthocyanins), wavebands centered at 970 or 1245 nm was ideal to study plant moisture fluctuations, and
iii. Lignin, cellulose, protein, and nitrogen have relatively low reflectance and strong absorption in SWIR bands by water that masks other absorption features.

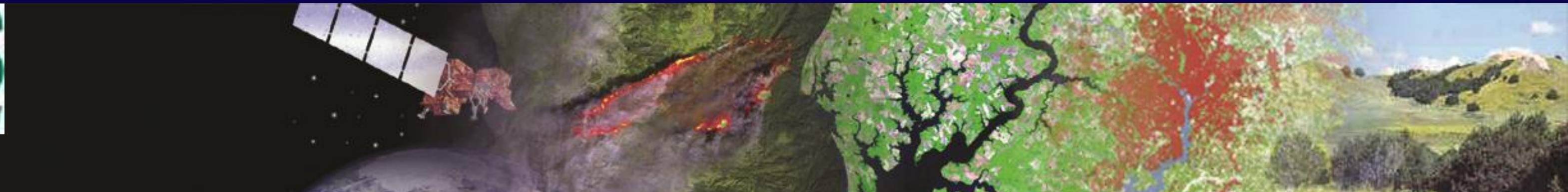

Targeted Hyperspectral Narrowbands (HNBs) in Study of Biochemical Properties

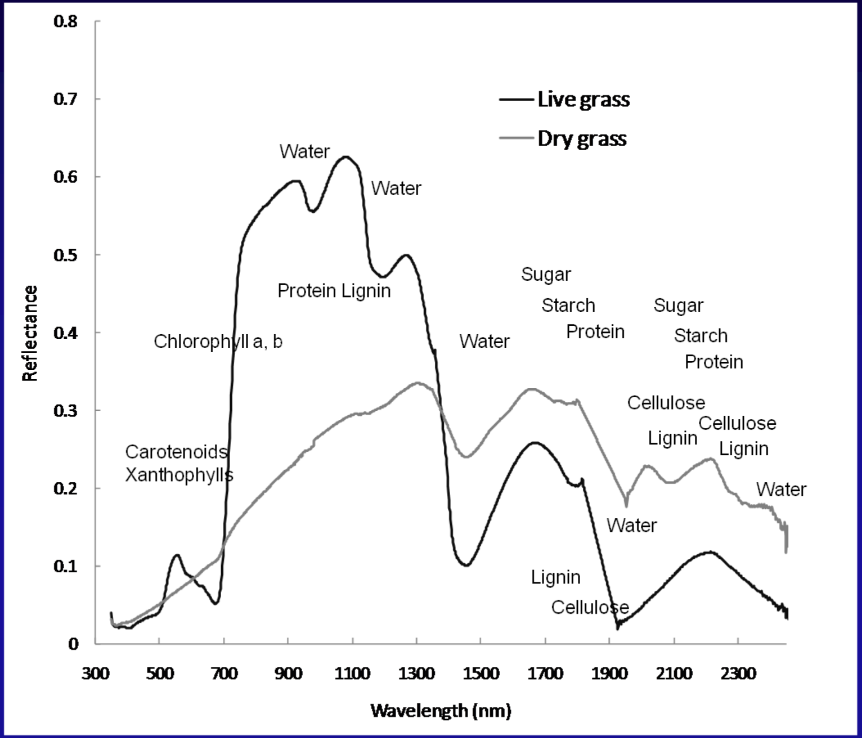

The reflectance spectra with characteristic absorption features associated with plant biochemical constitutents for live and dry grass (Adapted from Hill [13]).

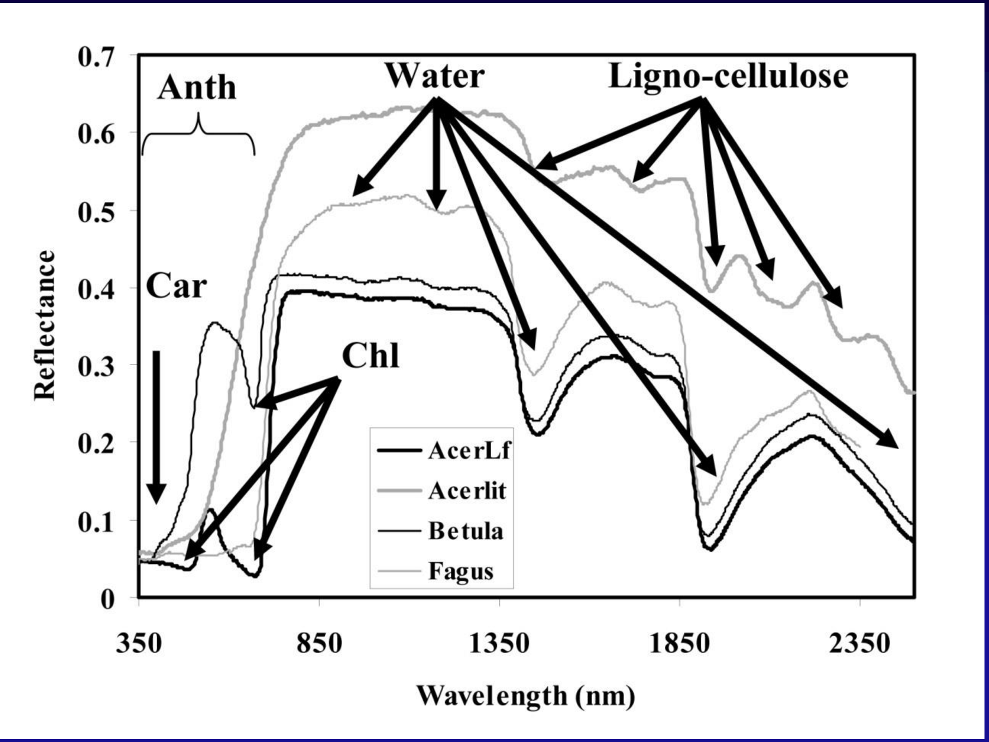

Reflectance spectra of leaves from a senesced birch (Betula), ornamental beech (Fagus) and healthy and fully senesced maple (AcerLf, Acerlit) illustrating Carotenoid (Car), Anthocyanin (Anth), Chlorophyll (Chl), Water and Ligno-cellulose absorptions.

See chapter 9; Thenkabail et al., 2012

See chapter 14; Thenkabail et al., 2012

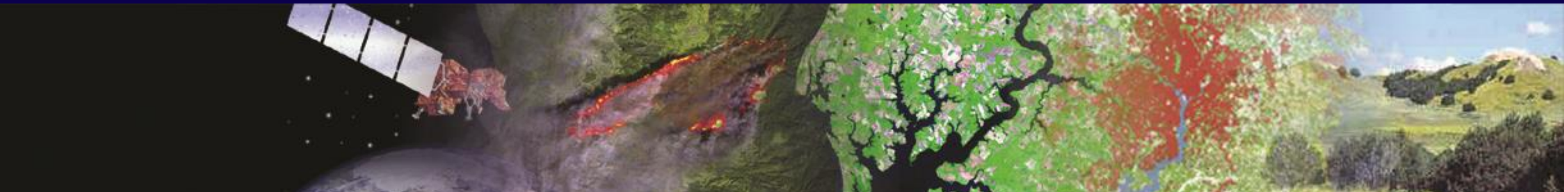

Targeted Hyperspectral Narrowbands (HNBs) in Study of Biophysical Properties

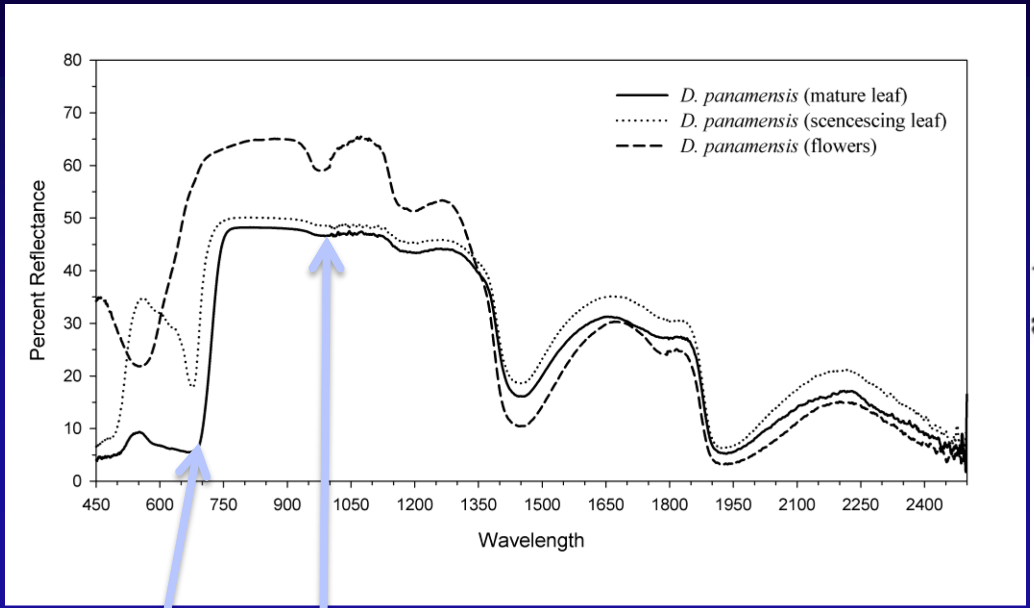

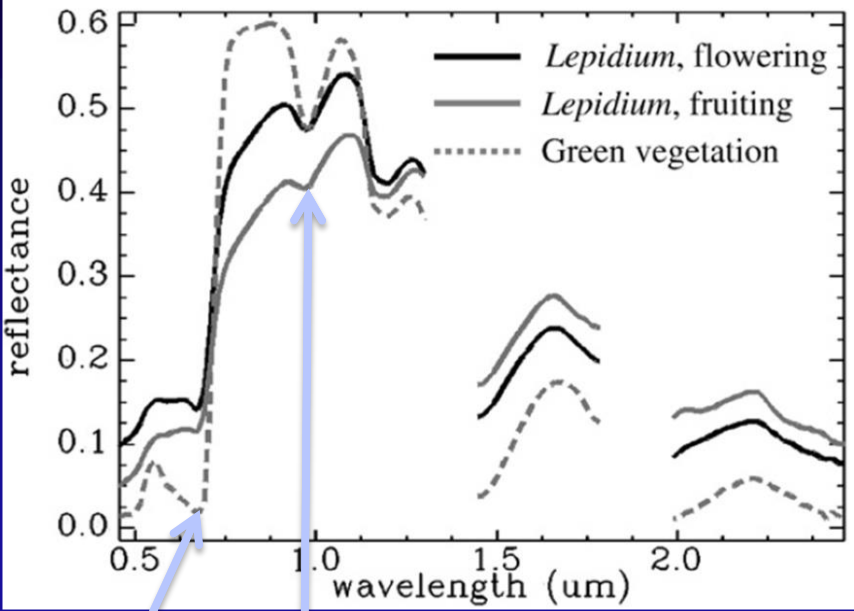

Greater the biomass, LAI, moisture, greater is absorption @ 680 nm

Greater the biomass, LAI, moisture, greater is absorption @ 970 nm

Greater the biomass, LAI, moisture, greater is absorption @ 680 nm

Greater the biomass, LAI, moisture, greater is absorption @ 970 nm

See chapter 18; in Thenkabail et al. 2012

See chapter 19; in Thenkabail et al., 2012

3. HVIs for Improved models of agricultural crops and vegetation biophysical and biochemical variables

HVIs provide significantly improved models of crop and vegetation quantities such as biomass, LAI, NPP, leaf nitrogen, chlorophyll, carotenoids, and anthocyanins.

Some of the Best Two-band Hyperspectral Vengetation Indices (HVIs)
In 400-2500 nm Waveband Range

Band number (#)	Hyperspectral narrowband (λ1)	Bandwidth (Δλ1)	Hyperspectral narrowband (λ2)	Bandwidth (Δλ2)	Hyperspectral vegetation index (HVI)	Best index under each catogory
I. Hyperspectral biomass and structural indices (HBSIs) [to best study biomass, LAI, palnt height, and grain yield]						
HBSI1	855	20	682	5	(855-682)/(855+682)	HBSI: Hyperspectral biomass and structural index
HBSI2	910	20	682	5	(910-682)/(910+682)	
HBSI3	550	5	682	5	(550-682)/(550+682)	
II. Hyperspectral biochemical indices (HBCIs) [pigments like carotenoids, anthocyanins as well as Nitrogen, chlorophyll]						
HBCI8	550	5	515	5	(550-515)/(550+515)	HBCI: Hyperspectral biochemical index
HBCI9	550	5	490	5	(550-490)/(550+490)	
III. Hyperspectral Red-edge indices (HREIs) [to best study plant stress, drought]						
HREI14	700-740	40	first-order derivative integrated over red-edge (700-740 nm)			HREI: Hyperspectral red-edge index
HREI15	855	5	720	5	(855-720)/(855+720)	
IV. Hyperspectral water and moisture indices (HWMIs) [to best study plant water and mosture]						
HWMI17	855	20	970	10	(855-970)/(855+970)	HWMI: Hyperspectral water and moisture index
HWMI18	1075	5	970	10	(1075-970)/(1075+970)	
HWMI19	1075	5	1180	5	(1075-1180)/(1075+1180)	
HWMI20	1245	5	1180	5	(1245-1180)/(1245+1180)	
V. Hyperspectral Light-use efficiency Index (HLEI)[to best study light use efficiency or LUE]						
HLUE24	570	5	531	1	(570-531)/(570+531)	HLEI: Hyperspectral light-use efficiency index
VI. Hyperspectral legnin cellulose index (HLCI) [to best study plant legnin, cellulose, and plant residue]						
HLCI25	2205	5	2025	1	(2205-2025)/(2205+2025)	HLCI: Hyperspectral legnin cellulose index

Some of the Best Two-band Hyperspectral Vengetation Indices (HVIs)
In 400-2500 nm Waveband Range

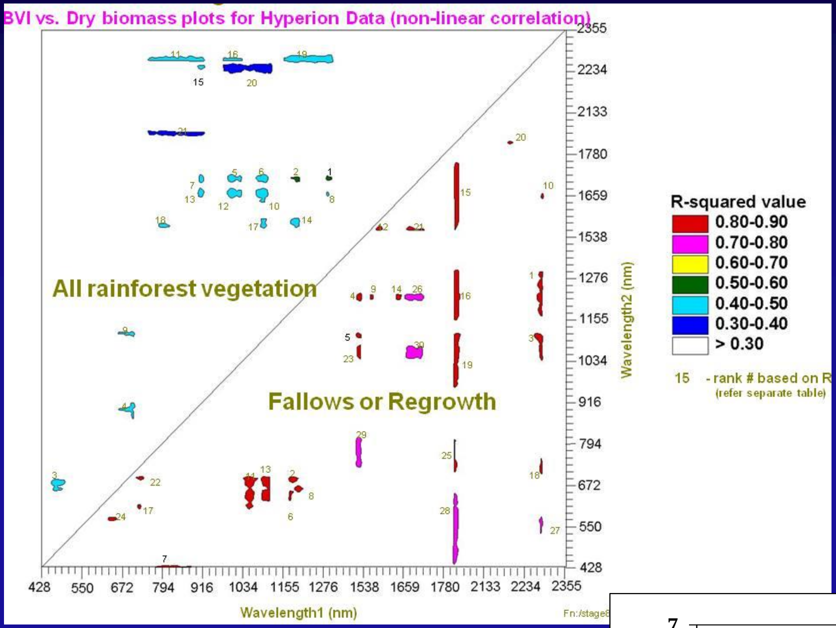

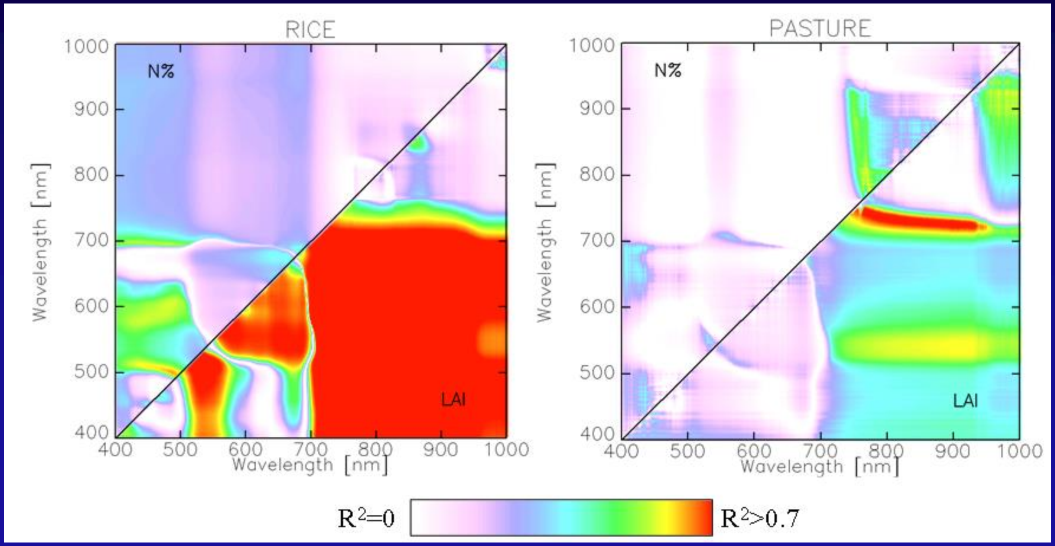

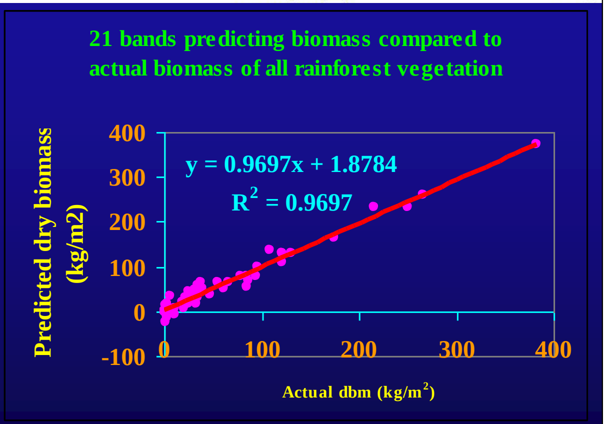

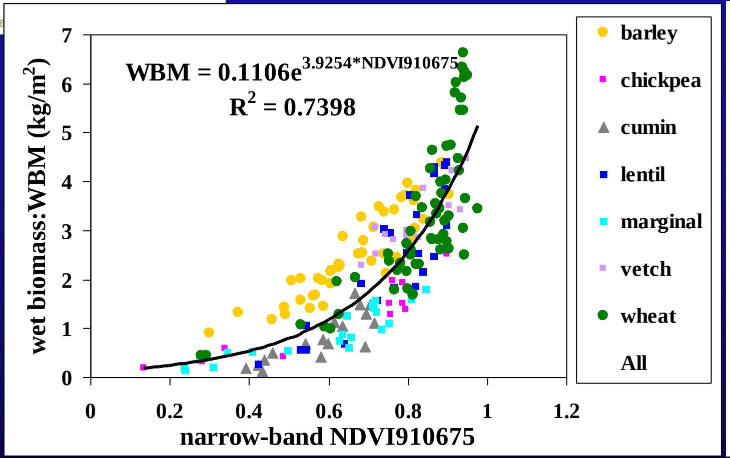

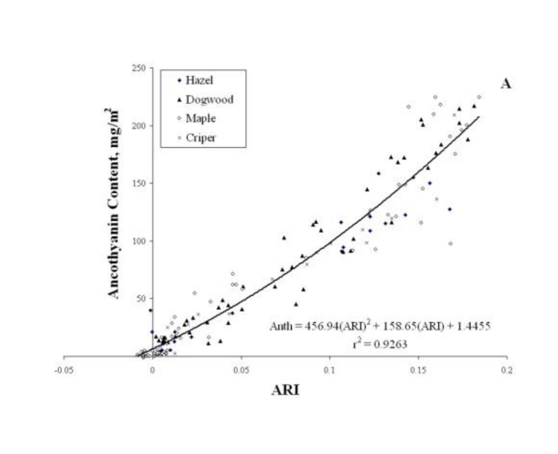

USGS
science for a changing world

U.S. Geological Survey
U.S. Department of Interior

Some of the Best Two-band Hyperspectral Vengetation Indices (HVIs)
In 400-2500 nm Waveband Range

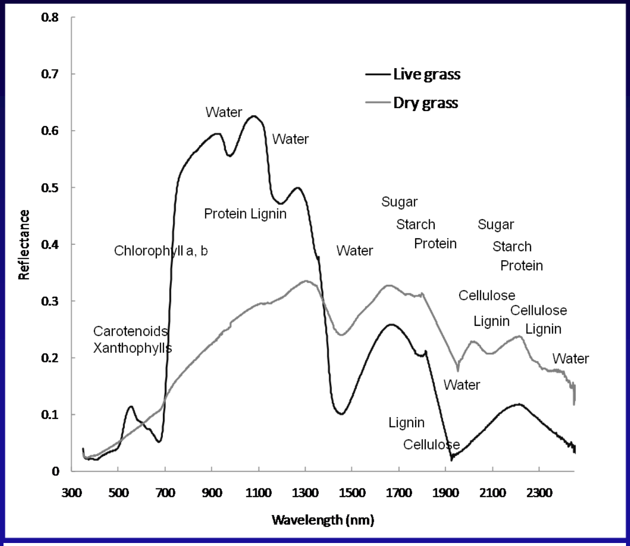

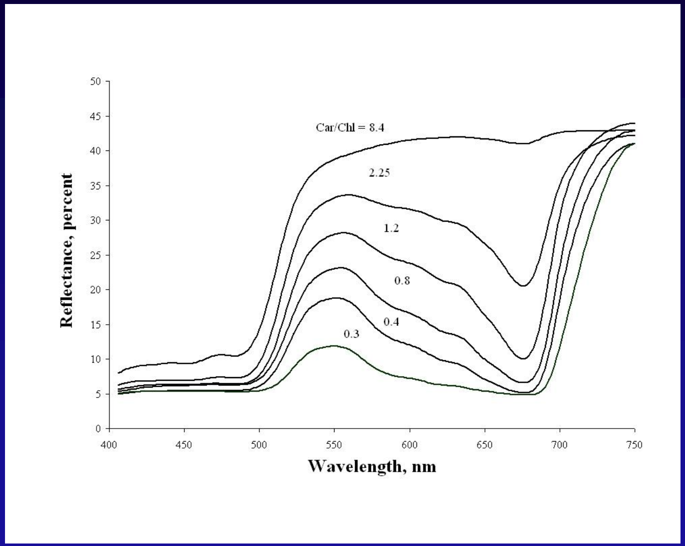

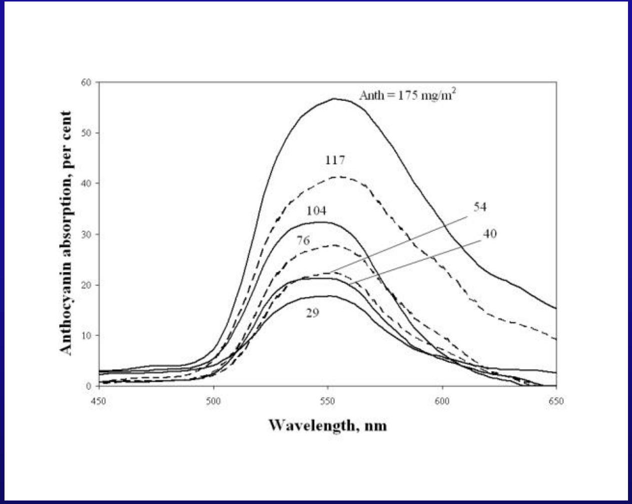

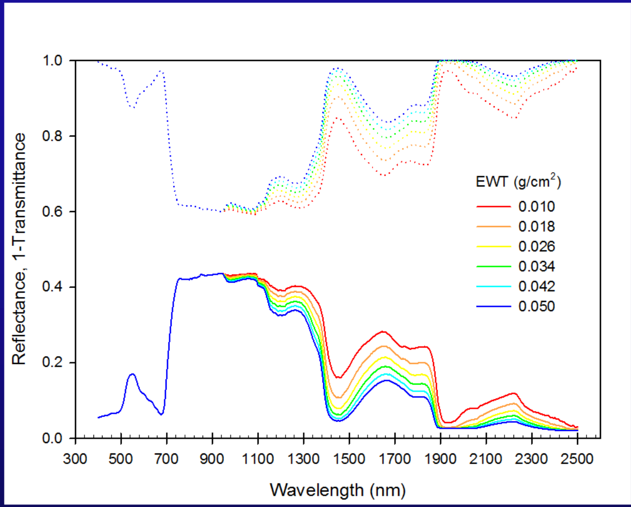

It is also important to know what specific wavebands are most suitable to study particular biophysical and/or biochemical properties. As examples, plant moisture sensitivity is best studied using a narrowband (5 nm wide or less) centered at 970 nm, while plant stress assessments are best made using a red-edge band centered at 720 nm (or an first order derivative index derived by integrating spectra over 700-740 nm range), and biophysical variables are best retrieved using a red band centered at 687 nm. These bands are, often, used along with a reference band to produce an effective index such as a two-band normalized difference vegetation index involving a near infrared (NIR) reference band centered at 890 nm and a red band centered at 687 nm.

Gitelson et al.

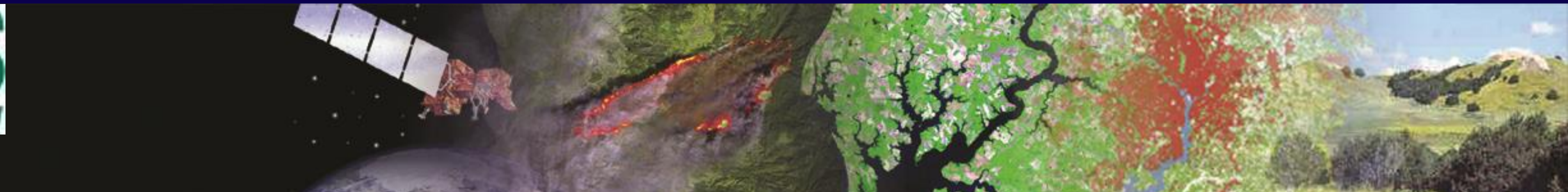

Knowledge Gain and Knowledge Gaps: Hyperspectral Remote Sensing of Crops and Vegetation

Targeted Hyperspectral Vegetation Indices (HVIs) in Study of Crops and Vegetation

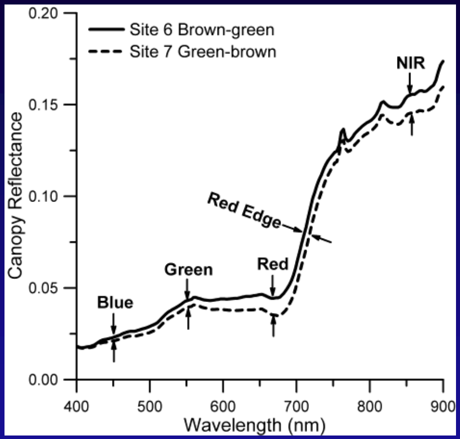

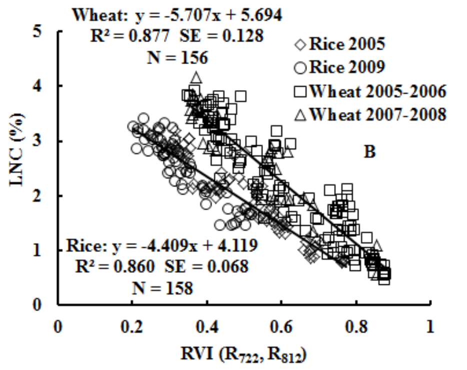

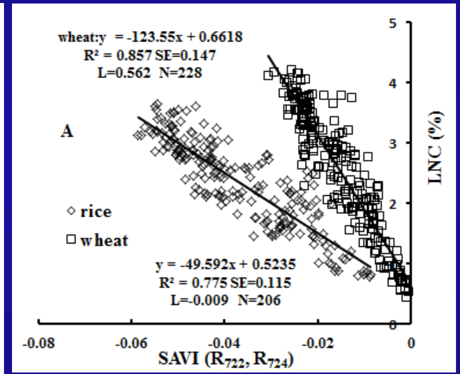

Index	Equation	Reference
Structure (LAI, green biomass, fraction)		
*NDVI	$(R_{NIR}-R_{red})/(R_{NIR}+R_{red})$	Rouse et al.[15]
*SR	R_{NIR}/R_{red}	Jordan [3]
*EVI	$2.5*(R_{NIR}-R_{red})/(R_{NIR}+6*R_{red}-7.5*R_{blue}+1)$	Huete et al.[23]
*NDWI	$(R_{857}-R_{1241})/(R_{857}+R_{1241})$	Gao [29]
**WBI	R_{900}/R_{970}	Peñuelas et al.[28]
*ARVI	$(R_{NIR}-[R_{red}-\gamma*(R_{blue}-R_{red})])/(R_{NIR}+[R_{red}-\gamma*(R_{blue}-R_{red})])$	Kaufman & Tanré [22]
*SAVI	$[(R_{NIR}-R_{red})/(R_{NIR}+R_{red}+L)]*(1+L)$	Huete [21]
**1DL_DGVI	$\sum_{\lambda_{626\,nm}}^{\lambda_{795\,nm}} \lvert R'(\lambda_i)-R'(\lambda_{626\,nm})\rvert \Delta\lambda_i$	Elvidge & Chen [1]
**1DZ_DGVI	$\sum_{\lambda_{626\,nm}}^{\lambda_{795\,nm}} \lvert R'(\lambda_i)\rvert \Delta\lambda_i$	Elvidge & Chen [1]
*VARI	$(R_{green}-R_{red})/(R_{green}+R_{red}-R_{blue})$	Gitelson et al.[13]
*VIgreen	$(R_{green}-R_{red})/(R_{green}+R_{red})$	Gitelson et al.[13]
Biochemical		
Pigments		
**SIPI	$(R_{800}-R_{445})/(R_{800}-R_{680})$	Peñuelas et al. [31]
**PSSR	(R_{800}/R_{675}); (R_{800}/R_{650})	Blackburn [30]
**PSND	$[(R_{800}-R_{675})/(R_{800}+R_{675})]$; $[(R_{800}-R_{650})/(R_{800}+R_{650})]$	Blackburn [32]
**PSRI	$(R_{680}-R_{500})/R_{750}$	Merzlyak et al. [33]
Chlorophyll		
**CARI	$[(R_{700}-R_{670})-0.2*(R_{700}-R_{550})]$	Kim [34]
**MCARI	$[(R_{700}-R_{670})-0.2*(R_{700}-R_{550})]*(R_{700}/R_{670})$	Daughtry et al. [35]
$**CI_{red\ edge}$	$R_{NIR}/R_{red\ edge}-1$	Gitelson et al. [36]
Anthocyanins		
**ARI	$(1/R_{green})-(1/R_{red\ edge})$	Gitelson et al.[40]
**mARI	$[(1/R_{green})-(1/R_{red\ edge})]*R_{NIR}$	Gitelson et al. [36]
**RGRI	R_{red}/R_{green}	Gamon & Surfus [7]
**ACI	R_{green}/R_{NIR}	Van den Berg & Perkins [41]
Carotenoids		
**CRI1	$(1/R_{510})-(1/R_{550})$	Gitelson et al.[42]
**CRI2	$(1/R_{510})-(1/R_{700})$	Gitelson et al. [42]
Water		
*NDII	$(R_{NIR}-R_{SWIR})/(R_{NIR}+R_{SWIR})$	Hunt & Rock [12]
*NDWI, **WBI	See Above	See Above
*MSI	R_{SWIR}/R_{NIR}	Rock et al. [43]
Lignin &Cellulose/Residues		
**CAI	100*[0.5*(R2031+R2211)-R2101]	Daughtry [47]
**NDLI	$[\log(1/R_{1754})-\log(1/R_{1680})]/[\log(1/R_{1754})+\log(1/R_{1680})]$	Serrano et al. [48]
Nitrogen		
**NDNI	$[\log(1/R_{1510})-\log(1/R_{1680})]/[\log(1/R_{1510})+\log(1/R_{1680})]$	Serrano et al. [48]
Physiology		
Light Use Efficiency		
RGRI,SIPI	See Above	See Above
**PRI	$(R_{530}-R_{570})/(R_{530}+R_{570})$	Gamon et al. [9]
Stress		
*MSI	See Above	See Above
**REP	l(max first derivitive: 680-750 nm)	Horler et al. [10]
**RVSI	$[(R_{714}+R_{752})/2-R_{733}$	Merton & Huntington [52]

Note: Narrowbands targeted to study specific vegetation biophysical and biochemical variable: Each waveband in Table was uniquely targeted to study specific vegetation biophysical, and biochemical properties and\or captures specific events such as plant stress. For example, a waveband centered at 550 nm provides excellent sensitivity to plant nitrogen, a waveband centered at 515 nm is best for pigments (carotenoids, anthocyanins), and a waveband centered at 970 nm or 1245 nm was ideal to study plant moisture fluctuations;

Chapters 8, 14, 21; Thenkabail et a 2012

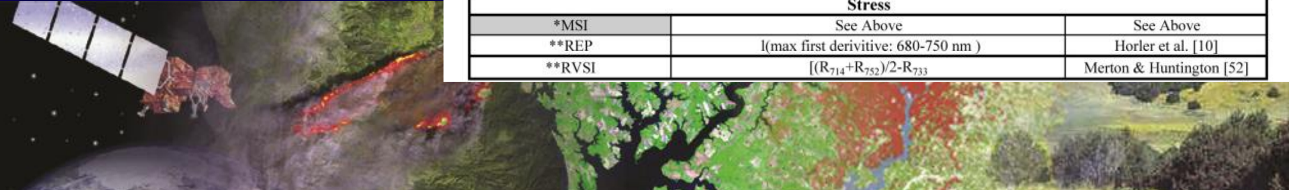

Some of the Best Two-band Hyperspectral Vengetation Indices (HVIs)
In 400-2500 nm Waveband Range

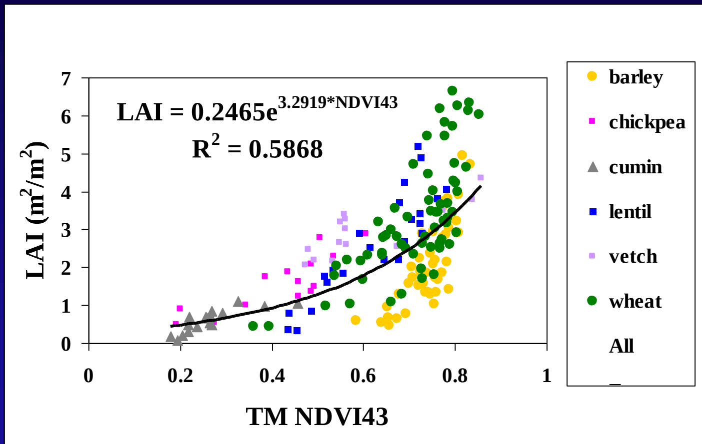

Broad-band NDVI43 vs. LAI

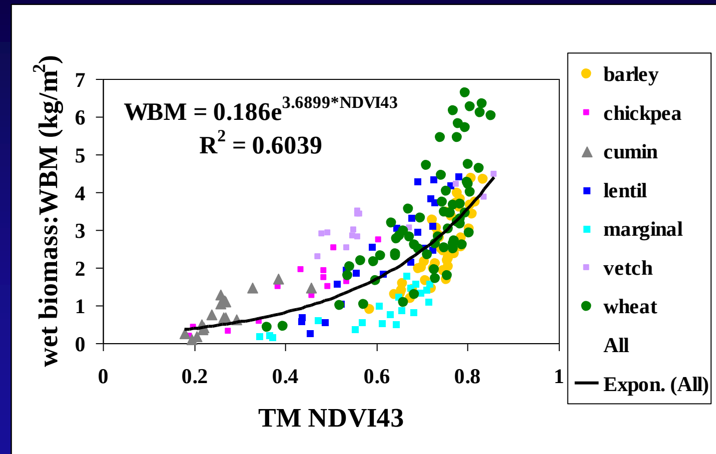

Broad-band NDVI43 vs. WBM

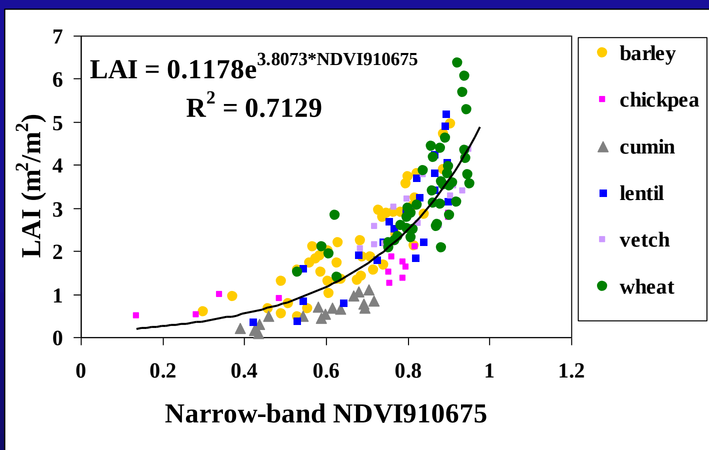

Narrow-band NDVI43 vs. LAI

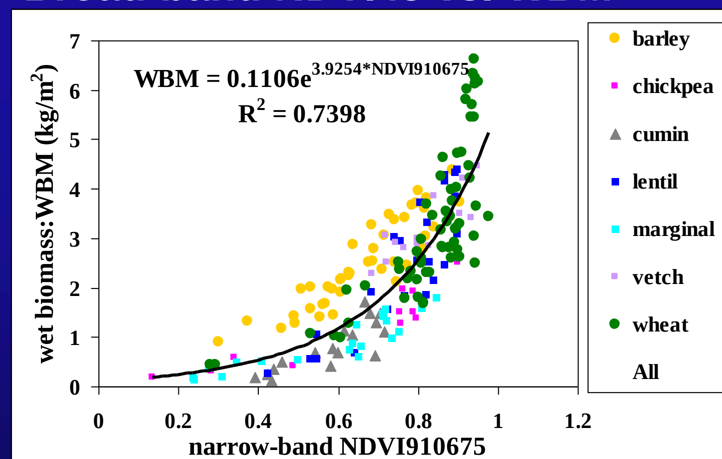

Narrow-band NDVI43 vs. WBM

Note: Improved models of vegetation biophysical and biochemical variables: The combination of wavebands in Table 28.1 or HVIs derived from them provide us with significantly improved models of vegetation variables such as biomass, LAI, net primary productivity, leaf nitrogen, chlorophyll, carotenoids, and anthocyanins. For example, stepwise linear regression with a dependent plant variable (e.g., LAI, Biomass, nitrogen) and a combination of "N" independent variables (e.g., chosen by the model from Table 28.1) establish a combination of wavebands that best model a plant variable

Narrow-band indices explain about 13 percent greater variability in modeling crop variables.

Crop or Vegetation Type or Species Separation

4. Distinct separation of vegetation types or species
Separating vegetation specific narrowbands, often, help discriminate two crop types or their variables distinctly when compared with broadbands.

Knowledge Gain and Knowledge Gaps: Hyperspectral Remote Sensing of Crops and Vegetation

Crop Type Separation

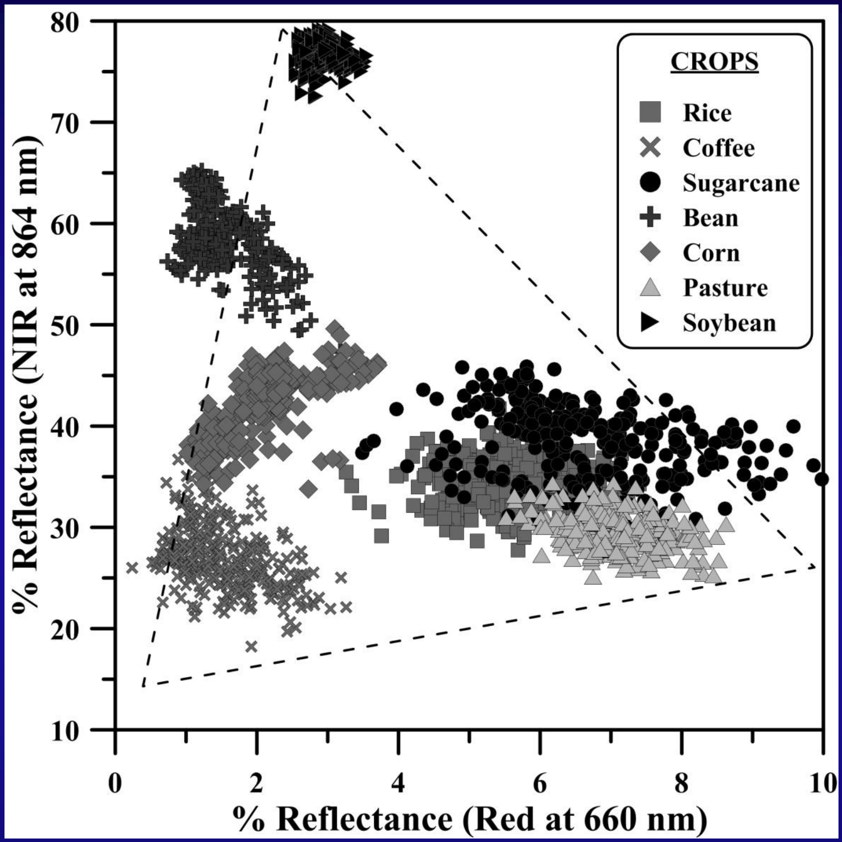

Relationships between red and near infrared (NIR) Hyperion bands for the studied crop types. The triangle is discussed in the text.

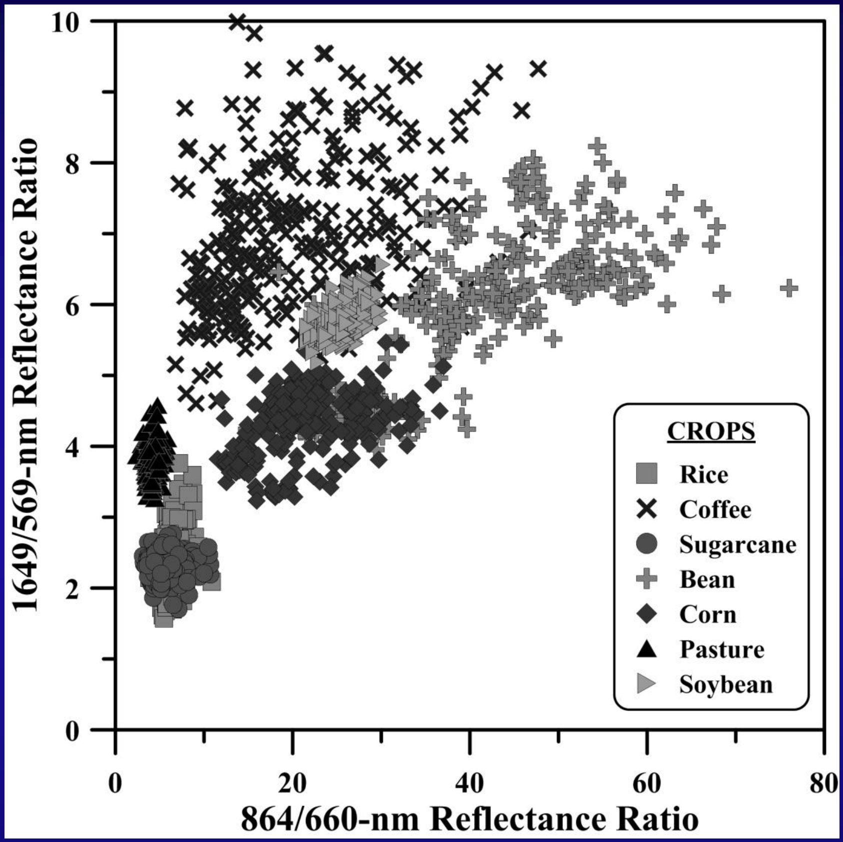

Variation in NIR-1/red and SWIR-1/green reflectance ratios for the crop types under study.

Note: see chapter 17

Crop Type Separation

Broad-band (Landsat-5 TM) Red vs. Green

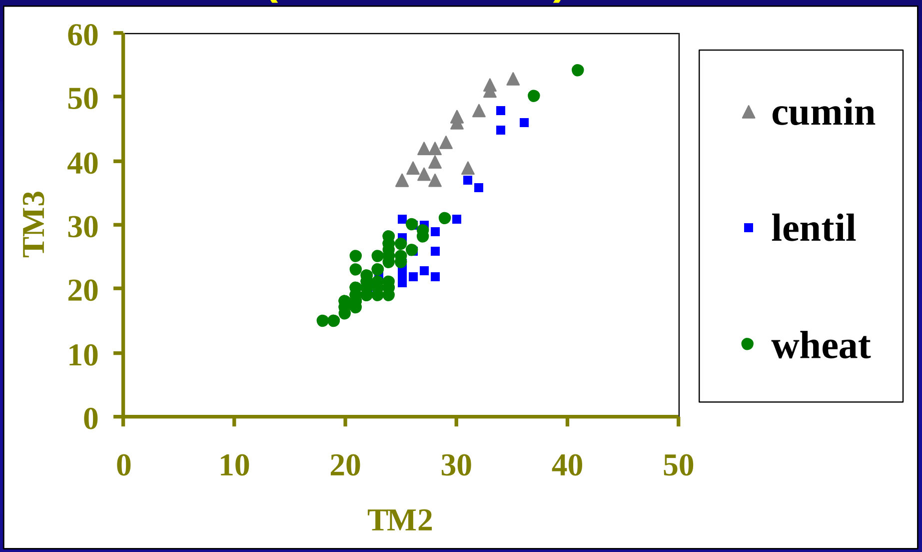

Narrow-band Red vs. Green

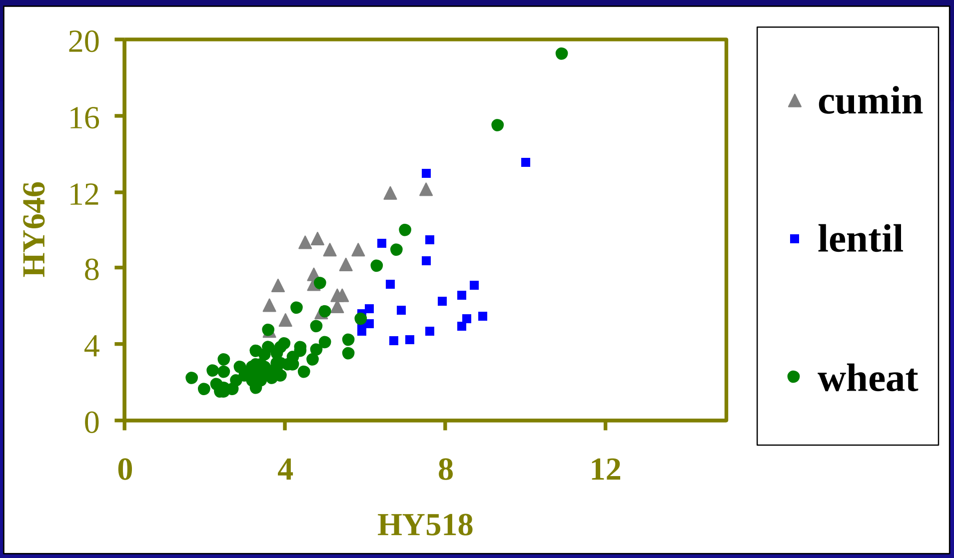

Numerous narrow-bands provide unique opportunity to discriminate different crops and vegetation.

USGS
science for a changing world

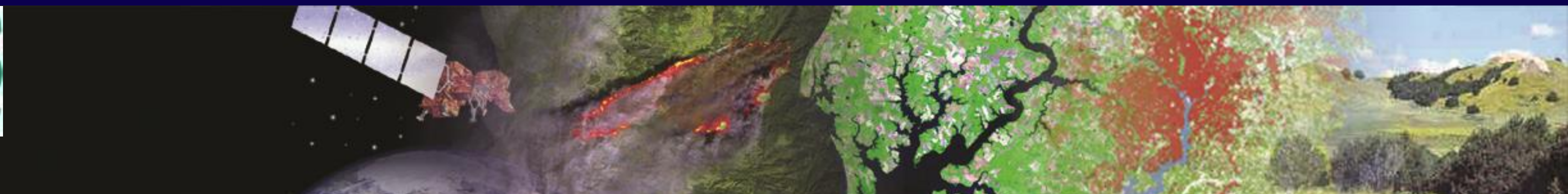

Classification Accuracies using Hyperspectral vs. Multispectral

5. Improved accuracies in crop or vegetation type or species classification

Hyperspectral narrowbands (HNBs) help provide significantly improved accuracies (10%–30%) in classifying vegetation types or species types compared to broadband data.

Classification Accuracies using Various Combinations of Selective Hyperspectral Bands

Best 4 bands	**550, 680, 850, 970**
Best 6 bands	**550, 680, 850, 970, 1075, 1450**
Best 8 bands	**550, 680, 850, 970, 1075, 1180, 1450, 2205**
Best 10 bands	**550, 680, 720, 850, 970, 1075, 1180, 1245, 1450, 2205**
Best 12 bands	**550, 680, 720, 850, 910, 970, 1075, 1180, 1245, 1450, 1650, 2205**
Best 16 bands	**490, 515, 550, 570, 680, 720, 850, 900, 970, 1075, 1180, 1245, 1450, 1650, 1950, 2205**
Best 20 bands	**490, 515, 531, 550, 570, 680, 720, 850, 900, 970, 1075, 1180, 1245, 1450, 1650, 1725, 1950, 2205, 2262, 2359**

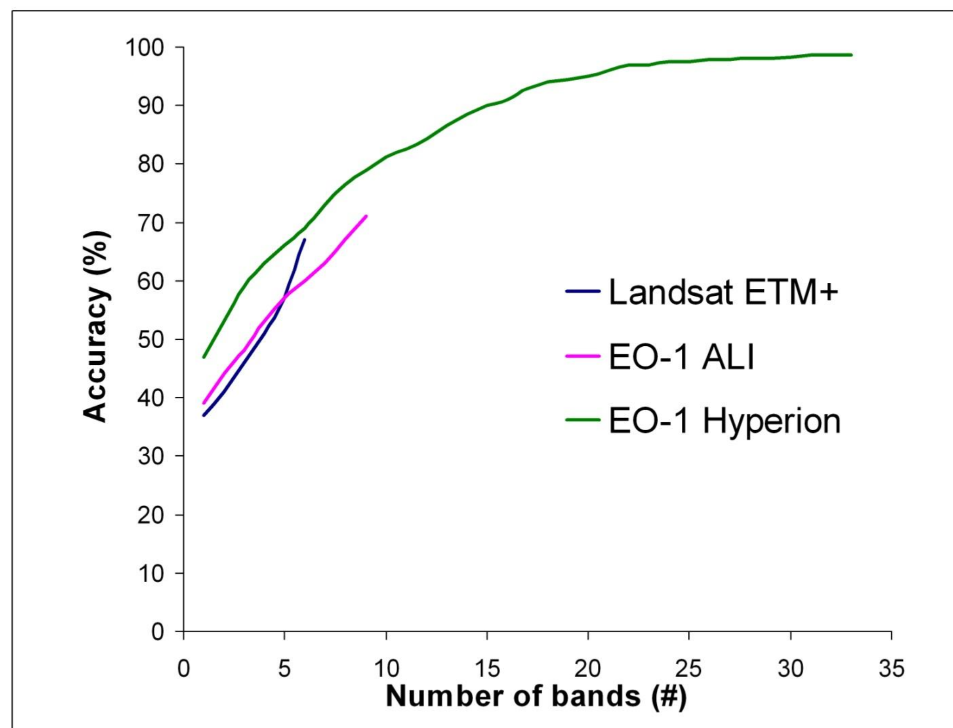

Whole Spectral Analysis Versus Selective Optimal Bands

6. Whole Spectral Analysis (e.g., continuous and entire spectra over 400–2500 nm) using such methods as partial least squares regression (PLSR), wavelet analysis, continuum removal, and spectral angle mapper (SAM) is very useful in many instances even if data volumes are very high.

Note:

1. Studying the structure of plant canopy (e.g., erectophile vs. planophile) through slope of the spectra in the NIR shoulder (760–900 nm);

2. blueshift in the red-edge (700–740 nm) portion of the spectrum indicates stress due to many causes such as drought and heavy metals and a redshift (shift of the red-edge position toward longer wavelengths) indicates chlorophyll accumulation.

Whole Spectral Analysis Versus Selective Optimal Bands

NIR shoulder (760 nm to 900 nm) for mature\senescing rice versus Rice in Vegetative phases

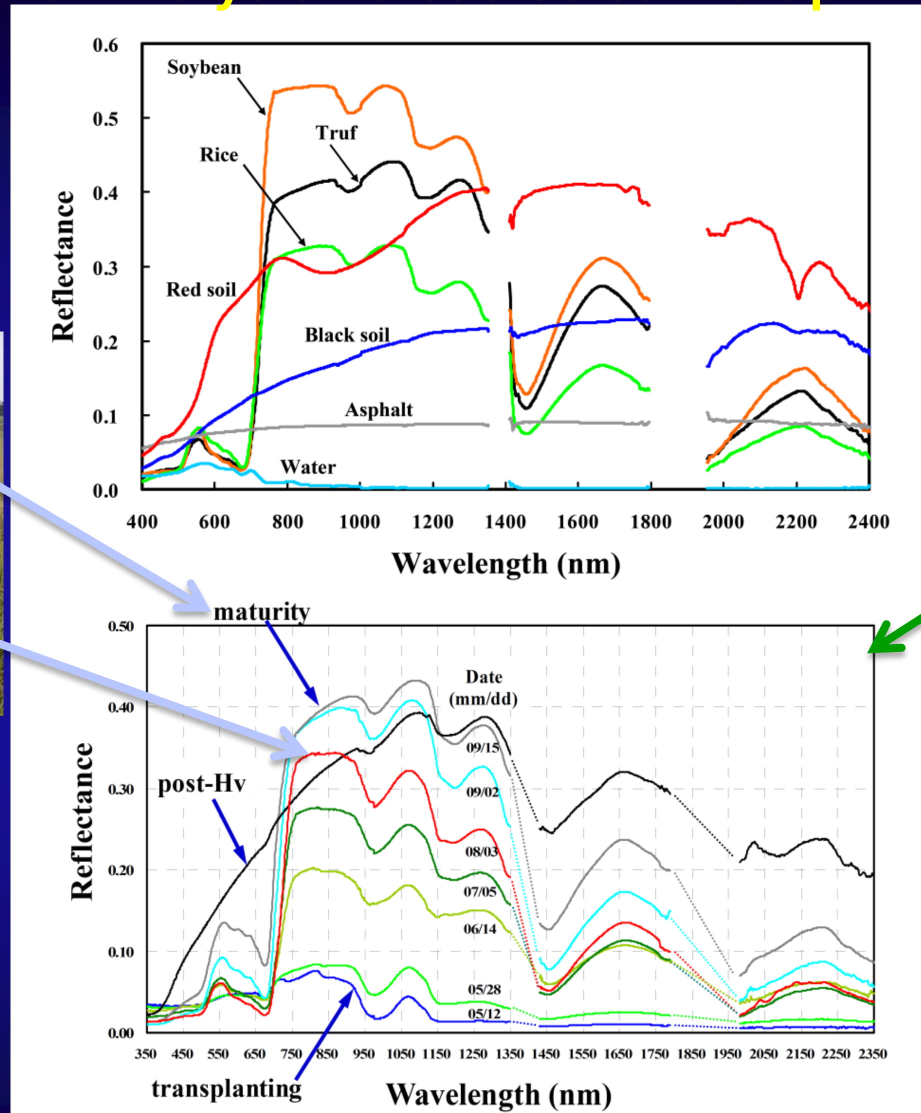

Typical reflectance spectra in agro-ecosystem surfaces (upper), and <u>seasonal changes</u> of spectra in a paddy rice field (lower).

See chapter 3

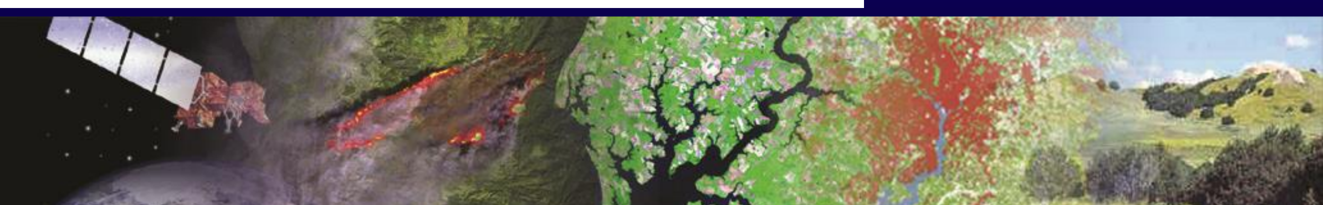

Knowledge Gain and Knowledge Gaps: Hyperspectral Remote Sensing of Crops and Vegetation

Whole Spectral Analysis Versus Selective Optimal Bands

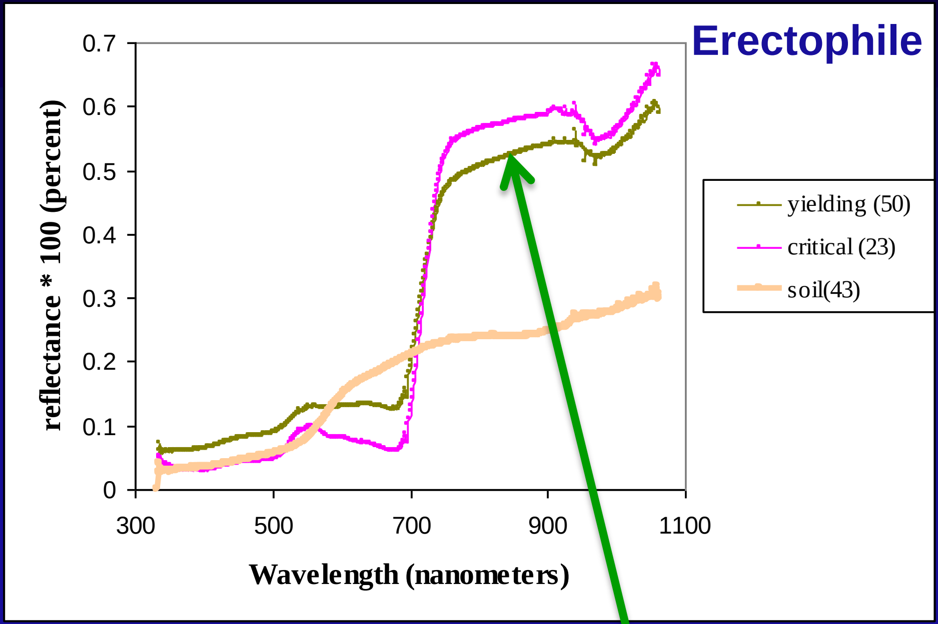

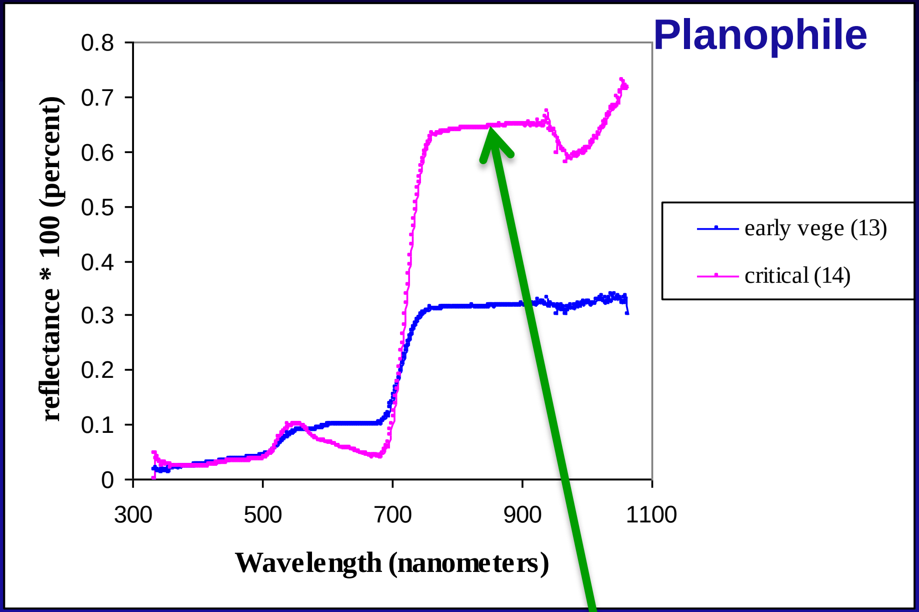

USGS
science for a changing world

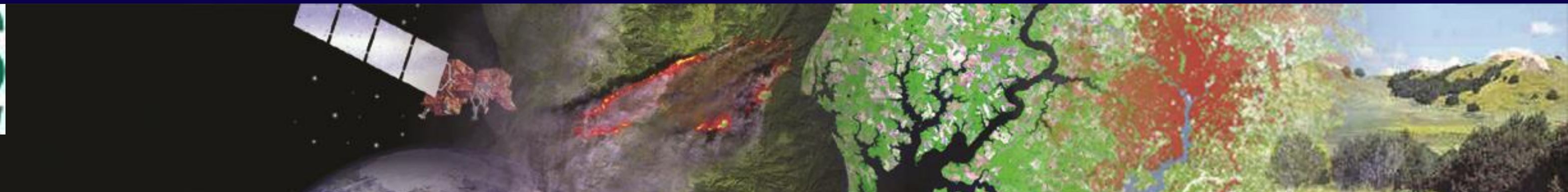

7. Hyperspectral Data Also Provides Data Continuity for Existing Sensors

Using hyperspectral narrowband data one can produce any broadband data (e.g., Landsat, Resourcesat, SPOT). Thereby, hyperspectral sensors not only help advance remote sensing science through imaging spectroscopy, but also facilitate data continuity of broadband sensors such as Landsat, SPOT, and IRS.

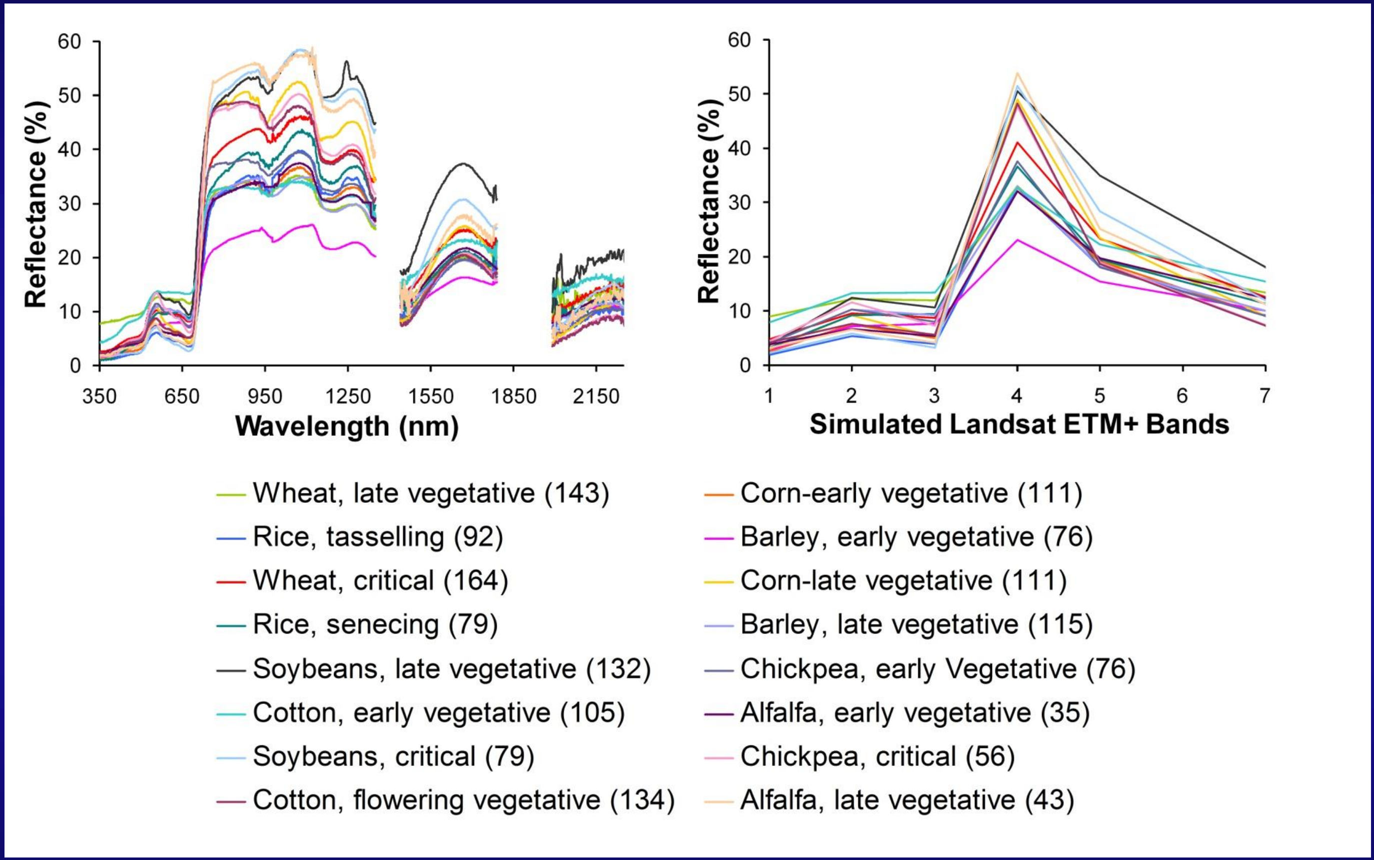

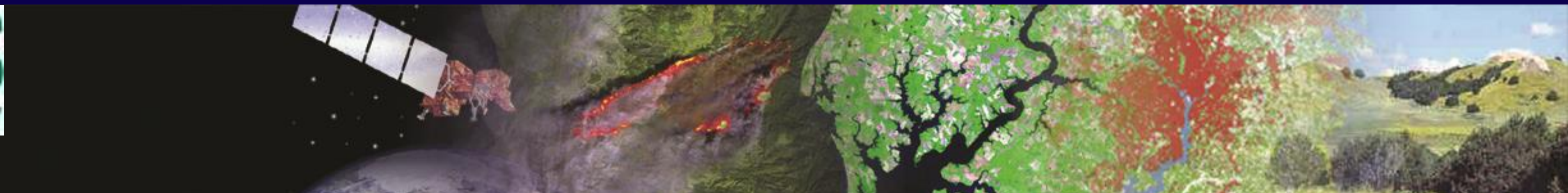

7. Hyperspectral Data Also Provides Data Continuity for Existing Sensors

Generating Broadbands (e.g., Landsat, IKONOS) from Narrowbands (e.g., HyspIRI)

Hyperspectral image data cube

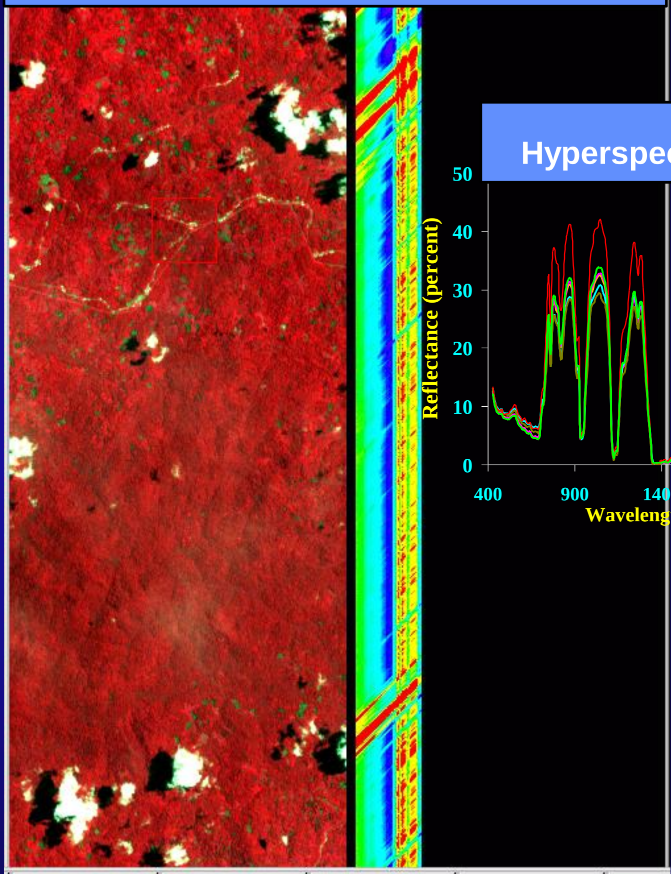

Hyperspectral image spectra

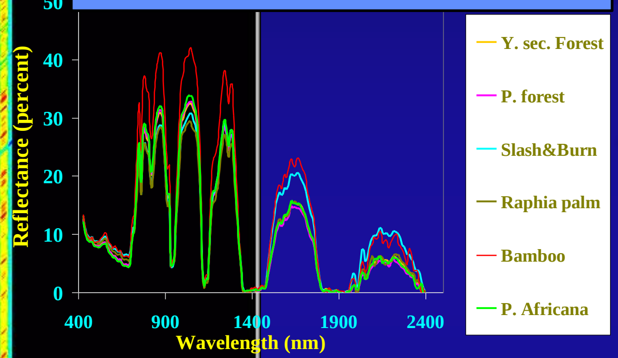

Generated Landsat ETM+ for data continuity: 6 non-thermal broadbands at 30 m of Landsat ETM+ Generated from a Hyperspectral Sensor

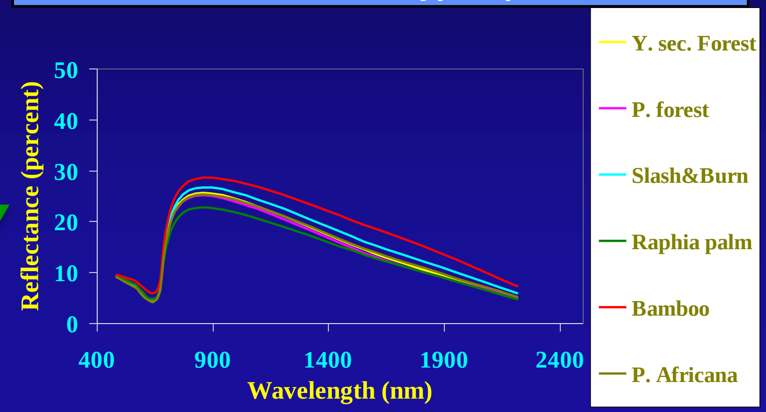

Generated IKONOS 4 m data: 4 broadbands at 4 m of IKONOS Generated from a Hyperspectral Sensor

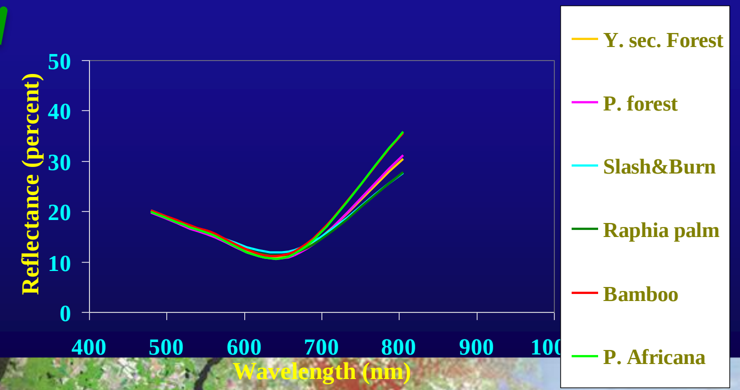

Imaging spectroscopy: 242 hyperspectral bands, each of 5 or 10 nm wide, in 400-2500 nm spectral range.

USGS
science for a changing world

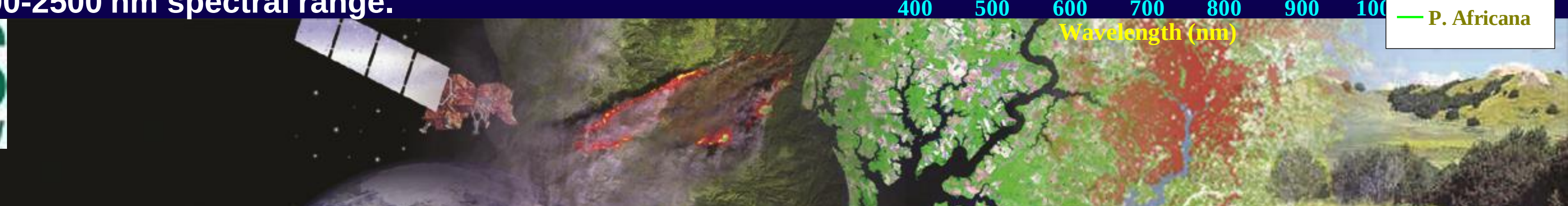

Hyperspectral (Imaging Spectroscopy) Narrowband Study of Agricultural Crops
Hyperspectral Narrowbands versus Multispectral Broadbands

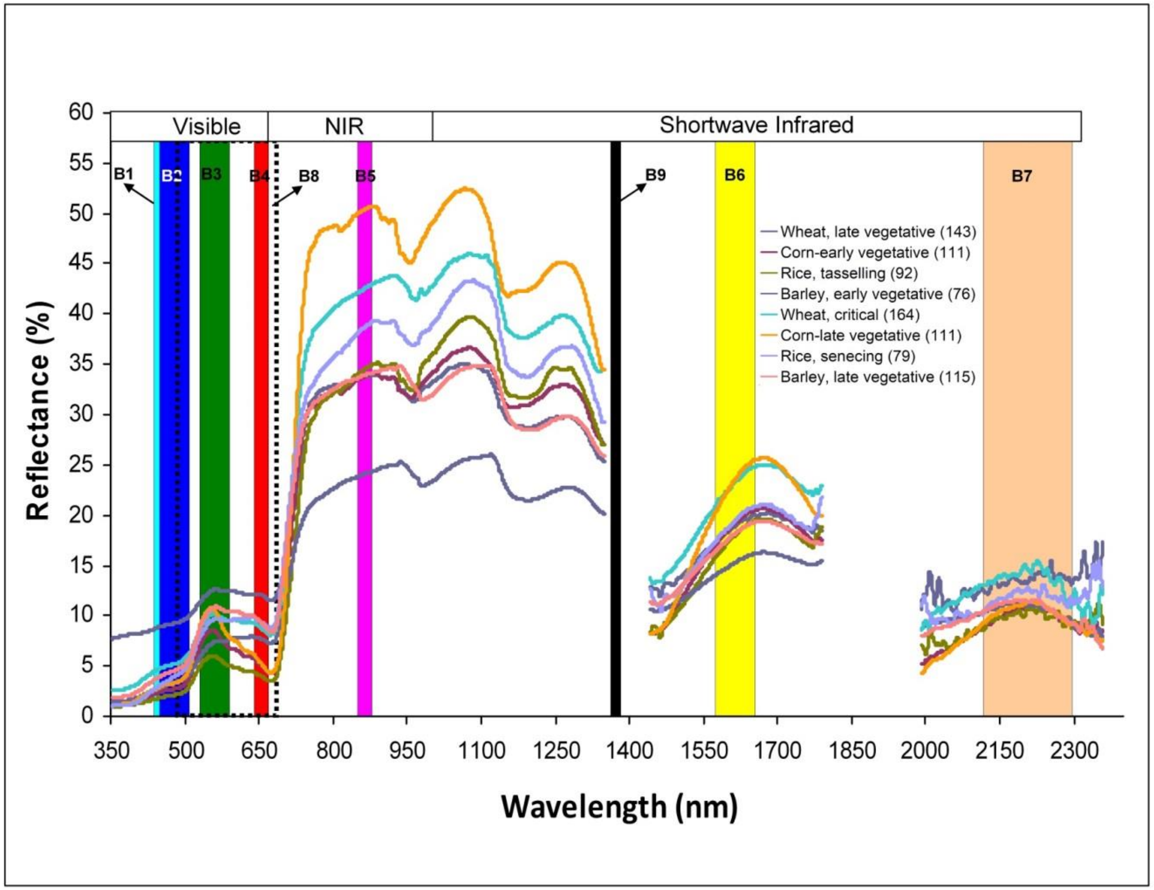

Optimal hyperspectral narrowbands (HNBs). Current state of knowledge on hyperspectral narrowbands (HNBs) for agricultural and vegetation studies (inferred from [8]). The whole spectral analysis (WSA) using contiguous bands allow for accurate retrieval of plant biophysical and biochemical quantities using methods like continuum removal. In contrast, studies on wide array of biophysical and biochemical variables, species types, crop types have established: (a) optimal HNBs band centers and band widths for vegetation/crop characterization, (b) targeted HVIs for specific modeling, mapping, and classifying vegetation/crop types or species and parameters such as biomass, LAI, plant water, plant stress, nitrogen, lignin, and pigments, and (c) redundant bands, leading to overcoming the Hughes Phenomenon. These studies support hyperspectral data characterization and applications from missions such as Hyperspectral Infrared Imager (HyspIRI) and Advanced Responsive Tactically Effective Military Imaging Spectrometer (ARTEMIS). Note: sample sizes shown within brackets of the figure legend refer to data used in this study.

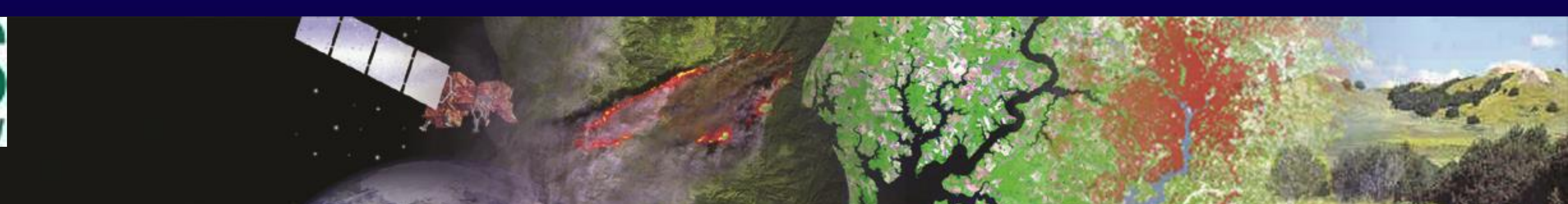

Knowledge Gain and Knowledge Gaps: Hyperspectral Remote Sensing of Crops and Vegetation

8. Spectral Signature Data Bank of Vegetation Species (e.g., P. Africana)

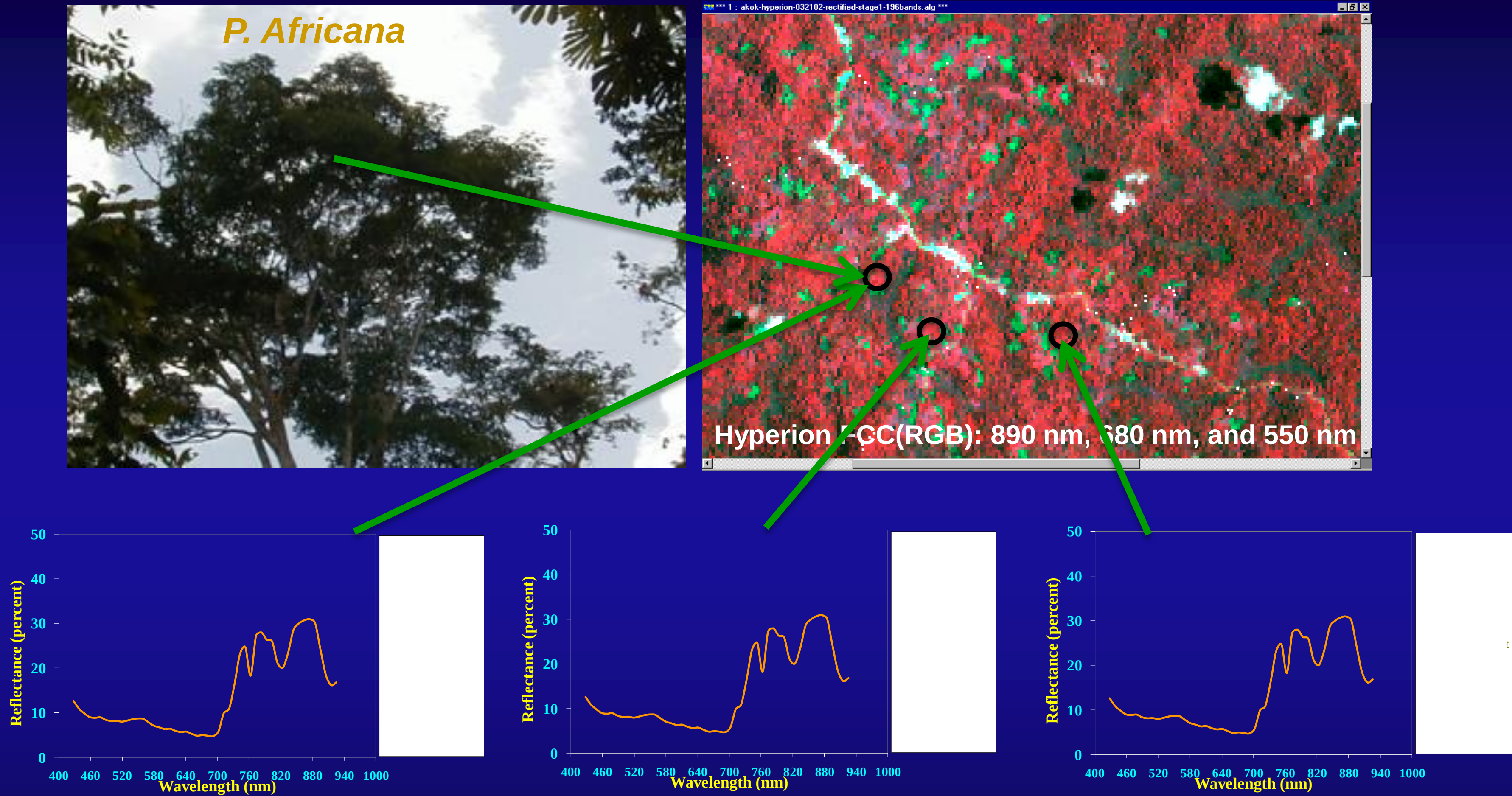

There are numerous uses of spectral data bank

9. Many Uses of Hyperspectral Data

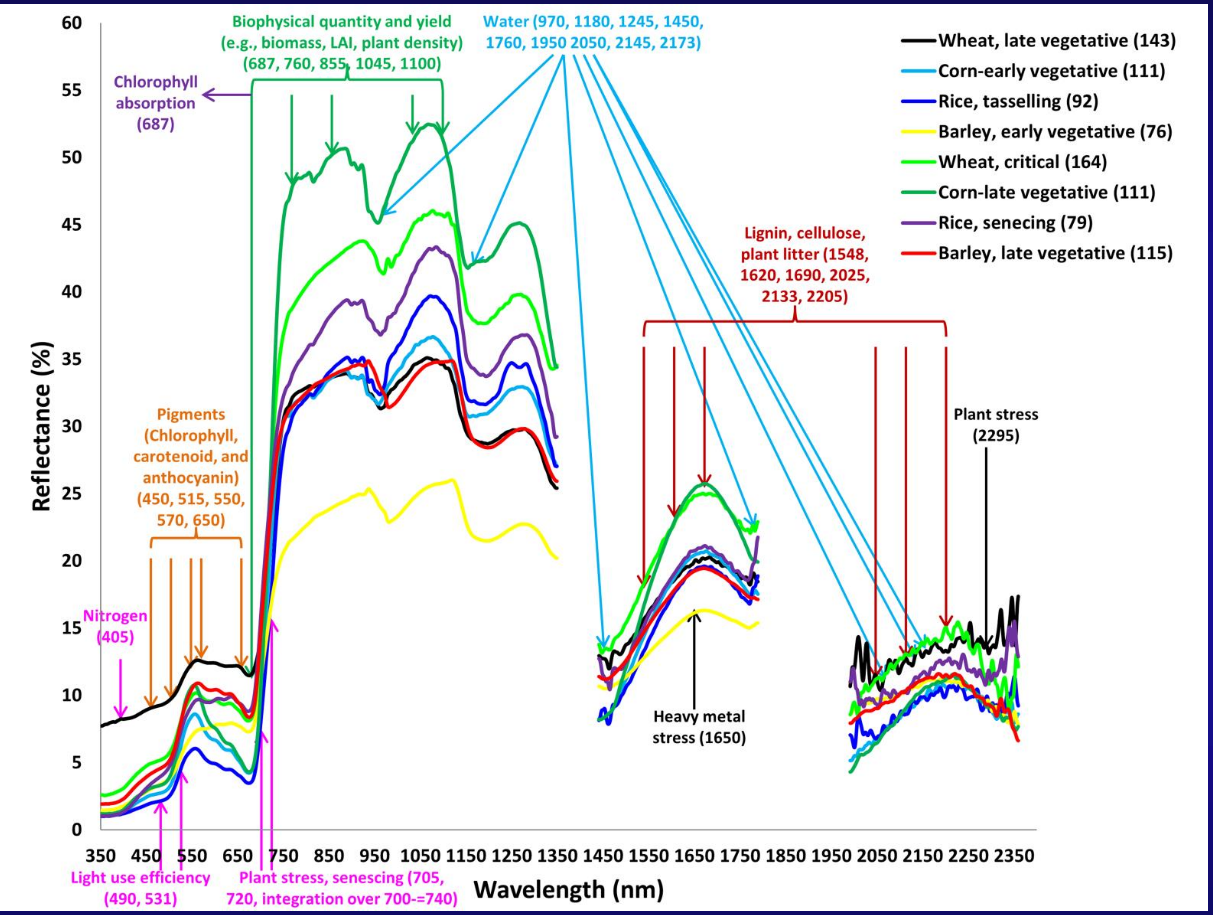

Optimal hyperspectral narrowbands (HNBs). Current state of knowledge on hyperspectral narrowbands (HNBs) for agricultural and vegetation studies (inferred from [8]). The whole spectral analysis (WSA) using contiguous bands allow for accurate retrieval of plant biophysical and biochemical quantities using methods like continuum removal. In contrast, studies on wide array of biophysical and biochemical variables, species types, crop types have established: (a) optimal HNBs band centers and band widths for vegetation/crop characterization, (b) targeted HVIs for specific modeling, mapping, and classifying vegetation/crop types or species and parameters such as biomass, LAI, plant water, plant stress, nitrogen, lignin, and pigments, and (c) redundant bands, leading to overcoming the Hughes Phenomenon. These studies support hyperspectral data characterization and applications from missions such as Hyperspectral Infrared Imager (HyspIRI) and Advanced Responsive Tactically Effective Military Imaging Spectrometer (ARTEMIS). Note: sample sizes shown within brackets of the figure legend refer to data used in this study.

Beyond Hyperspectral Data: Hyperspectral+LiDAR+Thermal

Strengths of hyperspectral data in biophysical and biochemical characterization of vegetation are well known.

LiDAR

However, better characterization and modeling of the vegetation height/depth, crown sizes, basal area, biomass, and structure will require LIDAR.

Thermal

Further plant water properties are better understood using thermal data.

Hyperspectral+LiDAR+Thermal

Given these facts, simultaneous acquisition and integration of hyperspectral data along with LIDAR and thermal data are considered the future of remote sensing.

Hyperspectral Data on Tropical Forests

Advances in Combining Hyperspectral and LIDAR over Tropical Forests

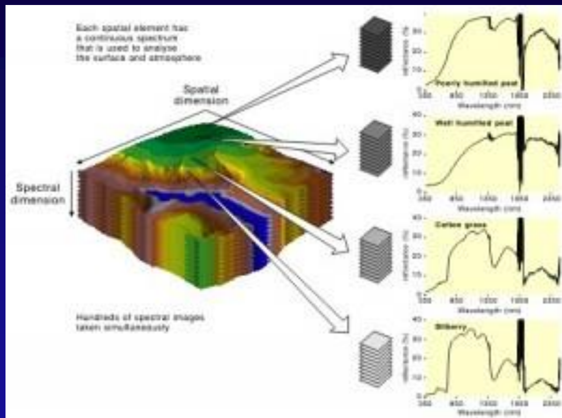

Hyperspectral for

canopy

biochemistry

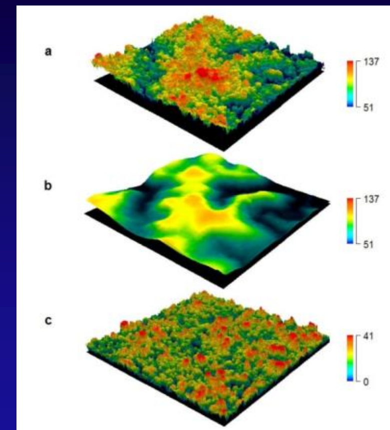

LIDAR for

canopy structure including

- height,
- crown shape,
- leaf area,
- biomass, and
- basal area

Hyperspectral + LIDAR for

characterize parameters such as

- height
- canopy cover
- leaf area
- canopy chlorophyll content, and
- canopy water content

Note: see chapter 20, Thomas et al.

Publications

Hyperspectral Remote Sensing of Vegetation

Remote Sensing Handbook: Vol. I, II, III; 82 Chapters (Editor: Prasad S. Thenkabail)

Taylor and Francis, Inc\CRC Press; November, 2015

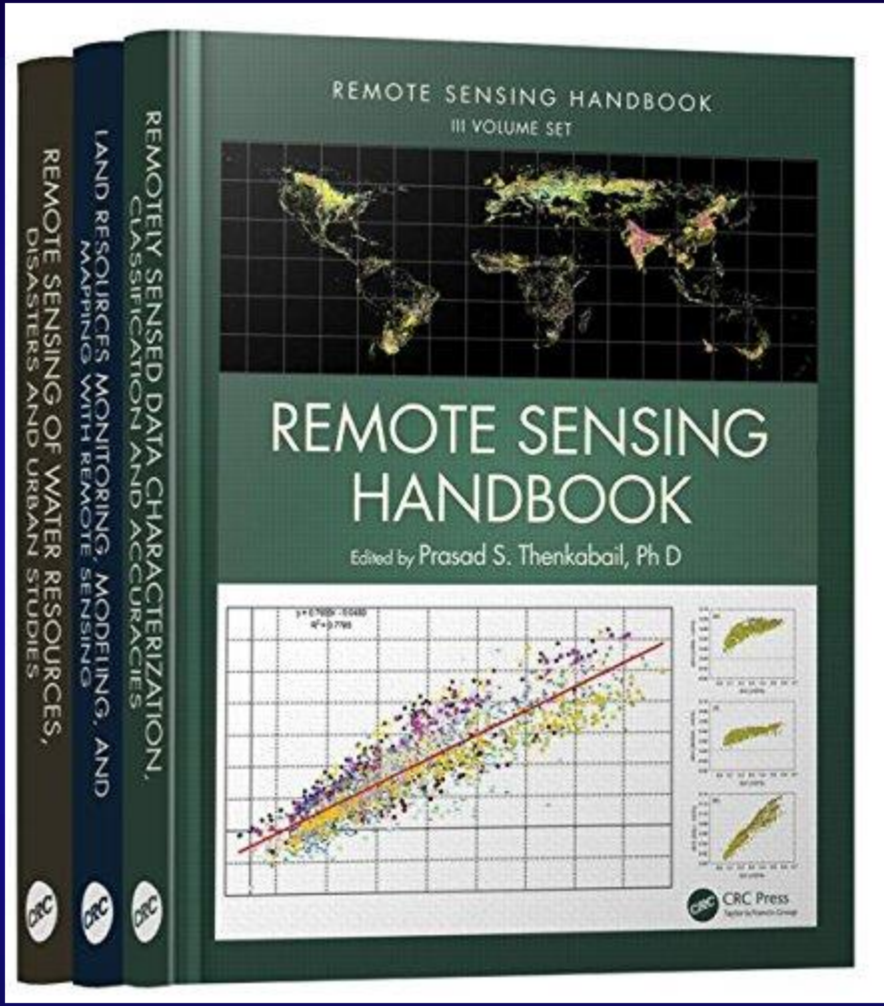

9

Hyperspectral Remote Sensing for Terrestrial Applications

Prasad S. Thenkabail
U. S. Geological Survey

Pardhasaradhi Teluguntla
U. S. Geological Survey
and
Bay Area Environmental Research Institute

Murali Krishna Gumma
International Crops Research Institute for the Semi Arid Tropics

Venkateswarlu Dheeravath
United Nations World Food Program

9.1 Introduction

Remote sensing data are considered hyperspectral when the data are gathered from numerous wavebands, contiguously over an entire range of the spectrum (e.g., 400–2500 nm). Goetz (1992) defined hyperspectral remote sensing as "The acquisition of images in hundreds of registered, contiguous spectral bands such that for each picture element of an image it is possible to derive a complete reflectance spectrum." However, Jensen (2004) defines hyperspectral remote sensing as "The simultaneous acquisition of images in many relatively narrow, contiguous and/or non contiguous spectral bands throughout the ultraviolet, visible, and infrared portions of the electromagnetic spectrum."

Overall, the three key factors in considering data to be hyperspectral are the following:

1. *Contiguity in data collection*: Data are collected contiguously over a spectral range (e.g., wavebands spread across 400–2500 nm).
2. *Number of wavebands*: The number of wavebands by itself does not make the data hyperspectral. For example, if there are numerous narrowbands in 400–700 nm wavelengths, but have only a few broadbands in 701–2500 nm, the data cannot be considered hyperspectral. However, even relatively broad bands of width, say, for example, 30 nm bandwidths spread equally across 400–2500 nm, for a total of ~70 bands, are considered hyperspectral due to contiguity. AQ1

K22130_C009.indd 201 4/2/2015 3:39:19 PM

science for a changing world

Hyperspectral Remote Sensing (Imaging Spectroscopy) for Vegetation Studies
References Pertaining to this Presentation

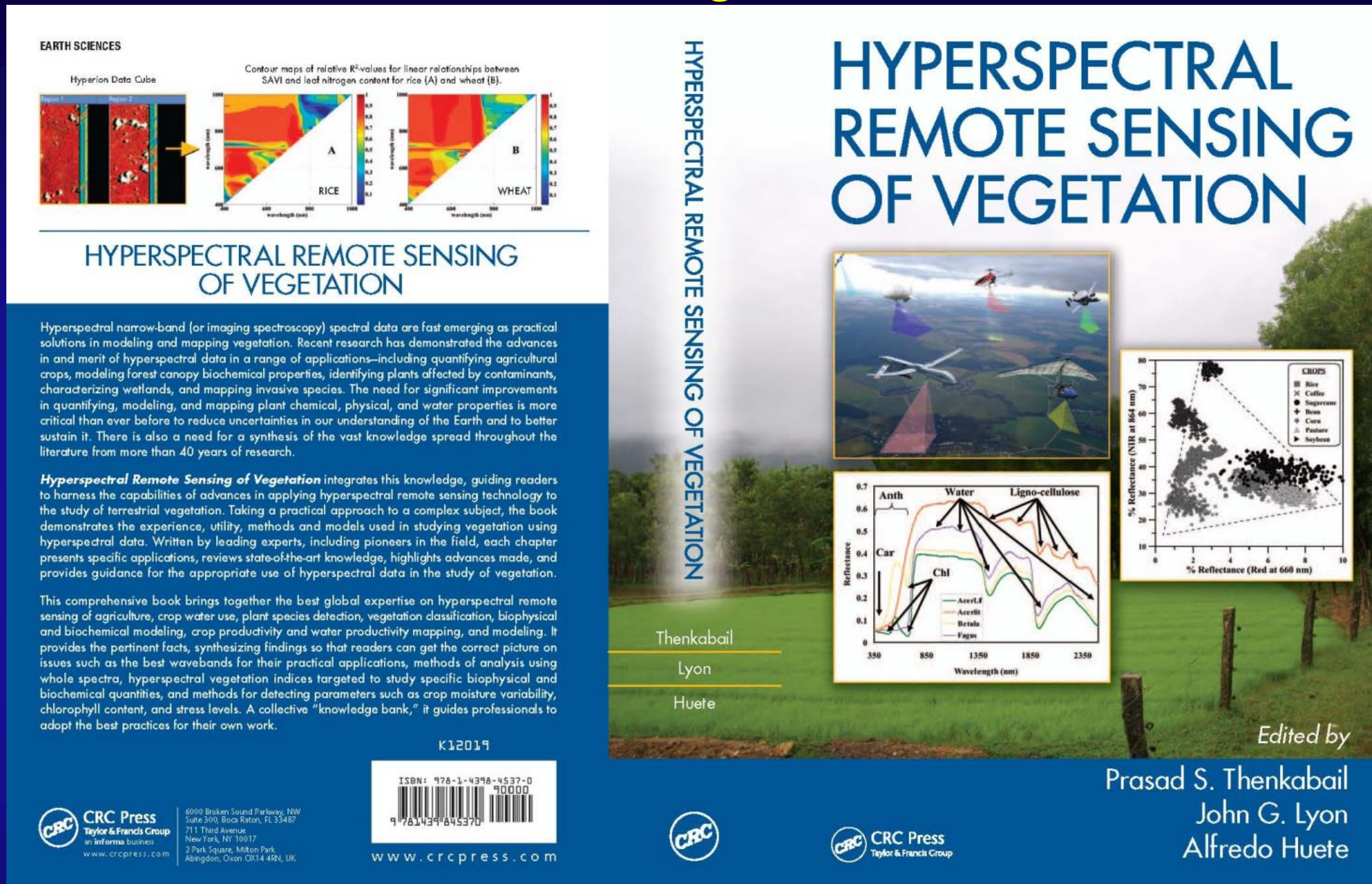

Thenkabail, P.S., Lyon, G.J., and Huete, A. 2012. Book entitled: "Advanced Hyperspectral Remote Sensing of Terrestrial Environment". 28 Chapters. CRC Press- Taylor and Francis group, Boca Raton, London, New York. Pp. 700+ (80+ pages in color). To be published by October 31, 2012.

USGS
science for a changing world
U.S. Geological Survey
U.S. Department of Interior

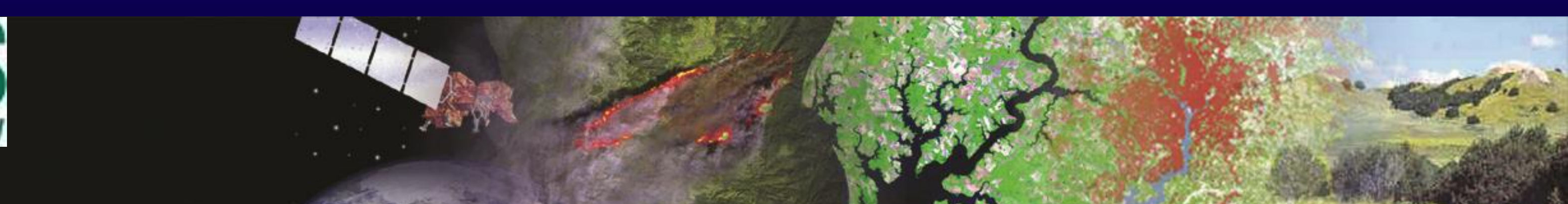

Hyperspectral Remote Sensing (Imaging Spectroscopy) for Vegetation Studies

References Pertaining to this Presentation

Thenkabail, P.S., 2014. Guest Editor of Special Issue on "Hyperspectral Remote Sensing of Vegetation and Agricultural Crops" Photogrammetric Engineering and Remote Sensing. 80(4).

Marshall, M.T., Thenkabail, P.S. 2014. Biomass modeling of four leading World crops using hyperspectral narrowbands in support of HyspIRI mission. Photogrammetric Engineering and Remote Sensing. 80(4): 757-772.

Thenkabail, P.S., Gumma, M.K., Teluguntla, P., and Mohammed, I.A., 2014. Hyperspectral Remote Sensing of Vegetation and Agricultural Crops. Highlight Article. Photogrammetric Engineering and Remote Sensing. 80(4): 697-709.

Thenkabail, P.S., 2014. Research Advances in Hyperspectral Remote Sensing. Special Issue Foreword. Photogrammetric Engineering and Remote Sensing. 80(4): 721-723.

Thenkabail, P.S., Gumma, M.K., Teluguntla, P., and Mohammed, I.A., 2014. Cover Page of Special Issue Hyperspectral Hyperion Images and Spectral Libraries of Agricultural Crops. Photogrammetric Engineering and Remote Sensing. 80(4): Cover Page.

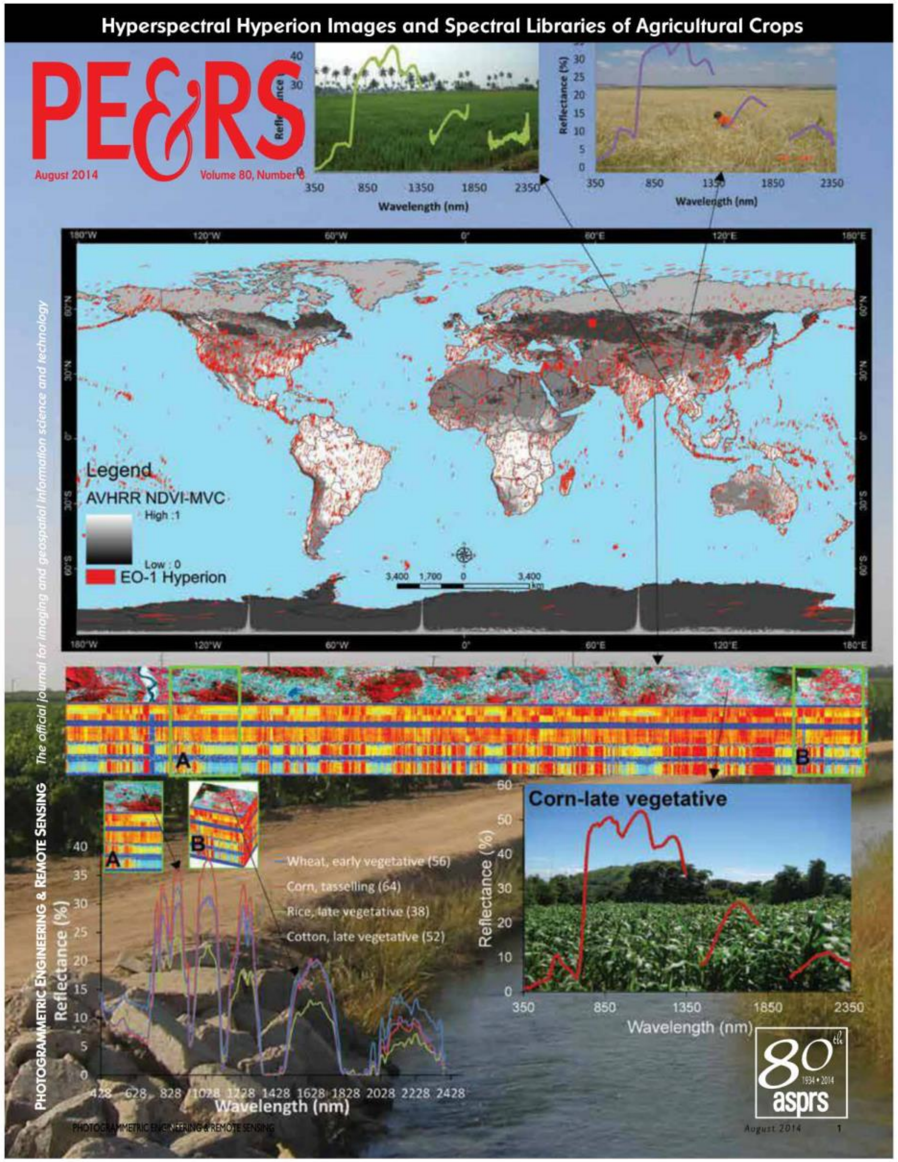

U.S. Geological Survey
U.S. Department of Interior

Hyperspectral Remote Sensing (Imaging Spectroscopy) of Agricultural Crops

Recent (April, 2013) Publication

Thenkabail, P.S., Mariotto, I., Gumma, M.K.,, Middleton, E.M., Landis, and D.R., Huemmrich, F.K., 2013. Selection of hyperspectral narrowbands (HNBs) and composition of hyperspectral twoband vegetation indices (HVIs) for biophysical characterization and discrimination of crop types using field reflectance and Hyperion/EO-1 data. IEEE JOURNAL OF SELECTED TOPICS IN APPLIED EARTH OBSERVATIONS AND REMOTE SENSING, Pp. 1-13, VOL. 6, NO. 2, APRIL 2013.

Selection of Hyperspectral Narrowbands (HNBs) and Composition of Hyperspectral Twoband Vegetation Indices (HVIs) for Biophysical Characterization and Discrimination of Crop Types Using Field Reflectance and Hyperion/EO-1 Data

Prasad S. Thenkabail, Isabella Mariotto, Murali Krishna Gumma, Elizabeth M. Middleton, David R. Landis, and K. Fred Huemmrich

Abstract—**The overarching goal of this study was to establish optimal hyperspectral vegetation indices (HVIs) and hyperspectral narrowbands (HNBs) that best characterize, classify, model, and map the world's main agricultural crops. The primary objectives were: (1) crop biophysical modeling through HNBs and HVIs, (2) accuracy assessment of crop type discrimination using Wilks' Lambda through a discriminant model, and (3) meta-analysis to select optimal HNBs and HVIs for applications related to agriculture. The study was conducted using two Earth Observing One (EO-1) Hyperion scenes and other surface hyperspectral data for the eight leading worldwide crops (wheat, corn, rice, barley, soybeans, pulses, cotton, and alfalfa) that occupy ~70% of all cropland areas globally. This study integrated data collected from multiple study areas in various agroecosystems of Africa, the Middle East, Central Asia, and India. Data were collected for the eight crop types in six distinct growth stages. These included (a) field spectroradiometer measurements (350–2500 nm) sampled at 1-nm discrete bandwidths, and (b) field biophysical variables (e.g., biomass, leaf area index) acquired to correspond with spectroradiometer measurements. The eight crops were described and classified using ~20 HNBs. The accuracy of classifying these 8 crops using HNBs was around 95%, which was ~25% better than the multi-spectral results possible from Landsat-7's Enhanced Thematic Mapper+ or EO-1's Advanced Land Imager. Further, based on this research and meta-analysis involving over 100 papers, the study established 33 optimal HNBs and an equal number of specific two-band normalized difference HVIs to best model and study specific biophysical and biochemical quantities of major agricultural crops of the world. Redundant bands identified in this study will help overcome the Hughes Phenomenon (or "the curse of high dimensionality") in hyperspectral data for a particular application (e.g., biophysical characterization of crops). The findings of this study will make a significant contribution to future hyperspectral missions such as NASA's HyspIRI.**

Index Terms—**Hyperion, field reflectance, imaging spectroscopy, HyspIRI, biophysical parameters, hyperspectral vegetation indices, hyperspectral narrowbands, broadbands.**

Manuscript received March 12, 2012; revised May 10, 2012, October 02, 2012; accepted March 06, 2013.

P. S. Thenkabail is with the Western Geographic Science Center, U. S. Geological Survey, Flagstaff, AZ 86001 USA (corresponding author, e-mail: pthenkabail@usgs.gov).

I. Mariotto is with the Environmental Science Program, Department of Geological Sciences, University of Texas at El Paso, El Paso, TX 79968 USA.

M. K. Gumma is with the International Rice Research Institute (IRRI), South Asia Breeding Hub, ICRISAT, 502 324 Andhra Pradesh, India.

E. M. Middleton is with the Biospheric Sciences Laboratory (Code 618), NASA/Goddard Space Flight Center, Greenbelt, MD 20771 USA.

D. R. Landis is with the Sigma Space Corp., Inc., Lanham, MD 20706 USA.

K. F. Huemmrich is with the University of Maryland Baltimore County, Baltimore, MD 21228 USA.

Color versions of one or more of the figures in this paper are available online at http://ieeexplore.ieee.org.

Digital Object Identifier 10.1109/JSTARS.2013.2252601

I. Introduction and Rationale

NUMEROUS studies (e.g., [1], [2]) have shown that the Hyperion imaging spectrometer onboard the Earth Observing One (EO-1) satellite has provided significantly enhanced data over conventional multi-spectral remote sensing systems. Hyperspectral narrowbands (HNBs) and hyperspectral vegetation indices (HVIs) derived from EO-1 and field spectral measurements in the 400–2500 nm spectrum allow us to study very specific characteristics of agricultural crops. These include biomass, leaf area index (LAI), pigment content (e.g., chlorophyll, carotenoid, anthocyanin), stress (e.g., due to drought or disease), management properties (e.g., nitrogen application, tillage), and other biochemical properties (e.g., lignin, cellulose, plant residue) [23], [24]. The ability of hyperspectral data to significantly improve the characterization, discrimination, modeling, and mapping of crops and vegetation, when compared with broadband multispectral remote sensing, is well known [8]. This has led to improved and targeted modeling and mapping of specific agricultural characteristics, such as (a) biophysical and biochemical quantities [3]–[8], [13], (b) crop type/species discrimination [9]–[12], [15], (c) stress factors [14], [15], and (d) crop and water productivity, and energy balance [16]–[22]. These benefits will help us better understand a broad range of agricultural applications involving droughts [2], [3], food security [8]–[12], biodiversity [9], [11], and invasive species [9], [24]. Nevertheless, there are still significant knowledge gaps that require further research.

Contiguous bands of spectrometer data allow for accurate retrieval of plant biophysical and biochemical quantities using methods like continuum removal, first discussed by Clark and Roush in 1984 [25]–[28]. However, since information about agriculture is time sensitive, approximate analyses, quickly obtained using one or more HVIs may be more useful than

USGS science for a changing world

U.S. Geological Survey
U.S. Department of Interior

Hyperspectral Remote Sensing (Imaging Spectroscopy) for Vegetation Studies

References Pertaining to this Presentation

1. Thenkabail, P.S., 2015. Hyperspectral Remote Sensing for Terrestrial Applications. Chapter 9, In Thenkabail, P.S., (Editor-in-Chief), 2015. “Remote Sensing Handbook” Volume II: Land Resources: Monitoring, Modeling, and Mapping: Advances over Last 50 Years and a Vision for the Future, Book Chapter. Taylor and Francis Inc.\CRC Press, Boca Raton, London, New York. Pp. 800+. In Press (planned publication in November, 2015).

2. Thenkabail, P.S., Mariotto, I., Gumma, M.K.,, Middleton, E.M., Landis, and D.R., Huemmrich, F.K., 2013. Selection of hyperspectral narrowbands (HNBs) and composition of hyperspectral twoband vegetation indices (HVIs) for biophysical characterization and discrimination of crop types using field reflectance and Hyperion/EO-1 data. IEEE JOURNAL OF SELECTED TOPICS IN APPLIED EARTH OBSERVATIONS AND REMOTE SENSING, Pp. 427-439, VOL. 6, NO. 2, APRIL 2013.doi: 10.1109/JSTARS.2013.2252601

3. Marshall M. T., and Thenkabail P. 2015. Developing *in situ* Non-Destructive Estimates of Crop Biomass to Address Issues of Scale in Remote Sensing. *Remote Sensing*. 2015; 7(1):808-835. doi:10.3390/rs70100808

4. Marshall, M.T., Thenkabail, P.S. 2014. Biomass modeling of four leading World crops using hyperspectral narrowbands in support of HyspIRI mission. Photogrammetric Engineering and Remote Sensing. 80(4): 757-772.

5. Mariotto, I., Thenkabail, P.S., Huete, H., Slonecker, T., Platonov, A., 2013. Hyperspectral versus Multispectral Crop- Biophysical Modeling and Type Discrimination for the HyspIRI Mission. Remote Sensing of Environment. 139:291-305

USGS

science for a changing world

U.S. Geological Survey
U.S. Department of Interior

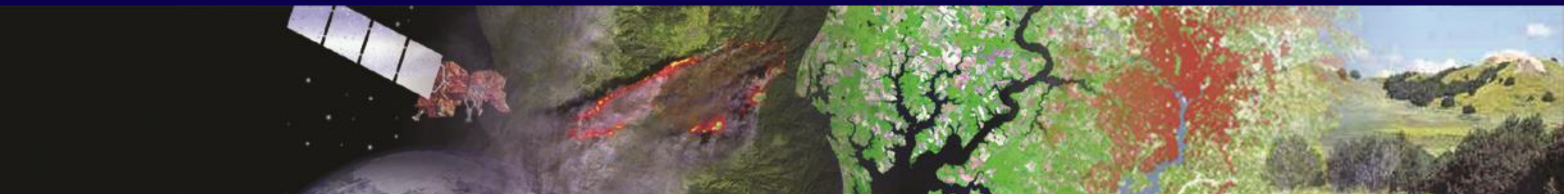

Hyperspectral Remote Sensing (Imaging Spectroscopy) for Vegetation Studies

References Pertaining to this Presentation

6. Thenkabail, P.S., Enclona, E.A., Ashton, M.S., Legg, C., Jean De Dieu, M., 2004. Hyperion, IKONOS, ALI, and ETM+ sensors in the study of African rainforests. Remote Sensing of Environment, 90:23-43.

7. Thenkabail, P.S., Enclona, E.A., Ashton, M.S., and Van Der Meer, V. 2004. Accuracy Assessments of Hyperspectral Waveband Performance for Vegetation Analysis Applications. Remote Sensing of Environment, 91:2-3: 354-376.

8. Thenkabail, P.S. 2003. Biophysical and yield information for precision farming from near-real time and historical Landsat TM images. International Journal of Remote Sensing. 24(14): 2879-2904.

9. Thenkabail P.S., Smith, R.B., and De-Pauw, E. 2002. Evaluation of Narrowband and Broadband Vegetation Indices for Determining Optimal Hyperspectral Wavebands for Agricultural Crop Characterization. Photogrammetric Engineering and Remote Sensing. 68(6): 607-621.

10. Thenkabail, P.S., 2002. Optimal Hyperspectral Narrowbands for Discriminating Agricultural Crops. Remote Sensing Reviews. 20(4): 257-291.

11. Thenkabail P.S., Smith, R.B., and De-Pauw, E. 2000b. Hyperspectral vegetation indices for determining agricultural crop characteristics. Remote sensing of Environment. 71:158-182.

12. Thenkabail P.S., Smith, R.B., and De-Pauw, E. 1999. Hyperspectral vegetation indices for determining agricultural crop characteristics. CEO research publication series No. 1, Center for earth Observation, Yale University. Pp. 47. Monograph\Book:ISBN:0-9671303-0-1. (Yale University, New Haven).